Variations of non-additive measures

Endre Pap

Department of Mathematics and Informatics, University of Novi Sad
Trg D. Obradovica 4, 21 000 Novi Sad, Serbia and Montenegro
e-mail: pape@eunet.yu

Abstract: General non-additive measures are investigated with the help of some related monotone measures (some types of variations and submeasures), which have some important additional properties.

Keywords: Set function, variation, submeasure.

1 Introduction

Non-additive set functions, as for example outer measures, semi-variations of vector measures, appeared naturally earlier in the classical measure theory concerning countable additive set functions or more general finite additive set functions. The pioneer in the theory of non-additive set functions was G.Choquet [2] from 1953 with his theory of capacities. This theory had influences on many parts of mathematics and different areas of sciences and technique.

Non-additive set functions are extensively used in the decision theory, mathematical economy, social choice problems, with early traces by Aumann and Shaplay in their monograph [1]. Recently, many authors have investigated different kinds of non-additive set functions, as subadditive and superadditive set functions, submeasures, k-triangular set functions, t-conorm and pseudo-addition decomposable measures, null-additive set functions , and many other types of set functions. Although in many results the monotonicity of the observed set functions was supposed, there are some results concerning also some classes of set functions which include also non-monotone set functions (for example superadditive set functions, k-triangular set functions).

On the other hand, fuzzy measures as monotone and continuous set functions were investigated by Sugeno [17] in 1974 with the purpose to evaluate non-additive quantity in systems engineering.This notion of fuzziness is different from the one given by Zadeh.Namely, instead of taking membership grades of a set, we take (in the fuzzy measure approach) the measure that a given unlocated element belongs to a set. There are many different type of fuzzy measures which are used . For example belief, possibility, decomposable measures. Specially in different branches of mathematics there are many types of non-additive set functions. They appeared in the potential theory, harmonic

analysis, fractal geometry, functional analysis, theory of nonlinear differential equations, theory of difference equations and optimizations. There are many different fields in which the interest on non-additive set functions is growing up. In the theory of the artificial intelligence, belief functions have been applied to model uncertainty. Belief functions, corresponding plausibility measures and other kinds of non-additive set functions are used in statistics. Non-additive expected utility theory has been applied for example in multi-stage decision and economics. Many aggregation operators are based on integrals related to non-additive measures [9, 10, 12]. We can compare additive set functions (which are base for the classical measure theory) and non-additive set functions in the following simple way. For a fixed set $A \in \Sigma$ the classical measure $\mu : \Sigma \to [0, +\infty]$ gives that for every set B from Σ such that $A \cap B = \emptyset$ we have that $\mu(A \cup B) - \mu(B)$ is always equal to a constant $\mu(A)$, i.e., it is independent of B. In contrast, for non-additive set function m the difference $m(A \cup B) - m(B)$ depends on B and can be interpreted as the effect of A joining B.

In this paper we will correspond to every set function ([1, 2, 13, 14, 15, 17, 18]) special positive set functions with some additional properties. Motivated by the notion of the variation of the classical measure ([15, 16]) we introduce axiomatically the notion of the variation of the general set function and prove that it always exists, but in general case it is not unique. One of them so called disjoint variation is based on the partition of the set and the other so called chain variation is based on the chains of sets, see [1, 4, 14]. In this paper we will prove that these variations have some additional properties with respect to the starting non-additive set function. Among others that disjoint variation is superadditive on any family of disjoint sets, see [14].

2 Variations

We start with some results from the classical measure theory. Let Σ be a σ-algebra of subsets of the given set X. A set function $\mu : \Sigma \to \mathbb{R}$ is additive (signed finitely additive measure) if we have

$$\mu(A \cup B) = \mu(A) + \mu(B)$$

for all $A, B \in \Sigma$ with $A \cap B = \varnothing$. A set function $\mu : \Sigma \to \mathbb{R}$ is $\sigma-$additive (signed measure) if we have

$$\mu\left(\bigcup_{i=1}^{\infty} E_i\right) = \sum_{i=1}^{\infty} \mu(E_i)$$

for all pairwise disjoint sequences $\{E_i\}$ from Σ, i.e., $E_n \cap E_m = \varnothing$ for $n \neq m$.

For an arbitrary but fixed subset A of X and an additive set function μ its variation $\overline{\mu}$ is defined by

$$\overline{\mu}(A) = \sup_{I} \sum_{i \in I} \mid \mu(D_i) \mid,$$

where the supremum is taken over all finite families $\{D_i\}_{i\in I}$ of pairwise disjoint sets of Σ such that $\cup_{i\in I} D_i = A$. It is well-known that if $\mu : \Sigma \to \mathbb{R}$ is finitely (or countable) additive the $\overline{\mu}$ is finitely (countable) additive. If μ is signed additive set function then μ is countable additive if and only if $\overline{\mu}$ is countable additive.

We consider now general set functions m, $m : \mathcal{D} \to [-\infty, +\infty]$, with $m(\varnothing) = 0$ (extended real-valued set function), see [14], where $\mathcal{D}$ denote a family of subsets of a set X with $\varnothing \in \mathcal{D}$. m is (finite) real-valued set function if $-\infty < m(A) < +\infty$ for all $A \in \mathcal{D}$, and m is monotone if $A \subset B$ implies $m(A) \leq m(B)$ for every $A, B \in \mathcal{D}$. m is non-negative if it is finite and $m(A) \geq 0$ for all $A \in \mathcal{D}$, and $m : \mathcal{D} \to [0, +\infty]$ is positive.

We introduce for an arbitrary set function axiomatically a generalization of the variation.

Definition 1 *Let m be a set function defined on $\mathcal{D}$ with values in $\mathbb{R}$ (or $[0, +\infty]$), with $m(\varnothing) = 0$. Then variation of m is a set function $\eta : \mathcal{D} \to [0, +\infty]$ with the following properties:*

(i) For every $A \subset X$ we have

$$0 \leq \eta(A) \leq +\infty;$$

(ii) $\eta(\varnothing) = 0$;

(iii) $\mid m(A) \mid \leq \eta(A)$ $(A \in \mathcal{D})$;

(iv) η *is monotone, i.e., if* $B \subset A$, *then* $\eta(B) \leq \eta(A)$;

(v) $\eta(A) = 0$ *if and only if* $m(B) = 0$ *for every subset* B *of* A *from* $\mathcal{D}$.

We easily obtain: For every $A \subset X$ we have

$$\eta(A) \geq \sup\{\mid m(B) \mid :\ B \subset A,\ \ B \in \mathcal{D}\}.$$

Namely, if B is a arbitrary subset of A which belongs to $\mathcal{D}$ we have by the properties (iv) and (iii)

$$\eta(A) \geq \eta(B) \geq \mid m(B) \mid .$$

3 The existence of variations

Theorem 1 *For every set function m defined on $\mathcal{D}$ and with values in $\mathbb{R}$ (or $[0, +\infty]$), with $m(\varnothing) = 0$, always exists its variation, which in general case is not uniquely determined.*

We introduce two special set functions related to a given set function m which are base for the proof of the preceding theorem.

Definition 2 *For an arbitrary but fixed subset A of X and a set function m we define the disjoint variation $\overline{m}$ by*

$$\overline{m}(A) = \sup_I \sum_{i\in I} \mid m(D_i) \mid, \tag{1}$$

where the supremum is taken over all finite families $\{D_i\}_{i\in I}$ *of pairwise disjoint sets of* $\mathcal{D}$ *such that* $D_i \subset A$ $(i \in I)$.

Definition 3 *For an arbitrary but fixed* $A \in \mathcal{D}$ *and a set function* m *we define the chain variation* $\mid m \mid$ *by*

$$\mid m \mid (A) = \sup\{\sum_{i=1}^{n} \mid m(A_i) - m(A_{i-1}) \mid:$$

$$\varnothing = A_0 \subset A_1 \subset \cdots \subset A_n = A, A_i \in \mathcal{D}, i = 1, \ldots, n\}. \tag{2}$$

We remark that the supremum in the previous definition is taken over all finite chains between $\varnothing$ and A.

Proof of Theorem 1. Let $m : \mathcal{D} \to \mathbb{R}$. We prove that $\overline{m}$ and $\mid m \mid$ are variations.

First we consider $\overline{m}$:

(i) Follows by the definition of $\overline{m}$.

(ii) Only family is $I = \{\varnothing\}$, and so we have

$$\overline{m}(\varnothing) = \sup \Sigma \mid m(\varnothing) \mid = 0.$$

(iii) Since one of the families I of disjoint sets of $\mathcal{D}$ contained in A is the family $I = \{A\}$ we obtain by the definition of $\overline{m}$ the desired inequality.

(iv) Since for any family $\{D_i\}_{i\in I}$ of disjoint sets of $\mathcal{D}$ with property $D_i \subset B$ $(i \in I)$, by $B \subset A$, we have $D_i \subset A$, too, we obtain

$$\sum_{i\in I} \mid m(D_i) \mid \leq \overline{m}(A),$$

and so $\overline{m}(B) \leq \overline{m}(A)$.

(v) Let us suppose that $\overline{m}(A) = 0$ for an arbitrary set $A \subset X$. Then by (v) we obtain

$$\overline{m}(B) = 0 \quad \text{for each} \quad B \subset A, \ \ B \in \mathcal{D}.$$

Suppose now that $\overline{m}(B) = 0$ for each $B \subset A$, $B \in \mathcal{D}$. Then for each finite family $\{D_i\}_{i\in I}$ of disjoint sets such that $D_i \subset A$ $(i \in I)$ we obtain

$$\sum_{i\in I} \mid m(D_i) \mid = 0.$$

This implies $\overline{m}(A) = 0$.

We consider now $\mid m \mid$:

(i) Follows by (2).

(ii) Every chain connecting $\varnothing$ with $\varnothing$ consists only of empty set, therefore

$$\begin{aligned} \mid m \mid (\varnothing) \quad &= \quad \sup\{\sum \mid m(A_i) - m(A_{i-1}) \mid: \\ &\qquad \varnothing = A_0 \subset A_n = \varnothing\} = 0. \end{aligned}$$

(iii) One of the chain which connects $\varnothing$ and the set A consists only of $\varnothing$ and A, i.e., $\varnothing = A_0 \subset A_n = A$, therefore

$$\begin{aligned} \mid m(A) \mid &= \sup\{\mid m(A) - m(\varnothing) \mid: \\ \varnothing = A_0 \subset A_n = A\} &\leq \mid m \mid (A). \end{aligned}$$

(iv) Some of chains from $\varnothing$ to A contain chains from $\varnothing$ to B, (exhaust all of them), therefore

$$\begin{aligned} \mid m \mid (B) &= \sup\{\sum_{i=1}^{n} \mid m(A_i) - m(A_{i-1}) \mid: \\ \varnothing = A_0 \subset A_1 \subset \cdots \subset A_n = B, A_i \in \mathcal{D},\ i = 1, ..., n\} \\ &\leq \sup\{\sum_{i=1}^{s} \mid m(A_i) - m(A_{i-1}) \mid: \\ \varnothing \subset A_0 \subset A_1 \subset \cdots \subset A_s = A, A_i \in \mathcal{D},\ \ i = 1, ..., s\} \\ &= \mid m \mid (A). \end{aligned}$$

(v) Suppose $\mid m \mid (A) = 0$. Then for every set $B \subset A,\ B \in \mathcal{D}$, we have by (v) $m(B) = 0$.

Conversely, if $m(B) = 0$ for every set $B \subset A,\ B \in \mathcal{D}$, then for any chain $\varnothing = A_0 \subset A_1 \subset ... \subset A_n = A$ we have $m(A_i) = 0,\ i = 1, 2, ..., n$, and so

$$\sum_{i=1}^{n} \mid m(A_i) - m(A_{i-1}) \mid = 0.$$

Hence $\mid m \mid (A) = 0$.

Finally we shall show that generally $\overline{m} \neq \mid m \mid$. Let $X = \{a, b\}$. Define $m : \mathcal{P}(X) \to \mathbb{R}$ by $m(\{a\}) = 2, m(\{b\}) = 3, m(\{a, b\}) = 4$. Then $\overline{m}(\{a, b\}) = 5 \neq 4 = \mid m \mid (\{a, b\})$. □

Remark 1 (i) If $\mathcal{D}$ is an algebra, then we can take for $A \in \mathcal{D}$ in (1) the supremum for all finite families $\{D_i\}_{i \in I}$ of disjoint sets such that $\bigcup_{i \in I} D_i = A$.
(ii) We note that the variation $\overline{m}$ given by (1) is defined on $\mathcal{P}(X)$.

Let $\mathcal{D}$ be a ring. A set function $m : \mathcal{D} \to \mathbb{R}$ is superadditive if for every $A, B \in \mathcal{D}$ with $A \cap B = \varnothing$ we have $m(A \cup B) \geq m(A) + m(B)$, and it is subadditive if for every $A, B \in \mathcal{D}$ with $A \cap B = \varnothing$ we have $m(A \cup B) \leq m(A) + m(B)$.

Theorem 2 *Let m be a set function defined on Σ with values in $\mathbb{R}$ (or $[0, +\infty]$), with $m(\varnothing) = 0$. Then the set function $\overline{m}$ given by (1) is superadditive, i.e.,*

$$\sum_{i \in I} \overline{m}(E_i) \leq \overline{m}\left(\bigcup_{i \in I} E_i\right)$$

for each family $\{E_i\}_{i \in I}$ of disjoint sets of X.

Proof. Suppose that $m \neq 0$. We take two arbitrary but fixed disjoint subset E_1 and E_2 of X such that $\overline{m}$ is different from zero on at least one of them. We take an arbitrary but fixed real number r such that

$$\overline{m}(E_1) + \overline{m}(E_2) > r. \tag{3}$$

Therefore there exist two real numbers r_1 and r_2 such that $r = r_1 + r_2$ and

$$\overline{m}(E_1) > r_1 \quad \text{and} \quad \overline{m}(E_2) > r_2.$$

Then there exists a finite family $\{D_i^1\}_{1 \leq i \leq n}$ of disjoint sets from Σ with $D_i^1 \subset E_1$ $(i = 1, 2, \ldots, n)$ such that

$$\sum_{i=1}^{n} \mid m(D_i^1) \mid > \ r_1, \tag{4}$$

and a finite family $\{D_i^2\}_{1 \leq j \leq k}$ of disjoint sets from Σ, with $D_j^2 \subset E_2$ $(j = 1, 2, \ldots, k)$, such that

$$\sum_{j=1}^{k} \mid m(D_j^2) \mid > \ r_2. \tag{5}$$

The family of sets

$$\{D_1^1, D_2^1, \ldots, D_n^1, D_1^2, D_2^2, \ldots, D_k^2\}$$

consists of disjoint sets from Σ which are contained in $E_1 \cup E_2$ and by (1) we obtain

$$\overline{m}(E_1 \cup E_2) \geq \sum_{i=1}^{n} \mid m(D_i^1) \mid + \sum_{j=1}^{k} \mid m(D_j^2) \mid .$$

Therefore by the inequalities (4) and (5)

$$\overline{m}(E_1 \cup E_2) > r_1 + r_2 = r. \tag{6}$$

Since the number r was arbitrary such that the inequality (3) is satisfied, we conclude that

$$\overline{m}(E_1) + \overline{m}(E_2) \leq \overline{m}(E_1 \cup E_2)$$

since the opposite inequality is impossible by (6).

The preceding inequality holds by induction for every finite family $\{E_i\}_{i \in J}$ of disjoint subsets of X, i.e.,

$$\sum_{i \in J} \overline{m}(E_i) \leq \overline{m} \left(\bigcup_{i \in J} E_i \right).$$

For an arbitrary family $\{E_i\}_{i \in I}$ of disjoint subset of X we obtain by the preceding step that for each finite subset J of I

$$\overline{m} \left(\bigcup_{i \in I} E_i \right) \geq \overline{m} \left(\bigcup_{i \in J} E_i \right) \geq \sum_{i \in J} \overline{m}(E_i).$$

Therefore

$$\overline{m}\left(\bigcup_{i\in I} E_i\right) \geq \sum_{i\in I} \overline{m}(E_i).$$

□

Open problem: *Find all variations of a given arbitrary set function m.*

We shall give a partial answer on this problem, when we require some additional properties of the variation.

Theorem 3 *Let m be a set function defined on Σ with values in $\mathbb{R}$ (or $[0,+\infty]$), with $m(\varnothing)=0$. Then $\overline{m}$ given by (1) is the smallest variation of m (defined on $\mathcal{P}(X)$) which is superadditive.*

Proof. By Theorem 2 variation $\overline{m}$ is superadditive. Then theorem follows by the properties of any superadditive variation η of m taking an arbitrary finite family $\{D_i\}_{i\in I}$ of disjoint sets from Σ contained in A, i.e.,

$$\eta(A) \geq \eta\left(\bigcup_{i\in I} D_i\right) \geq \sum_{i\in I} \eta(D_i) \geq \sum_{i\in I} \mid m(D_i) \mid .$$

Hence $\eta(A) \geq \overline{m}(A)$. □

Open problem: *Find all variations of a given arbitrary set function m.*

We shall give a partial answer on this problem, when we require some additional properties of the variation.

Theorem 4 *Let m be a set function defined on Σ with values in $\mathbb{R}$ (or $[0,+\infty]$), with $m(\varnothing)=0$. Then $\overline{m}$ given by (1) is the smallest variation of m (defined on $\mathcal{P}(X)$) which is superadditive.*

4 Submeasures

For non-negative monotone set function m with an additional topological property we can correspond a submeasure ξ (monotone and subadditive set function) which is closely topologically connected with m, see for more details [6, 7, 13, 14].

Theorem 5 *Let $\mathcal{D}$ be a ring and $m : \mathcal{D} \to [0,\infty)$ be monotone. Then there exists a submeasure ξ on $\mathcal{D}$ such that*

$$m(E_n) \to 0 \Leftrightarrow \xi(E_n) \to 0,$$

if and only if m satisfies the following condition:

$$(ac) \quad m(A_n) + m(B_n) \to 0, \quad \textit{then} \quad m(A_n \cup B_n) \to 0.$$

The work was supported by the grant MNTRS-1866 and the Vojvodina Academy of Sciences and Arts..

References

[1] R. J. Aumann, L. S. Shapley, *Values of Non-Atomic Games*, Princ. Univ. Press, 1974.

[2] G. Choquet, Theory of capacities, *Ann. Inst. Fourier (Grenoble)* 5 (1953-54), 131-292.

[3] D. Denneberg, *Non-Additive Measure and Integral,* Kluwer Academic Publishers, Dordrecht, 1994.

[4] N. Dinculeanu, *Vector Measures*. Pergamon Press, New York, 1967.

[5] I. Dobrakov, *On submeasures-I*, Dissertationes Math. 112, Warszawa, 1974.

[6] L. Drewnowski, Topological rings of sets, continuous set functions, integration, I, II, III, *Bull. Acad. Polon. Sci. Ser. Math. Astronom. Phys.* 20 (1972), 269-276, 277-286, 439-445.

[7] L. Drewnowski, On the continuity of certain non-additive set functions, *Colloquium Math.* 38 (1978), 243-253.

[8] M. Grabish, T. Murofushi, M. Sugeno, Fuzzy measure of fuzzy events defined by fuzzy integrals, *Fuzzy Sets and Systems* 50 (1992) , 293-313.

[9] M. Grabisch, H.T. Nguyen and E.A. Walker, *Fundamentals of Uncertainty Calculi with Applications to Fuzzy Inference.* Kluwer Academic Publishers, Dordercht, 1995.

[10] M. Grabisch, T. Murofushi, M. Sugeno, eds.: *Fuzzy Measures and Integrals. Theory and Applications*. Physica-Verlag, Heidelberg, 2000.

[11] E. P. Klement, R. Mesiar, E. Pap, Integration with respect to decomposable measures, based on a conditionally distributive semiring on the unit interval, *Internat. J. Uncertain. Fuzziness Knowledge-Based Systems* 8 (2000), 701-717.

[12] E. P. Klement, R. Mesiar, E. Pap, Measure-based aggregation operators, *Fuzzy Sets and Systems* 142 (2004), 3-14.

[13] E. Pap, On non-additive set functions. *Atti. Sem. Mat. Fis. Univ. Modena* 39 (1991), 345-360.

[14] E. Pap, *Null-Additive Set Functions*. Kluwer Academic Publishers, Dordrecht, Ister Science, Bratislava, 1995.

[15] E. Pap (Ed.), *Handbook of Measure Theory*. Elsevier, North-Holland, 2002.

[16] W. Rudin, *Real and Complex Analysis*. Mc Graw-Hill, 1966.

[17] M. Sugeno, *Theory of fuzzy integrals and its applications*. Ph.D.Thesis, Tokyo Institute of Technology, 1974.

[18] Z. Wang, G. Klir, *Fuzzy measures*. Plenum Press, New York, 1992.

Assessment of the Completeness of Mineral Exploration by the Application of Fuzzy Arithmetic and Prior Information

György Bárdossy [1], **János Fodor** [2]

[1] Hungarian Academy of Sciences, Budapest, Hungary
Tel.: +36-1-3117-993, e-mail: h4750bar@helka.iif.hu

[2] Department of Biomathematics and Informatics
Szent István University, Budapest, Hungary
Tel.: +36-1-478-4213, e-mail: Fodor.Janos@aotk.szie.hu

Abstract: The completeness of an exploration project is of crutial importance for making decision to start or to give up a mining investment, or to continue the exploration to get complementary information. The authors discuss this problem on the example of the Halimba bauxite deposit, Hungary. Resource calculations were carried out in 12 subsequent stages by fuzzy arithmetic with the aim to quantify the uncertainties of ore tonnage and grade. Prior information and prior probabilities were applied to complete the exploration data. Ranges of influence for the main variables were calculated by variograms. Spatial variability and spatial continuity of the ore bodies were mathematically evaluated. The authors found that the main geological, mining and economic factors must be evaluated separately and ranked according to their importance.

Keywords: resource assessment, fuzzy arithmetic, prior information, prior probabilities

1 Introduction

Exploration of solid mineral deposits is generally an expensive task. Even more expensive and risky is the successive mining investment. It is of paramount importance therefore to optimize the exploration expenses and to minimize the risks of the mining investment. This double task was considered so far as a purely geological and mining- engineering problem, however, in our opinion, the application of some new mathematical methods may considerably improve the results. The aim of this paper is to show the application of these new methods by a case study. The Halimba bauxite deposit in Hungary has been chosen as example.

2 Basic Concepts

The completeness of an exploration campaign is generally expressed by the resource assessment (tonnage and grade) and its overall reliability. The spatial distribution and spatial variability of ore grade and the spatial continuity of ore within the deposit are further important aspects (Henley 2000, Wellmer 1989, Yamamoto 1999). However the traditional methods of resource assessment are not able to quantify the reliability of the estimation results. The fuzzy set theory has been applied by the authors for this purpose on some solid mineral deposits with success (Bárdossy, Fodor 2004). Fuzzy sets have been applied for the resource assessment of skarn tin deposits by Luo and Dimitrakopoulos (2003).

A further improvement can be achieved by applying the concept of Bayesian probabilities. It is well known that the so called frequentist approach requires repeated identical experiments. However, this requirement can be fulfilled only rarely at the geologic investigations. The Bayesian approach, on the other hand, is able to evaluate unrepeatable phenomena as well. Bayesian probability depends only on the state of knowledge about the given problem and it changes with time as new pieces of information are acquired (Bárdossy, Fodor 2004). Mineral exploration has also this changing character as new pieces of information are obtained about the given deposit by drilling new boreholes etc. For this reason,it is reasonable to apply also prior information and Bayesian probabilities for the evaluation of exploration results and other geoscientific problems (Wood and Curtis 2004).

3 Initial Data

The bauxite deposit of Halimba, selected for this case study has been explored since 1943 and up to the present more than 2600 core boreholes have been performed. Underground mining started in 1950 and is still running. Computerised relational databases have been established (AutoCad) for the main data obtained about the deposit, particularly for the chemical composition of the ore. The sector of the test calculations – called Halimba II east – has been intensively explored during the last three years. It covers an area of 15 hectars with 237 borehole sites and it is situated int he southern part of the deposit (Figure 1). A 10 to 40 m thick bed consisting of bauxite, clayey bauxite and bauxitic clay covers the karstified surface of Upper Triassic dolomite and limestone. The overburden is of Middle Eocene age. The entire deposit is of fluvial origin. The area of the studied sector is of flood-plain facies. The bauxite accumulated during short inundation phases, forming very irregular ore bodies within a continuous clayey bauxitic layer. Underground mining operations started in the western part of the study area in 2003. They confermed the above outlined deposit model.

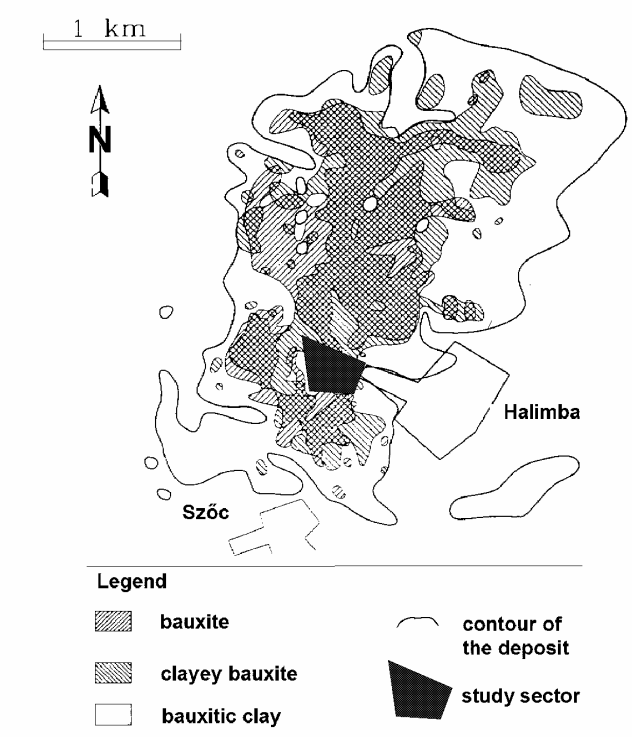

Figure 1
The Halimba bauxite deposit, Hungary

First the spatial variability of the main variables has been evaluated by us applying the well known methods of geostatistics (Goovaerts 1997). Ranges of influence have been calculated by the Variowin program for the thickness of the bauxitic bed, for the bauxite ore and for the Al_2O_3, SiO_2,Fe_2O_3,CaO and MgO contents of the bauxite.

Our basic idea was to follow the changes that occurred as the exploration progressed. For this reason resource assessments were carried out by us after every 20 new boreholes finished. Thus a growing number of boreholes served as a base of the successive resource assessments. Altogether 12 resource assessments have been performed.

The three basic components of any resource assessment of solid mineral deposits are the area of the deposit, the thickness of the ore and its bulk density. Fuzzy numbers have been constructed for all the three components. The „support" of the fuzzy number extends from the minimum to the maximum possible value. In the case of the deposit area the minimum value is determined by straight lines connecting the extreme productive boreholes. The maximum possible area is obtained by connecting the closest improductive boreholes around the productive

area. The „core" of the fuzzy number represents the geologically most possible area, determined by the deposit model and its contour line.

This is a relatively simple and unambiguous task in the case of well explored deposits. However, in the early stages of exploration the number of boreholes is often not sufficient for the above outlined constructions. In that cases we extrapolated from the given productive borehole the range of influence of the bauxite thickness in all directions, obtaining this way the minimum possible area. The maximum possible area was obtained by taking in all directions twice the range of influence. In this case an interval has been chosen also for the core of the fuzzy number, expressing the larger uncertainty of the deposit area. The extrapolated resource boundaries are replaced gradually by straight lines connecting the neighbouring boreholes, as new boreholes are drilled. According to our experience, exploration should not be finished before replacing all the extrapolated boundaries by the connecting straight lines. Thus the trapesoidal fuzzy numbers are gradually replaced by triangular ones. As an example the area of the resource assessment at the end of the third stage is shown in Figure 2, and that at the end of the last (12^{th}) stage in Figure 3.

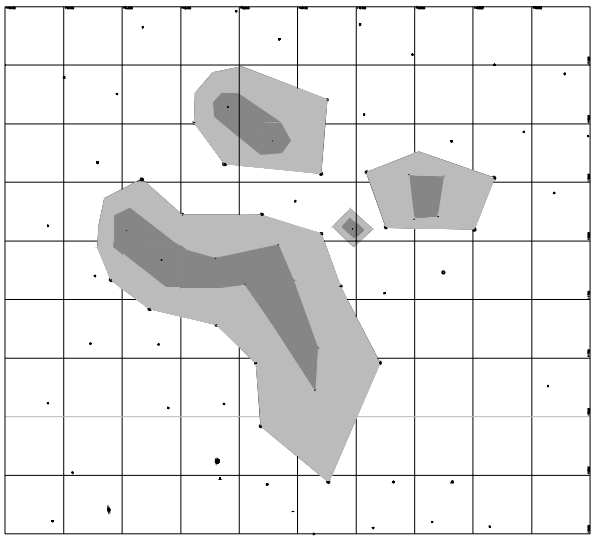

Figure 2
The area of the resource assessment at the end of the third stage

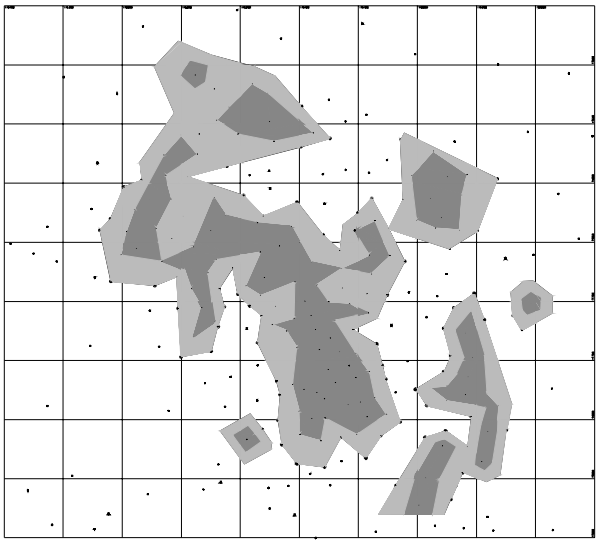

Figure 3
The area of the resource assessment at the end of the last stage

The fuzzy numbers representing the ore thickness correspond to the averages of the borehole results. Before calculating the averages, the main statistics of ore thickness have been calculated by us, applying the 12.0 version of the SPSS program. The histograms and the „skewness" values indicated a strong right-asymmetrical distribution. To eliminate the corresponding bias, „maximum likelihood" estimators have been calculated instead of the common averages. Tukey's biweight estimator was found to correspond best to an unbiased average. It has been applied in all cases when the skewness statistic exceeded 1,0. The minimum and the maximum values of the support of the fuzzy numbers correspond to the endpoints of the corresponding confidence interval, at 95% level of confidence. The core of the fuzzy number is an interval determined by the standard error of the mean.

The bulk density of the ore has been measured in the laboratory on borehole cores and in the mine on large samples, several hundred times. The distribution of the results is symmetrical. The mean value is 2,29 tons/m^3. The analytical error is less than 10 relative percents. The variability of the bulk density is very limited over the test area. For this reason the same fuzzy number has been applied for all the twelve resource assessments. In the same way as for the ore thickness, the support corresponds to the confidence interval at 95% level of confidence and the core to the standard error of the mean, plus the analytical error.

The tonnage of the resource is the product of the above discussed three components. Fuzzy multiplication was applied for the three corresponding fuzzy numbers. The uncertainty of the resource assessment is expressed in tons by the

length of the support and the core. Additionally relative deviations from the average values – expressed as percentages – were also calculated.

The average grade of the ore has been calculated in a similar way constructing average fuzzy numbers for all the listed chemical components. To avoid biases due to asymmetrical distribution histograms and skewness values were calculated and robust M-estimators were applied whenever the skewness exceeded the value 1,0. As in the case of tonnage, absolute and relative uncertainties have been calculated for all the evaluated chemical components.

As mentioned above, all the above listed calculations have been repeated 12 times, adding every time 20 new boreholes. Fuzzy numbers for selected stages are presented in Figure 4.

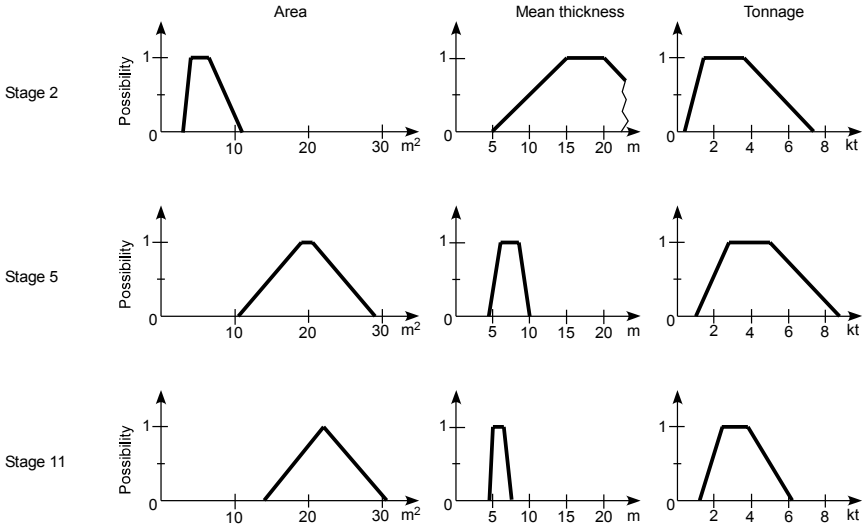

Figure 4
Fuzzy numbers expressing the area, mean thickness, and tonnage for stages 2, 5, 11

4 Evaluation of the Completeness of the Exploration

For the starting situation, that is before the drilling of the first bore hole in the sector, the following prior probabilities have been assumed, based on the experiences of the neighbouring explored and mined sectors:

- the bauxite – clayey bauxite bed is continuous over the exploration sector *0.8 probability*
- the bed is not continuous over the exploration sector *0.2 probability*

Second item of the prior probabilities:

- - commercial bauxite ore bodies are situated within the above bed *0.6 probability*
- - no commercial bauxite ore bodies occur within the bed *0.4 probability*

The end situation – after the 12th stage – confirmed both larger prior probabilities.

For the first two stages of exploration the number of productive boreholes was not sufficient to calculate reliable variograms. For this reason, the already calculated ranges of influence of the neighbouring sectors were applied, supposing similar values in the study area. At the end of the third stage variograms could be calculated for the ore thickness. By applying different „lags" and variogram models ranges of influence from 10 to 20 m length were obtained. With growing number of boreholes the variograms became more accurate and after the 12th stage 15 m range of influence was accepted for the entire exploration area. However, locally even smaller ranges of influence exist, as confirmed by the latest mining operations. As outlined later, these changes significantly influenced the results of the successive resource assessments.

At the end of each exploration stage circles were constructed around each borehole, expressing the range of influence. The boreholes were placed in a „random-stratified" grid, with the aim to optimize the contouring of the very irregularly shaped ore bodies. For this reason „unknown" slices remained between some neighbouring boreholes. Prior probabilities have been calculated for these slices separately and if they exceeded the 0.5 value, they have been included into the resource assessment. This procedure ameliorated considerably the fitting of the resource contours to the real boundaries of the ore bodies.

Different variables have been chosen for the quantitative evaluation of the completeness of exploration,first of all the tonnage of the resources. In Figure 5 the successive changes of the minimum and maximum values of the support are represented. The minimum value of the tonnage steeply increases in the first four stages of exploration, followed by much smaller increase in the later stages. The fluctuation of the diagram reflects the randomness of the results at some stages. The possible maximum tonnage also increases steeply in the first stages, but it is followed by an unexpected gradual decrease untill the eighth stage. The last stages show a slight increase. The peculiar form of this diagram can be explained by the higher uncertainty of the maximum tonnage, influenced by the position of the closest improductive boreholes and by the extrapolation of the contour line in the first stages of exploration. The peak between the third and fourth stages is clearly a random effect, that may occur in the first stages of any exploration campaign. As exploration progresses, the difference between the two diagrams diminishes, as the area between the manimum and maximum contours becomes narrower.

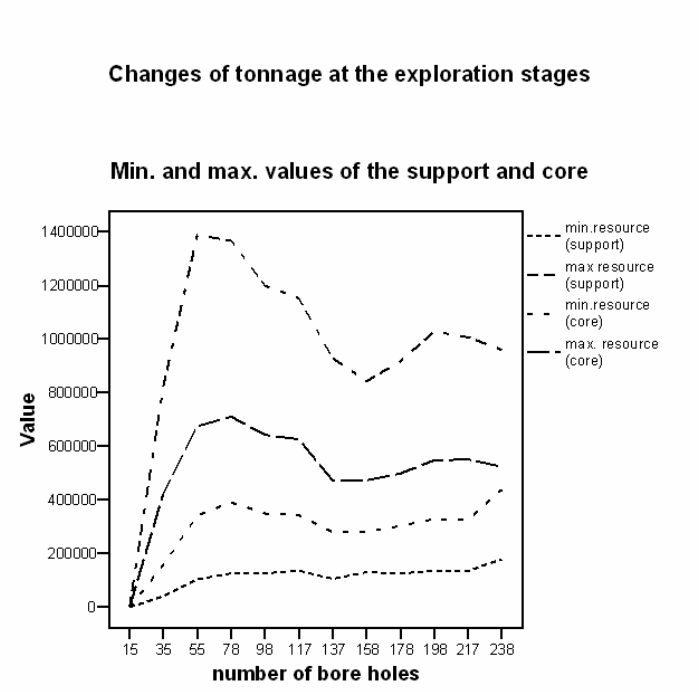

Figure 5
Quantitative evaluation of tonnage: successive changes of the maximum and minimum of the support and the core, respectively

The tonnage expressed by the core of the fuzzy numbers has a much shorter uncertainty interval, presented also in Figure 5. The random overestimation of the tonnage between the third and fourth stages is clearly visible on both diagrams, but it is gradually equalized in the later stages without reaching a constant value. Theoretically, the exploration is still not complete, but the changes of the tonnage are insignificant. Thus the tonnage of the resources alone is in favour of finishing the exploration drilling.

A further aspect of the evaluation is the relative uncertainty of the tonnage, expressed as a percentage of the mean (crisp) tonnage. We calculated it separately for the support and for the core of the corresponding fuzzy numbers. The results are presented in Figure 6. It is obvious that the uncertainty of the tonnage expressed by the support is much larger than that of the core. It decreases in the successive stages untill the eighth stage – from ±91% to ±73%. This is followed in the later stages by a fluctuation and a final value of ±69%. On the other hand, the relative uncertainty of the tonnages expressed by the core are much smaller. The starting ±46% relative uncertainty diminishes to ±9%. This indicates a near complete exploration result.

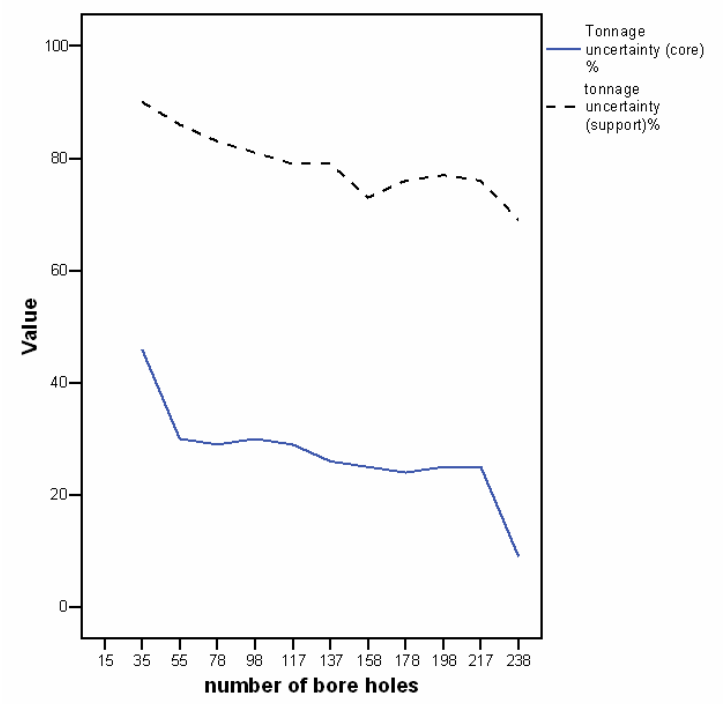

Figure 6
Relative uncertainty of the tonnage for the core and the support, respectively

The tonnage values of the fuzzy numbers and their relative uncertainties are presented in Table 1. Let us stress that these data represent a significant complement to the single-valued traditional resource estimation results. But even these data are insufficient in our opinion to make a reliable decision on the completenes of an exploration campaign. The main chemical components have been evaluated by us too, in function of the successive exploration stages.The resulting main statistics, calculated by the SPSS program are presented in Table 2.

The Al_2O_3 content has the smallest relative variance, ±7%. The distribution of this component is almost normal, thus the mean value is unbiased. It diminished from the second to the latest exploration stage from 52.8 to 51.2%, considered by us as a very small change. In the same time, the standard error of the mean diminished from ±1.0 to ±0.3%, indicating a high reliability of the results. It can be concluded that regarding the alumina content the exploration has been complete since the early stages.

The Fe_2O_3 content follows with ±14-16% relative variance. The distribution is symmetrical and the mean decreased from 25.3 to 24.6% as exploration progressed, close to the range of the analytical error. As with the Al_2O_3, the standard error of the mean diminished from ±1.0 to ±0.3%.

Table 1
Main results of the resource calculations

Stages	Number of boreholes	Deposit area				Tonnage				Length of the core interval	Relative uncertainty of the tonnage (%)	Length of the support interval	Relative uncertainty of the tonnage (%)
		a	b	c	d	a	b	c	d				
1	15	0	0	0	0	0	0	0	0	0	0	0	0
2	35	5300	8100	12000	17400	41700	158200	425400	826400	267200	46	784700	90
3	55	11800	26200	29800	46400	104400	342400	675200	1388400	332800	30	1284000	86
4	78	12610	29100	30800	47960	126100	391400	710900	1367200	319500	29	1241100	83
5	98	14090	29300	31000	46600	126600	350000	643000	1200000	293000	30	1073400	81
6	117	15630	30400	32100	47700	136500	344500	626700	1152500	282200	29	1016000	79
7	137	14090	29700	30000	45630	106000	279600	472600	929000	193000	26	823000	79
8	158	16980	30200	30700	44100	130900	281900	473800	843200	191900	25	712300	73
9	178	16700	32200	32400	47870	126400	303300	499100	917500	195800	24	791100	76
10	198	18940	35300	35300	52280	135900	329200	548000	1028500	218800	25	892600	77
11	217	20800	36000	36300	52200	136200	323800	549100	1002700	224100	25	870900	76
12	238	24300	41600	42000	60300	178800	439000	524200	960000	85200	9	781100	69

Legend:

a: lower bound of the support of trapezoidal fuzzy number [a,b,c,d]

b: lower bound of the core of trapezoidal fuzzy number [a,b,c,d]

c: upper bound of the core of trapezoidal fuzzy number [a,b,c,d]

d: upper bound of the support of trapezoidal fuzzy number [a,b,c,d]

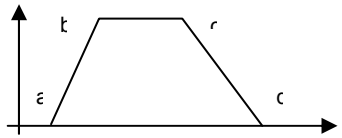

Thus the exploration is considered complete also in this respect.

The SiO_2 content of the ore is more variable, the relative variance ranging from ±39 to 45%. The distribution is almost symmetrical and the mean remained the same within the range of the analytical error. Only the standard error of the mean diminished from ±0.7 to ±0.2%, indicating a high reliability of the results. The exploration is complete also in this respect.

The CaO is one of the main contaminants in the bauxite. This is the most variable analysed chemical component, the relative variance ranging from ±83 to 114%. The distribution is strongly skewed, as indicated by the high positive skewness value. For this reason Tukey's M-estimator has been applied intead of the normal mean. It increased gradually from 0.6 to 1.0% to the last stage of the exploration. It cannot be predicted whether a further increase would occur with the drilling of new boreholes. The reason for this high variability is the presence of CaO in the form of secondary calcite precipitations, irregularly distributed within the ore bodies.Thus regarding the evaluated chemical components, the exploration can be considered as completed, except the CaO content.

A further aspect influencing the completeness of the exploration is the detection of the spatial distribution of the orebodies and the degree of their variability. The question is, how much increased the precision of these predictions by the exploration and can it be regarded complete after the twelfth stage? To answer these questions prior probabilities have been applied. The borehole sites have been ordered into five categories and a prior probability has been attached to each category, based on the overall exploration experiences of the entire deposit:

1.	the site is within the productive area	0.3 prior probability
2.	the site is on the border of the productive area	0.05
3.	the site is within the possible area	0.2
4.	the site is on the outer border of the possible area	0.05
5.	the site is within the improductive area	0.4
	altogether	1.0 prior probability

The borehole sites situated beyond the range of influence of bauxite thickness have not been categorized. In the next step all existing borehole sites were categorized based on the resource assessment maps of the 12 exploration stages and the changes of categories were presented in the form of a table. Table 3 shows these changes for 20 selected borehole sites, as the limited extent of this paper does not allow the presentation of all the 237 borehole sites. (The not categorized sites are indicated by question-marks). It is obvious that the number of not categorized sites diminishes in the successive exploration stages. Several boreholes have been drilled at such sites having no prior information.

Table 2
Main statistics of selected chemical components at the end of exploration stages

Chemical components	Stage 12	Stage 8	Stage 6	Stage 4	Stage 2
SiO2					
Mean (%)	5.30	5.70	5.70	5.50	5.40
Standard error of the mean (%)	± 0.20	± 0.20	± 0.30	± 0.30	± 0.70
Standard deviation (%)	± 2.10	± 2.30	± 2.30	± 2.2	± 2.40
Coefficient of variation (%)	39.00	40.00	41.00	40.00	45.00
Skewness	0.02	-0.05	-0.03	0.03	-0.16
Min (%)	1.30	1.30	1.30	1.30	1.30
Max (%)	9.90	9.50	9.50	9.50	9.40
Al2O3					
Mean (%)	51.20	51.60	51.90	51.90	52.80
Standard error of the mean (%)	± 0.30	± 0.40	± 0.40	± 0.50	± 1.00
Standard deviation (%)	± 3.60	± 3.70	± 3.50	±3.20	± 3.70
Coefficient of variation (%)	7.00	7.00	7.00	6.00	7.00
Skewness	0.24	-0.09	0.45	0.88	-0.89
Min (%)	38.70	38.70	42.90	44.00	44.00
Max (%)	64.10	63.10	63.10	63.10	59.50
Fe2O3					
Mean (%)	24.60	24.60	24.30	24.30	25.30
Standard error of the mean (%)	± 0.30	± 0.40	± 0.40	± 0.60	± 1.00
Standard deviation (%)	± 3.80	± 3.90	± 3.50	± 3.80	± 3.50
Coefficient of variation (%)	16.00	16.00	15.00	16.00	14.00
Skewness	-0.89	0.65	-0.77	-0.94	0.38
Min (%)	10.30	11.10	11.10	11.10	20.10
Max (%)	36.70	36.70	32.60	32.60	32.60
CaO					
Mean (%)	1.00	0.90	0.89	0.76	0.60
Standard error of the mean (%)	± 0.08	± 0.09	± 0.12	± 0.19	± 0.27
Standard deviation (%)	± 0.83	± 0.81	± 0.85	± 0.87	± 0.55
Coefficient of variation (%)	83.00	90.00	96.00	114.00	91.00
Skewness	1.32	1.54	1.74	2.57	1.54
Min (%)	0.11	0.11	0.11	0.11	0.20
Max (%)	3.90	3.90	3.90	3.90	1.38

This „haphazard" approach leaded to some negative results, as illustrated by the Table 3. The categories of the borehole sites often changed in positive or negative

sense indicating the incompleteness of the exploration. Theoretically, exploration should be considered complete if the site-category would not change in the final two or three exploration stages, before the drilling of the given borehole. Unfortunately, this condition was only partly fulfilled even for the last, twelfth stage. Thus, in this respect the exploration cannot be accepted as complete.

Table 3
Prior categorization of selected borehole sites

Borehole	Exploration stages										
	1	2	3	4	5	6	7	8	9	10	11
H-2564	?	5	3	3	3	3	3	3	3	3	**2**
H-2557	5	5	5	5	5	5	5	5	5	5	**1**
H-2556	?	?	?	?	?	?	?	?	?	?	**5**
H-2555	?	?	?	?	?	?	?	?	?	?	**5**
H-2554	?	(1)	(1)	3	3	3	3	3	3	3	**2**
H-2553	?	(2)	(1)	3	3	3	3	3	3	3	**2**
H-2552	?	(3)	3	3	3	3	3	3	3	3	**2**
H-2551	?	(1)	(1)	1	1	1	1	1	1	1	**3**
H-2550	5	5	3	3	3	3	3	3	3	3	**2**
H-2549	?	5	5	5	5	5	5	3	3	3	**4**
H-2548	?	?	?	?	?	?	?	?	?	?	**5**
H-2547	?	5	3	3	3	3	3	3	3	3	**3**
H-2546	?	5	(1)	1	1	1	1	1	1	1	**1**
H-2545	?	5	(4)	(4)	(4)	(4)	(4)	(4)	4	**4**	n.a.
H-2544	?	?	5	?	?	?	?	5	3	**2**	n.a.
H-2543	5	5	5	?	?	?	?	?	?	**5**	n.a.
H-2542	5	5	5	?	?	?	?	?	?	**4**	n.a.
H-2541	?	?	?	?	?	?	?	?	5	**2**	n.a.
H-2540	?	?	?	?	?	?	?	?	?	**2**	n.a.
H-2539	?	?	?	?	?	?	?	?	?	**4**	n.a.

Legend:

1. Site within the productive area.

2. Site on the border of the productive area

3. Site within the possible area.

4. Site on the outer border of the possible area.

5. Site within improductive area (clayey bauxite and bauxitic clay).

( ) Site categorized by extrapolation.

? Not categorized site, outside the ranges of influence.

Bold numbers: categories after drilling the corresponding borehole site.

Table 4
Summary results of the prior categorization of the first seven exploration stages

Categories	Productive	Possible	Improductive	Sum of row
Productive	20	16	14	50
Possible	10	17	11	38
Improductive	0	2	12	14
Sum of column	30	35	37	102

A more complete evaluation can be obtained if several exploration stages are considered together. Table 4 shows the results of the first seven stages.(Obviously, the first stage can not be evaluated). Even more interesting results were obtained, when evaluating all stages together, as presented in Table 5. From the 203 prior probabilities 92 were confirmed by the drilling of the corresponding bore-holes. Even more important is that in 97 cases the prior probabilities were changed positively and only in 14 cases negatively. These result underline the effectiveness of the exploration campaign.

Table 5
Summary results of the prior categorization of all the 12 exploration stages

Categories	Productive	Possible	Improductive	Sum of row
Productive	28	35	37	100
Possible	12	32	25	69
Improductive	0	2	32	34
Sum of column	40	69	94	203

A further aspect, important for the planning of a mining investment, is the completeness of the contouring of the orebodies. In our case this means that the orebodies should be surrounded from all sides by improductive boreholes. The evaluation is simple: the exploration is incomplete at all places where the contour of the orebody is determined only by extrapolation. In the study area four places remained incomplete in this respect after ending the 12^{th} stage. An overall relative index can be computed when comparing the length of the completely contoured borders with the length of the extrapolated ones.

A further aspect is the rate of lateral changes in the thickness and altitude of the orebodies. This aspect is very important in the case of underground mining, as it can be a limiting factor for the choice of the excavation and production systems. We evaluated this aspect by calculating the specific rates of lateral changes for the bauxite thickness of neighbouring boreholes. An example of this evaluation is presented in Figure 7. In the ore bodies of our test sector these specific rates of lateral changes are often very strong and they may vary quickly in the different directions, making difficulties in the choice of the mining methods. Note that the boreholes beyond the range of influence were excluded from this evaluation. The entire productive sector has been evaluated in this way. The exploration is complete in this respect.

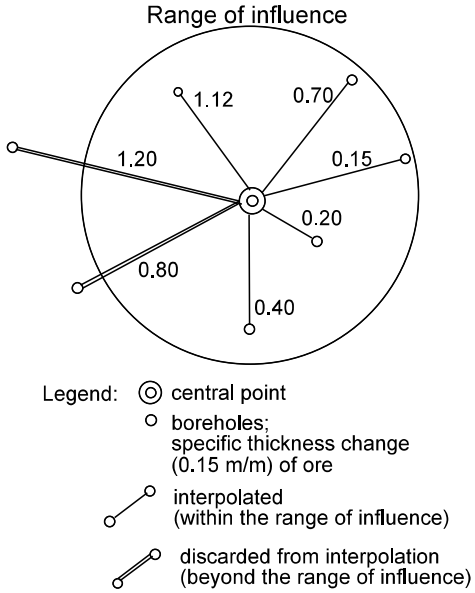

Figure 7
Evaluation of the specific rate of changes for ore thickness in an underground mine around a measured central point

It is mathematically possible to aggregate all the discussed aspects into one fuzzy completeness index of the exploration, following the methodology of Luo and Dimitrakopoulos (2003) for their fuzzy mineral favourability index. This is a useful estimator for the stakeholder, but for the mining engineer, planning and starting the mining operations, it is more useful to evaluate and to compare all the discussed aspects separately. We recommend therefore the stepwise evaluation of each aspect after every exploration stage and making decisions after ranking them in both respects of completeness (reliability) and the additional costs of the drilling of further boreholes.

5 Verification of the Exploration Results

The underground mining operations quickly followed the above outlined exploration, offering us a possibility to check the validity of our evaluations. In the western part of the deposit boreholes were drilled from the galleries at 5 meter intervals vertically up and down and also laterally. The bauxite has been sampled and analysed at every one meter interval. The bauxite ore of more than 2 meters thickness have been excavated.

All these data have been evaluated by us by applying the AutoCAD program and the resulting 2 meters contour has been constructed. This line has been compared with our last (12^{th}) resource assessment map – for the selected part of the deposit (Figure 8). The productive area of our resource assessment is completely confirmed by this contour line. It runs generally within the possible area, and at some places it even extends beyond it. There is no positive or negative bias (over- or under estimation) in this respect. Thus our deposit model, applied to our resource assesment has been confirmed by the mining operations.

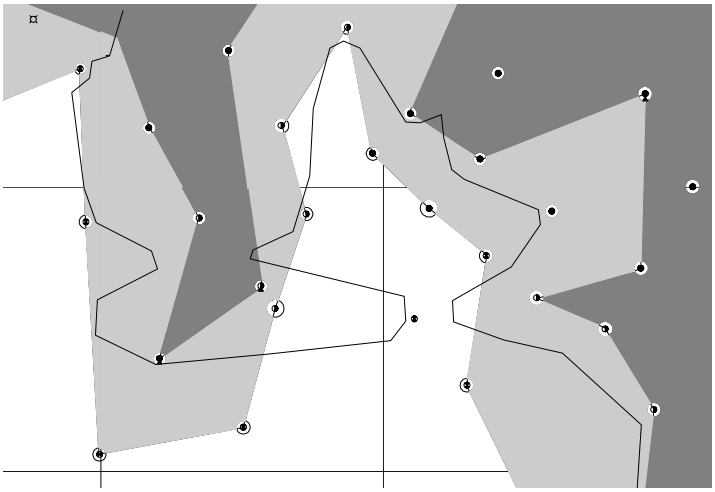

Figure 8
Comparison of estimation and reality

Conclusions

The completeness of a mineral exploration can be best evaluated by a joint application of the fuzzy set theory and Bayesian (prior) probabilities. The establishment of appropriate computerized databases is indispensable for these tasks.

The method consists of the stepwise evaluation of successive exploration stages (contouring the productive and possible areas and calculating the resources).

According to our experiences, completeness of exploration is achieved at different stages of exploration regarding the different evaluated variables. The criterion for completeness should be the decrease or complete equalization of the given variable.

Even in the case of best planned and evaluated exploration random effects (over- or under-estimation of the given variable) cannot be excluded, mainly in the early stages of the exploration campaign.

A reliable deposit model is the precondition of any evaluation in this respect. The model can be verified by the evaluation of the successive mining operations.

This methodology can be applied to other types of solid mineral deposits as well, taking into account their specific deposit models.

References

[1] Bárdossy, Gy., R. Szabó, J., Varga, G. 2003: A new method of resource estimation for bauxite and other solid mineral deposits. – BHM, 148. Jg. pp. 57-64. Leoben

[2] Bárdossy, Gy., Fodor, J. 2004: Evaluation of Uncertainties and Risks in Geology. – Springer Verlag. Berlin, Heidelberg, London, New York. 221 pages

[3] Henley, S. 2000: Resources, reserves and reality. – Earth Sciences Computer Applications. Vol. 15. No. 10. pp 1-2

[4] Luo, X., Dimitrakopoulos, R. 2003: Data-driven fuzzy analysis in quantitative mineral resource assessment. – Computers and Geosciences. 29. pp. 3-13

[5] Wellmer, F. W. 1989: Economic Evaluations in Exploration. – Springer Verlag. Berlin, Heidelberg, London, New York. 150 pages

[6] Wood, R. Curtis, A. 2004: Geological prior information, and its applications in solving geo-scientific problems. – In: „Geological Prior Information" Eds: A. Cueris and R. Wood. – Geol. Society of London Special Publication. 239. (in press)

[7] Yamamoto, K. 1999: Quantification of uncertainty in ore reserve estimation. Applications to Chapada Copper Deposit, Brazil. – Natural Resources Research. 8. pp. 153-163

Soft Computing Based Point Correspondence Matching for Automatic 3D Reconstruction

Annamária R. Várkonyi-Kóczy [1, 2], **András Rövid** [1, 2]

[1]Dept. of Measurement and Information Systems,
[2]Integrated Intelligent Systems Japanese-Hungarian Laboratory
Budapest University of Technology and Economics,
Magyar tudósok krt. 2, H-1521 Budapest, Hungary
e-mails: rovid@mit.bme.hu, koczy@mit.bme.hu

Abstract: In computer vision image point correspondence matching plays an important role. With the help of the point correspondence matching algorithms for example some of methods concerning the field of stereo vision can be automatized. This paper presents a method for quickly and reliably selecting and matching of the most interesting image points (feature points).

Keywords: Feature points, image point correspondence, 3D modeling, noise cancellation, edge detection, corner detection, fuzzy reasoning

1 Introduction

Feature matching is a key component in many computer vision applications, for example in stereo vision, motion tracking, and identification. The most significant problem in stereo vision is how to find the corresponding points in two, let us call them left and right images, referred to as the correspondence problem. In the field of computer vision several applications require to match feature points of images taken form different camera positions. Stereo techniques can be distinguished by several attributes, e.g., whether they use area-based or feature-based techniques, are applied to static or dynamic scenes, use passive or active techniques, or produce sparse or dense depth maps. The extremely long computational time needed to match stereo images is still the main obstacle on the way to the practical application of stereo vision techniques. In applications such as robotics, where the environment being modeled is continuously changing, these operations must also be fast to allow a continuous update of the matching set, from which 3D information is extracted [1] [2]. The correspondence search in stereo images is commonly reduced to significant features as computing time is still an important criterion in stereo vision. There exist several stereo vision techniques, from which

the most popular are the Area-based and the Feature-based stereo techniques. The first kind of the mentioned techniques finds corresponding points based on the correlation between the corresponding areas in left and right images [3]. First, a point of interest is chosen in one of the images. A correlation measure is then applied to search for a corresponding point with a matching neighborhood in the other image. Area-based techniques have the disadvantage of being sensitive to photometric variations during the image acquisition process and are sensitive to distortions, which reason in the first place is the changing viewing position. Feature-based stereo techniques, on the other hand, match features in the left image to those in the right image. Features are selected as the most prominent parts in the image, such as, for example, edge points or edge segments, corner points etc. Feature-based techniques have the advantage of being less sensitive to photometric variations and of being faster than the area-based stereo method, because there are fewer candidates for matching corresponding points [4]. If we combine the Area-based stereo techniques with the Feature-based stereo techniques we can get better results. In this paper a new approach of feature points correspondence matching is presented. The paper is organized as follows: In Section 2 the preprocessing phase of the input pictures is detailed, Section 3 shows how to find edge and corner points, while Section 4 presents the matching algorithm of these feature points. In Section 5 experimental results are summarized and Section 6 is devoted to the conclusions.

2 Preprocessing of the Images, Noise Elimination

A major task in the field of digital processing of measurement signals is to extract information from sensor data corrupted by noise [5] [6]. For this purpose we will use a special fuzzy system characterized by an IF-THEN-ELSE structure and a specific inference mechanism. Different noise statistics can be addressed by adopting different combinations of fuzzy sets and rules [5] [6]. Let $x(\mathbf{r})$ be the pixel luminance at location $\mathbf{r}=[r_1,r_2]$ in the noisy image where r_1 is the horizontal and r_2 the vertical coordinate of the pixel. Let $\mathbf{N}$ be the set of eight neighboring pixels (see Fig. 1a). The input variables of the fuzzy filter are the amplitude differences defined by:

$$\Delta x_j = x_j - x_0, j = 1,...,8 \tag{1}$$

where the x_j, j=1,…,8 values are the neighboring pixels of the actually processed pixel x_0 (see Fig. 1a).

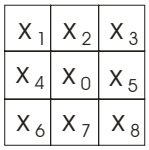

Figure 1a
The neighboring pixels of the actually processed pixel x_0

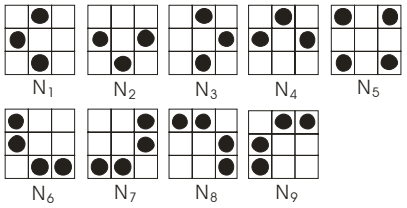

Figure 1b
Pixel patterns $N_1,...,N_9 \subseteq N$

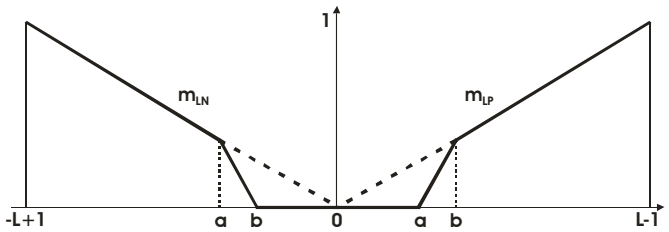

Figure 2
Membership function m_{LP}. Parameters *a* and *b* are appropriate constant values

Let y_0 be the luminance of the pixel having the same position as x_0 in the output signal. This value is determined by the following relationship:

$$y_0 = x_0 + \Delta y \tag{2}$$

where Δy is calculated thereinafter (see eq. (5)). Let the rule-base deal with the pixel patterns $N_1,...,N_9 \subseteq N$ (see Fig. 1b).

The value y_0 can be calculated, as follows [7]:

$$\lambda = MAX\left\{MIN\left\{m_{LP}(\Delta x_j) : x_j \in N_i\right\}, i = 1,...,9\right\} \tag{3}$$

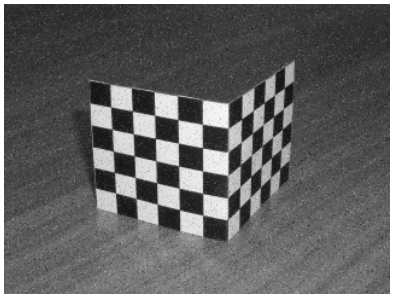

3a

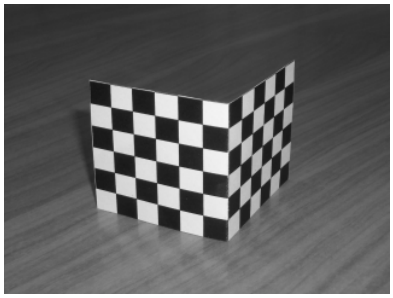

3b

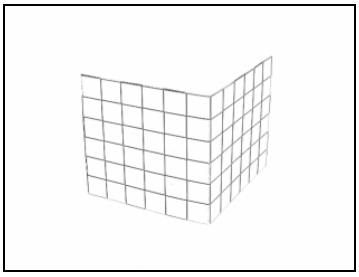

3c

Figure 3a represents the image corrupted by impulse noise, 3b shows the image after fuzzy filtering and in figure 3c the image after the fuzzy based edge detection can be followed

$$\lambda^* = MAX\left\{MIN\left\{m_{LN}(\Delta x_j) : x_j \in N_i\right\}; i = 1,...,9\right\} \tag{4}$$

$$\begin{aligned} \Delta y &= (L-1)\Delta\lambda \\ y_0 &= x_0 + \Delta y \end{aligned} \tag{5}$$

where $\Delta\lambda=\lambda-\lambda^*$, m_{LP} and m_{LN} correspond to the membership functions of fuzzy sets large positive and large negative and $m_{LP}(u)=m_{LN}(-u)$ (see Fig. 2). The filter is recursively applied to the input data. Using this fuzzy filter the impulse noise can effectively be eliminated. With the help of the parameters a, b the sensitivity of the noise elimination method can be modified, i.e., the shape of the membership functions m_{LN} and m_{LP} can be tuned. If after the noise cancellation noisy image points will remain in the image, they will also be detected as corner points in the next step (see Section 3) and therefore it is very advisable to eliminate them as effectively as possible. Otherwise, for example at one hand, at automatic 3D reconstruction of a scene these non eliminated noisy pixels will appear in the 3D space, as well and on the other hand, the efficiency of the point correspondence matching algorithms will brake down with the number of non-eliminated noisy pixels.

3 Detection of Feature Points

Edge detection in an image is a very important step for a complete image understanding system. In fact, edges correspond to object boundaries and are therefore useful inputs for 3D reconstruction algorithms. The proposed fuzzy based edge detection [7] can very advantageously be used for this purpose.

Let $x_{i,j}$ be the pixel luminance at location $[i,j]$ in the input image. Let us consider the group of neighboring pixels which belong to a 3x3 window centered on $x_{i,j}$ (see Fig. 1a). The output of the edge detector is yielded by the following equation [7]:

$$\begin{aligned} z_{i,j} &= (L-1)MAX\{m_{LA}(\Delta y_1), m_{LA}(\Delta y_2)\} \\ \Delta y_1 &= \left| x_{i-1,j} - x_{i,j} \right| \\ \Delta y_2 &= \left| x_{i,j-1} - x_{i,j} \right| \end{aligned} \tag{6}$$

where $z_{i,j}$ is the pixel luminance in the output image and m_{LA} is the used membership function (see Fig. 4). Pixels $x_{i\text{-}1,j}$ and $x_{i,j\text{-}1}$ are the luminance values of the left and the upper neighbors of the pixel at location $[i,j]$.

The fuzzy based technique compared to the classical methods provided better results with less (very small) processing time. Fig. 3 shows an example for the filtering and edge detection results. In Fig. 3a the original photo corrupted by noise can be seen, Fig. 3b presents the filtered image of Fig. 3a, while in Fig. 3c the result of the edge detection can be followed.

Corners are also local image features and are very useful at the 3D reconstruction of a scene. Using these feature points the processing time of the reconstruction of a scene can be reduced.

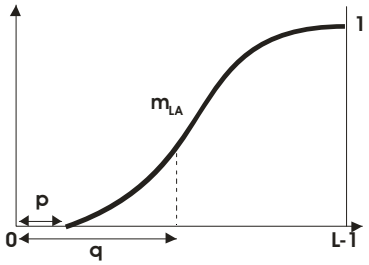

Figure 4

Membership function m_{LA}. Parameters p and q are appropriate constant values with the help of which the membership function m_{LA} can be shaped. Parameter q is for changing the curvature of the membership function and p is for setting the sensitivity of the proposed edge detector

Any corner detection algorithm should satisfy the following requirements:

- All the true corners should be detected
- No false corners should be detected
- Corner points should be well localized
- Corner detector should be robust with respect to noise

Förstner determines corners as local maxima of function $H(x,y)$ [8]:

$$H(x,y)=\frac{\left(\frac{\partial I}{\partial x}\right)^2\left(\frac{\partial I}{\partial y}\right)^2-\left(\frac{\partial I}{\partial x}\frac{\partial I}{\partial y}\right)^2}{\left(\frac{\partial I}{\partial x}\right)^2+\left(\frac{\partial I}{\partial y}\right)^2}, \tag{7}$$

where $I(x,y)$ is the intensity function and x, y are the coordinates of the pixels in the image. Starting from the algorithm of Förstner a new, improved corner detection algorithm can be developed by combining it with fuzzy reasoning. This can be used for the characterization of the continuous transition between the localized and not localized corner points, as well. The algorithm consists of the following steps: First, the picture, in which we have to find the corners, is preprocessed. As a result of the preprocessing procedure the noise is eliminated. For this purpose we apply the above described fuzzy filter [5] [6]. After noise-filtering, the first derivatives of the intensity function $I(x, y)$ are calculated in each image point. This is solved by using the following convolution masks:

$\begin{bmatrix}-1 & 0 & 1\\ -1 & 0 & 1\\ -1 & 0 & 1\end{bmatrix}$ for the determination of $\frac{\partial I}{\partial x}$ and

$\begin{bmatrix}-1 & -1 & -1\\ 0 & 0 & 0\\ 1 & 1 & 1\end{bmatrix}$ for determining $\frac{\partial I}{\partial y}$.

Table 1
Comparison some of corner detectors with fuzzy based one

	Correctly detected corners [%]	Incorrectly detected points [%]	Non detected points [%]
Fuzzy based corner detector	84	3,2	16
SUSAN corner detector	52	4,7	48
Harris corner detector k=0.001	71	15,3	29

For increasing the effectiveness of the corner detection it is proposed to smooth the entries I_x^2, I_y^2, I_xI_y, in eq. (7), (I_x and I_y stand for the first partial derivatives of the intensity function $I(x,y)$, x,y denote the 2D coordinates of the pixels). This can be done by applying a Gaussian 6x6 convolution kernel with σ=1 [8]. As the following step, the values $H(x,y)$ are calculated for each image point with the help of the previously determined smoothed I_x^2, I_y^2, and I_xI_y values. If the detected corners are neighbors, we should keep only the corner having the largest calculated value $H(x,y)$. The others are to be ignored. In most of the cases we can not unambiguously determine whether the analyzed image point is a corner or not based only on a certain concrete threshold value, therefore we have introduced fuzzy techniques in the inference of the proposed corner detection algorithm. As a result, the rate of the corner detection has been improved (see Table 1). By the score of the membership function of fuzzy set "corners" (see Fig. 5) we can determine a weighting factor, which characterizes "the rate of being a corner". The value of the membership function m_c is 1 for those image points for which the calculated value H equals or is larger than the given threshold value. With the help of the parameters p and q (see Fig. 5) the shape of the membership function can be modified and so the sensitivity of the described detector can be changed. Finally, the output of the proposed corner detector is yielded by the following relation:

$$C_{x,y} = (L-1)m_c(H), \tag{8}$$

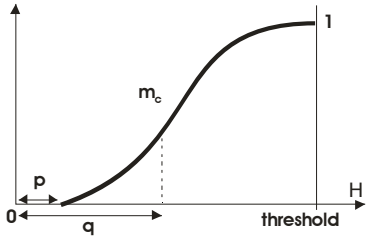

Figure 5

Membership function of fuzzy set "corners" (m_c). Axis H is the axis of the calculated $H(x,y)$ values. Parameters p and q are appropriate constant values with the help of which we membership function m_c can be shaped: parameter q is for changing the curvature of the membership function and p is for setting the sensitivity of the proposed corner detector.

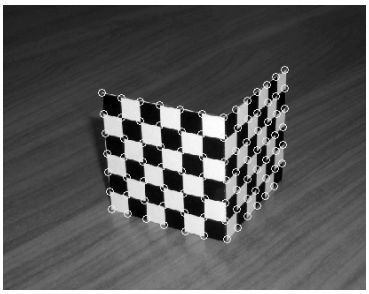

Figure 6

The image after fuzzy based corner detection. The circles indicate the detected corners.

where $C_{x,y}$ represents the gray-level intensity values of the output image, x and y are the horizontal and vertical coordinates of the processed image point, L is the largest gray level intensity value, and H stands for the calculated $H(x,y)$ values.

4 Matching the Corresponding Feature Points in Stereo Images

Feature matching is commonly referred to as the correspondence problem. The problem is how to automatically match corresponding features from two images, while at the same time not assigning matches incorrectly. The common approach for corners, is to take a small region of pixels around the detected corner (referred to as a correlation window) and compare this with a similar region around each of the candidate corners in the other image. Each comparison yields a score, a measure of similarity. The match is assigned to the corner with the highest matching score. The most popular measure of similarity is the cross-correlation. Most matching algorithms include constraints to complement the similarity measure. These may take the form of constraints on which corners are selected as candidate matches: a maximum disparity, or corners which agree with some known relationship between the images (such as the epipolar geometry). Constraints such as uniqueness or continuity may also be applied after candidate matches have been found. With the help of the epipolar constraint we can reduce the number of candidate image points. We have to search only along the epipolar line corresponding to the actually chosen image point in the source image. This epipolar line can be determined using the so called fundamental matrix [2]. The fundamental matrix defines a bilinear constraint between the coordinates of the corresponding image points. If for example $\mathbf{m_2}$ is the point in the second image

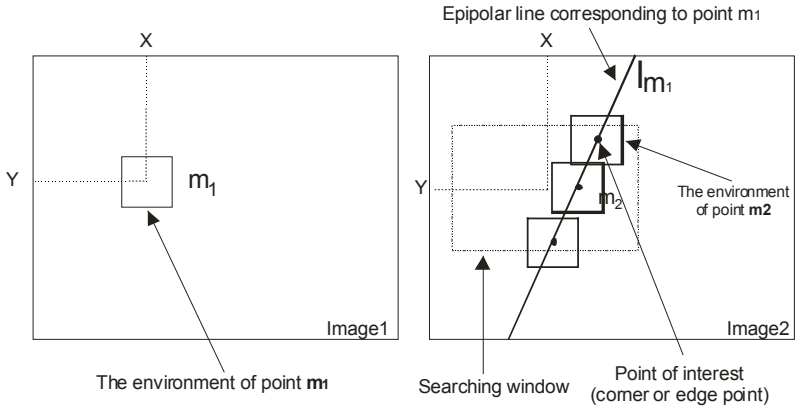

Figure 7
Illustration of the proposed point matching technique. In the left image a chosen corner is illustrated, while in the right image the candidate corner points can be seen.

corresponding to $\mathbf{m_1}$ (see Fig. 7), it must lie on the epipolar line $\mathbf{l_{m1}}$. The epipolar constraint can be written as:

$$\mathbf{m}_2^T \mathbf{F} \mathbf{m}_1 = 0 \tag{9}$$

Linear Solution for the Fundamental Matrix:

Each point match gives rise to one linear equation in the unknown entries of matrix **F**. The coefficients of this equation can easily be written in terms of the known coordinates of $\mathbf{m_1}$ and $\mathbf{m_2}$. Specifically, the equation corresponding to a pair of points $\mathbf{m_1}$ and $\mathbf{m_2}$ will be

$$\begin{aligned} &xx'f_{11} + xy'f_{12} + xf_{13} + yx'f_{21} + \\ &yy'f_{22} + yf_{23} + x'f_{31} + y'f_{32} + f_{33} = 0 \end{aligned} \tag{10}$$

where the coordinates of $\mathbf{m_1}$ and $\mathbf{m_2}$ are $(x, y, 1)^t$ and $(x',y',1)^t$, respectively. Combining the equations obtained for each match gives a linear system that can be written as $\mathbf{Aw} = \mathbf{0}$, where **w** is a vector containing the 9 coefficients of **F** (f_{ij}) and each row of **A** is built of the coordinates $\mathbf{m_1}$ and $\mathbf{m_2}$ of a single match. Since **F** is defined only up to an overall scale factor, we can restrict the solution for **w** to have norm 1. We usually have more than the minimum number (8) of points, but these are perturbed by noise so we will look for a least squares solution:

$$\min_{\|\mathbf{w}\|=1} \|\mathbf{Aw}\|^2 \tag{11}$$

As $\|\mathbf{Aw}\|^2 = \mathbf{w}^T \mathbf{A}^T \mathbf{Aw}$, we have to find the eigenvector associated with the smallest eigenvalue of the 9x9 symmetric, positive semidefinite normal matrix $\mathbf{A^T A}$. However, this formulation does not enforce the rank constraint, so a second step must be added to the computation to project the solution **F** onto the rank 2 subspace. This can be done by taking the Singular Value Decomposition (SVD) of matrix **F** and setting the smallest singular value to zero. Basically, SVD decomposes any real valued matrix **F** in the form of

$$\mathbf{F} = \mathbf{Q}\,\mathbf{D}\,\mathbf{R} \tag{12}$$

where **D** is diagonal and **Q** and **R** are orthogonal matrices. Setting the smallest diagonal element of **D** to 0 and reconstituting gives the desired result.

As we know, the images in which we have to find the corresponding feature points are taken from different camera positions. If the angle of the camera positions is relatively small, we have greater chance to match the mentioned feature points, because of the small deformation of image pixels between two views. In this case the corresponding points can be found with high reliability in each image. Feature point mentioned in this section can be either corners or edge points. Matches are found by evaluating the similarity between image regions and selecting the match of the pair of regions with the highest similarity (see Fig. 7). There are many

similarity measure definitions known in the literature [10]. In this paper, we introduce a new measure of similarity which is based on the combination of cross-correlation and a fuzzy measure:

$$M_s = \frac{\sum F_m(x,y) I_L(x,y) I_R(x,y)}{\sum F_m(x,y) I_L(x,y)^2 \sum F_m(x,y) I_R(x,y)^2}, \tag{13}$$

where I_L and I_R are the intensity functions of the input images (left and right image) and F_m stands for the fuzzy measure corresponding to the pixel with coordinates x,y. F_m can be calculated, as follows:

$$F_m(x,y) = MIN\{\mu_A(x), \mu_B(y)\}, \tag{14}$$

μ_A and μ_B are the membership functions in universes X and Y representing the closeness of the points in the environment to the analyzed corner point-candidate (see Fig. 8).

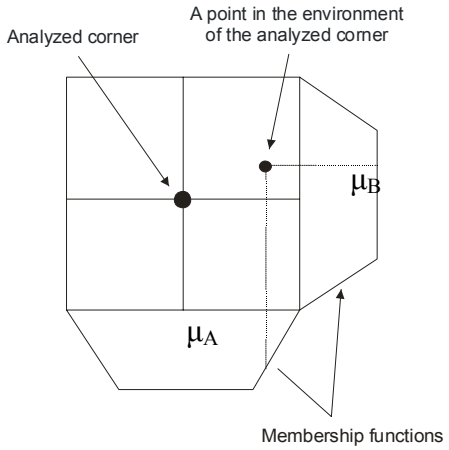

Figure 8
Fuzzy membership functions μ_A and μ_B of closeness used in eqs. 13, 14

5 Experimental Results

Fig. 9 represents two overlapped images, taken form two different camera positions. In the image the point correspondence is illustrated with the help of lines joining the corresponding image points. The end points of the lines represent the corresponding feature points of the overlapped images.

Figure 9
The two images in overlapped form with the corresponding feature points

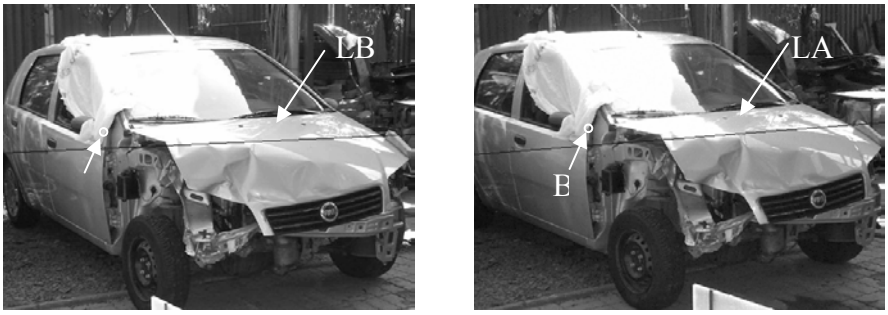

(a) (b)

Figure 10
The epipolar lines and an example of two corresponding feature points

Fig. 10a and Fig. 10b illustrate two images taken from different camera positions. On each of them an epipolar line corresponding to the pointed image pixel can be followed. To the image point *A* corresponds the epipolar line *LA* and to the image point *B* correspond the epipolar line *LB*. The corresponding image point of *A* is the image point *B* and inversely the point which corresponds to *B* is the image point *A*.

Conclusions

This paper introduces a new fuzzy based method for the matching of corresponding feature points in images, which are taken of the same scene from different camera positions. The method uses fuzzy based noise elimination and feature detection algorithms, with the help of which we can eliminate the non interesting points from the images and detect those feature points, which are the most interesting from the 3D reconstruction point of view. The method combines the area based and the feature based stereo techniques and applies fuzzy reasoning for the determination of a similarity measure, with the help of which we can decide which feature points can be the best candidates of being the corresponding

points. The method introduced in this paper can advantageously be used in many other fields, as well, e.g. in robot guiding, medicine, and 3D object reconstruction.

Acknowledgement

This work was sponsored by the Hungarian Fund for Scientific Research (OTKA T035190 and T049519) and the Hungarian-Portuguese Intergovernmental S&T Cooperation Programme (P-24/03).

References

[1] Zhang, Z., Deriche, R., Faugeras, O., Luong, Q.-T., "A Robust Technique for Matching Two Uncalibrated Images Through the Recovery of the Unknown Epipolar Geometry," *Artificial Intelligence*, 1995, pp. 87-119

[2] Rövid, A., A. R. Várkonyi-Kóczy, Várlaki, P., "3D Model Estimation from Multiple Images," *IEEE International Conference on Fuzzy Systems, FUZZ-IEEE'2004*, July 25-29, 2004, Budapest, Hungary, pp. 1661-1666

[3] Faugeras, O., Vieville, T., Theron, E., Vuillemin, J., Hotz, B., Zhang, Z., Moll, L., Bertin, P., Mathieu, H., Fua, P., Berry, G., Proy, C., "Real time correlation-based stereo: algorithm, implementations and applications," *Research Report 2013*, INRIA Sophia-Antipolis, France, August 1993, p. 45.

[4] Lee, C.-Y., Cooper, D. B., and Keren, D., "Computing Correspondence Based on Region and Invariants without Feature Extraction and Segmentation," *Proc. CVPR'93*, New York, USA, 1993, pp. 655-656

[5] Russo, F., "Fuzzy Filtering of Noisy Sensor Data," *In Proc. of the IEEE Instrumentation and Measurement Technology Conference*, Brussels, Belgium, 4-6 June 1996, pp. 1281-1285

[6] Russo, F., "Recent Advances in Fuzzy Techniques for Image Enhancement," *IEEE Transactions on Instrumentation and Measurement*, Vol. 47, No. 6, Dec. 1998, pp. 1428-1434

[7] Russo, F., "Edge Detection in Noisy Images Using Fuzzy Reasoning," *IEEE Transactions on Instrumentation and Measurement*, Vol. 47, No. 5, Oct. 1998, pp. 1102-1105

[8] Förstner W., "A feature based correspondence algorithm for image matching," *Int. Arch. Photogramm. Remote Sensing*, vol. 26, 1986, pp. 150-166

[9] Catté, F., Lions, P.-L., Morel, J.-M., Coll, T., "Image selective smoothing and edge detection by nonlinear diffusion," *SIAM Journal on Numerical Analysis*, 32:, 1992, pp. 1895-1909

[10] Bogdan, G., Meer, P., "Point Matching under Large Image Deformations and Illumination Changes*," IEEE Transactions on Pattern Analysis and Machine Intelligence*, VOL. 26, NO. 6, JUNE 2004, pp. 674-688

Approximation of the Continuous Nilpotent Operator Class

József Dombi, Zsolt Gera

University of Szeged, Institute of Informatics
E-mail: {dombi | gera}@inf.u-szeged.hu

Abstract: In this paper we propose an approximation of the class of continuous nilpotent operators. The proof is based on one hand the approximation of the cut function, and on the other hand the representation theorem of operators with zero divisors. The approximation is based on sigmoid functions which are found to be useful in machine intelligence and other areas, too. The continuous nilpotent class of operators play an important role in fuzzy logic due to their good theoretical properties. Besides them this operator family does not have a continuous gradient. The main motivation was to have a simple and continuously differentiable approximation which ensures good properties for the operator.

Keywords: nilpotent operators, sigmoid function, approximation

1 Introduction

The nilpotent operator class (see e.g. [1], [2], [3]) is commonly used for various purposes. In the following we will consider only the continuous nilpotent operators. In this well known operator family the cut function (denoted by [□]) plays a central role. We can get the cut function from x by taking the maximum of 0 and x and then taking the minimum of the result and 1. One can relax the restrictions of 0 and 1 to get the concept of the generalized cut function.

Definition 1 *Let the **cut function** be*

$$\left[x\right] = \min(1, \max(0, x)) = \begin{cases} 0 & \text{if } x < 0 \\ x & \text{if } 0 \le x \le 1 \\ 1 & \text{if } 1 < \text{x} \end{cases} \tag{1}$$

*Let the **generalized cut function** be*

$$[x]_{a,b} = [(x-a)/(b-a)] = \begin{cases} 0 & \text{if } x < a \\ (x-a)/(b-a) & \text{if } a \le x \le b \\ 1 & \text{if } b < x \end{cases} \qquad (2)$$

where $a,b \in R$ *and* $a < b$.

Remark. We will use [·] for parentheses, too, e.g. f [x] means f ([x]).

As it can be seen from the representation theorem of the nilpotent class, which we will show later, all nilpotent operators are constructed using the cut function. The formulas of the Lukasiewicz conjunction, disjunction, implication and negation are the following:

$$\begin{aligned} c(x,y) &= [x+y-1] \\ d(x,y) &= [x+y] \\ i(x,y) &= [y-x+1] \\ n(x) &= 1-x \end{aligned} \qquad (3)$$

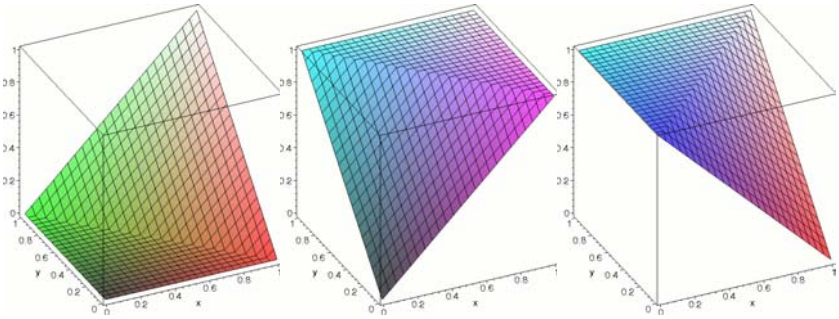

Figure 1
The truth tables of the Lukasiewicz conjunction, disjunction and implication

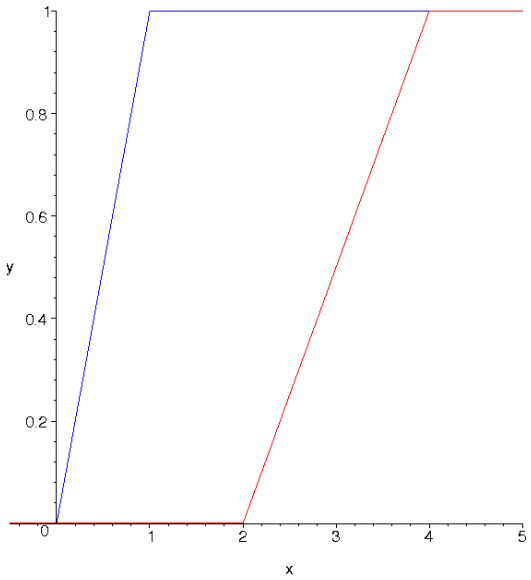

Figure 2
Two generalized cut functions

The truth tables of the former three can be seen on figure 1. The Lukasiewicz operator family used above has good theoretical properties. These are: the law of non-contradiction (that is the conjunction of a variable and its negation is always zero) and the law of excluded middle (that is the disjunction of a variable and its negation is always one) both hold, and the residual and material implications coincide. These properties make these operators to be widely used in fuzzy logic and to be the closest one to classic Boolean logic. Besides these good theoretical properties this operator family does not have a continuous gradient. So for example gradient based optimization techniques are impossible with Lukasiewicz operators. The root of this problem is the shape of the cut function itself.

2 Approximation of the Cut Function

A solution to above mentioned problem is a continuously differentiable approximation of the cut function, which can be seen on figure 3. In this section we'll construct such an approximating function by means of sigmoid functions. The reason for choosing the sigmoid function was that this function has a very important role in many areas. It is frequently used in artificial neural networks, optimization methods, economical and biological models.

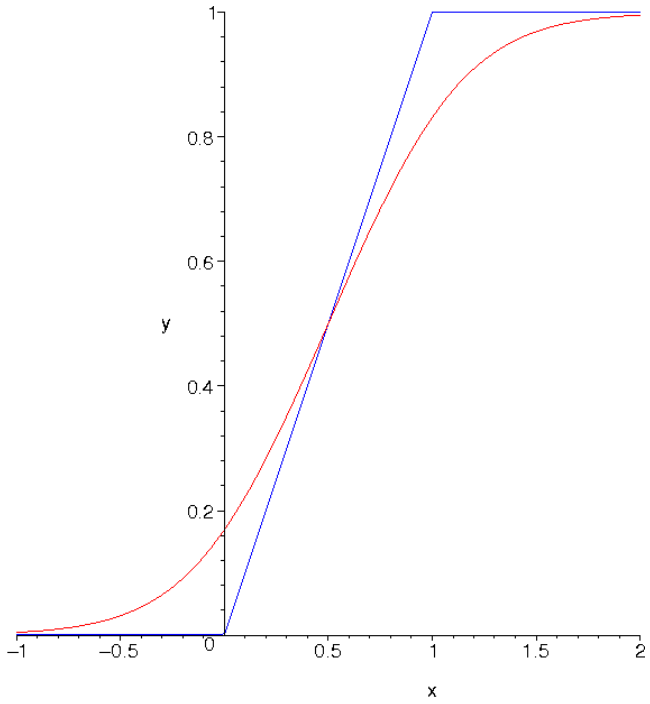

Figure 3
The cut function and its approximation

2.1 The Sigmoid Function

The sigmoid function (see figure 4) is defined as

$$\sigma_d^{(\beta)}(x) = \frac{1}{1+e^{-\beta(x-d)}} \tag{4}$$

where the lower index d is omitted if 0.

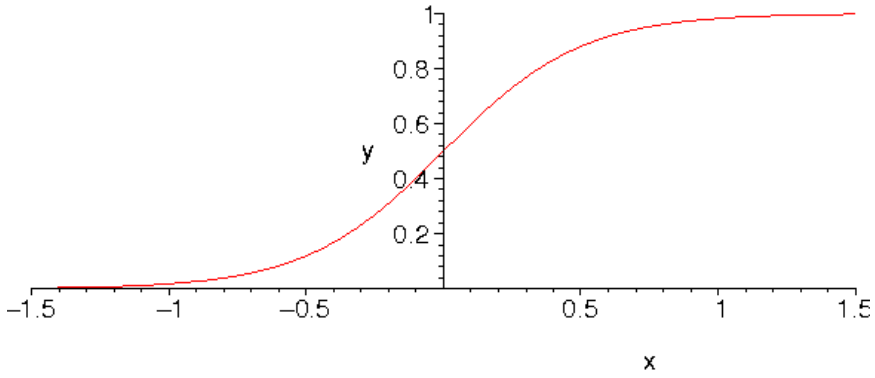

Figure 4
The sigmoid function with parameters d=0 and β=4

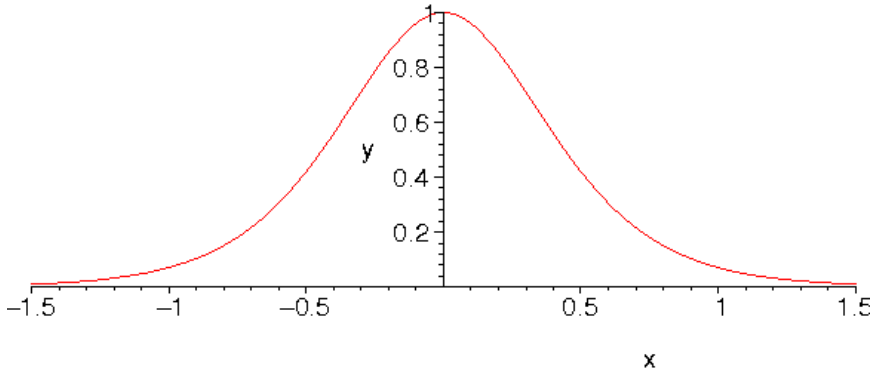

Figure 5
The first derivative of the sigmoid function

Let us examine some of its properties which will be useful later:

- its derivative can be expressed by itself (see figure 5):

$$\frac{\partial \sigma_d^{(\beta)}(x)}{\partial x} = \beta \sigma_d^{(\beta)}(x) \sigma_d^{(-\beta)}(x), \tag{5}$$

- its integral has the following form:

$$\int \sigma_d^{(\beta)}(x)\, dx = -\frac{1}{\beta} \ln \sigma_d^{(-\beta)}(x). \tag{6}$$

Because the sigmoid function is asymptotically 1 as x tends to infinity, the integral of the sigmoid function is asymptotically x (see figure 6).

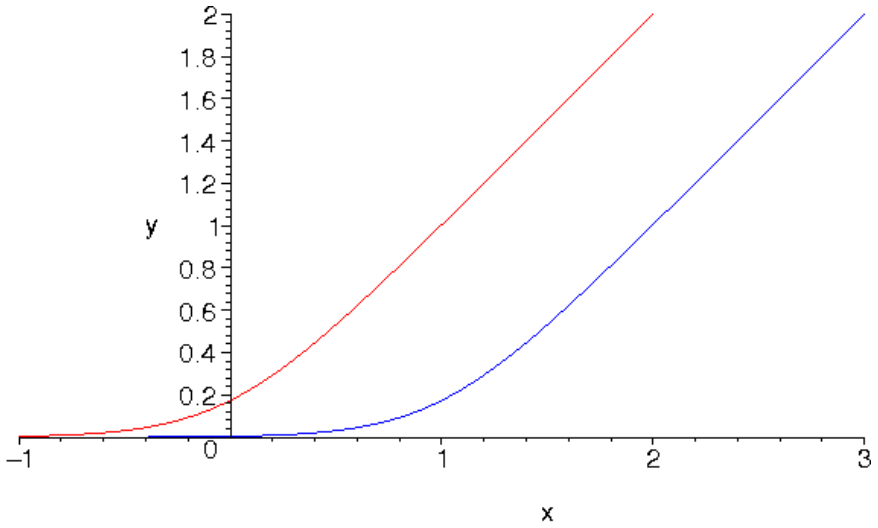

Figure 6
The integral of the sigmoid function, one is shifted by 1

2.2 The Squashing Function on the Interval [a,b]

In order to get an approximation of the generalized cut function, let us integrate the difference of two sigmoid functions, which are translated by a and b ($a < b$), respectively.

$$\frac{1}{b-a}\int \sigma_a^{(\beta)}(x)-\sigma_b^{(\beta)}(x)\,dx=\frac{1}{b-a}\left(\int \sigma_a^{(\beta)}(x)\,dx-\int \sigma_b^{(\beta)}(x)\,dx\right)=$$

$$=\frac{1}{b-a}\left(-\frac{1}{\beta}\ln\sigma_a^{(-\beta)}(x)+\frac{1}{\beta}\ln\sigma_b^{(-\beta)}(x)\right) \qquad (7)$$

After simplification we get the squashing function on the interval $[a,b]$:

Definition 2 *Let the* ***interval squashing function*** *on [a,b] be*

$$S_{a,b}^{(\beta)}(x)=\frac{1}{b-a}\ln\left(\frac{\sigma_b^{(-\beta)}(x)}{\sigma_a^{(-\beta)}(x)}\right)^{1/\beta}=\frac{1}{b-a}\ln\left(\frac{1+e^{\beta(x-a)}}{1+e^{\beta(x-b)}}\right)^{1/\beta}. \qquad (8)$$

The parameters a and b affect the placement of the interval squashing function, while the β parameter drives the precision of the approximation. We need to prove that $S_{a,b}^{(\beta)}(x)$ is really an approximation of the generalized cut function.

Theorem 3 *Let $a,b\in R$, $a < b$ and $\beta\in R^+$. Then*

$$\lim_{\beta\to\infty} S_{a,b}^{(\beta)}(x) = [x]_{a,b} \tag{9}$$

and $S_{a,b}^{(\beta)}(x)$ *is continuous in x, a, b and β.*

Proof. It is easy to see the continuity because $S_{a,b}^{(\beta)}(x)$ is a simple composition of continuous functions and because the sigmoid function has a range of [0,1] the quotient is always positive.

In proving the limit we separate three cases, depending on the relation between *a*,*b* and *x*.

- Case 1 ($x < a < b$): Since $\beta(x-a) < 0$, so $e^{\beta(x-a)} \to 0$ and similarly $e^{\beta(x-b)} \to 0$. Hence the quotient converges to 1 if $\beta \to \infty$, and the logarithm of one is zero.
- Case 2 ($a \le x \le b$):

$$\frac{1}{b-a}\ln\left(\lim_{\beta\to\infty}\left(\frac{1+e^{\beta(x-a)}}{1+e^{\beta(x-b)}}\right)^{1/\beta}\right) =$$

$$= \frac{1}{b-a}\ln\left(\lim_{\beta\to\infty}\left(\frac{e^{\beta(x-a)}(e^{-\beta(x-a)}+1)}{1+e^{\beta(x-b)}}\right)^{1/\beta}\right) =$$

$$= \frac{1}{b-a}\ln\left(\lim_{\beta\to\infty}\frac{e^{x-a}(e^{-\beta(x-a)}+1)^{1/\beta}}{(1+e^{\beta(x-b)})^{1/\beta}}\right) =$$

$$= \frac{1}{b-a}\ln\left(e^{x-a}\lim_{\beta\to\infty}\frac{(e^{-\beta(x-a)}+1)^{1/\beta}}{(1+e^{\beta(x-b)})^{1/\beta}}\right). \tag{10}$$

We transform the nominator so that we can take the e^{x-a} out of the limes. In the nominator $e^{-\beta(x-a)}$ remained which converges to 0 as well as $e^{\beta(x-b)}$ in the denominator so the quotient converges to 1 if $\beta \to \infty$. So as the result, the limit of the interval squashing function is $(x-a)/(b-a)$, which by definition equals to the generalized cut function in this case.

- Case 3 ($a < b < x$):

$$\frac{1}{b-a}\ln\left(\lim_{\beta\to\infty}\left(\frac{1+e^{\beta(x-a)}}{1+e^{\beta(x-b)}}\right)^{1/\beta}\right)=$$

$$=\frac{1}{b-a}\ln\left(\lim_{\beta\to\infty}\left(\frac{e^{\beta(x-a)}(e^{-\beta(x-a)}+1)}{e^{\beta(x-b)}(e^{-\beta(x-b)}+1)}\right)^{1/\beta}\right)=$$

$$=\frac{1}{b-a}\ln\left(\lim_{\beta\to\infty}\frac{e^{x-a}(e^{-\beta(x-a)}+1)^{1/\beta}}{e^{x-a}(e^{-\beta(x-b)}+1)^{1/\beta}}\right)=$$

$$=\frac{1}{b-a}\ln\left(\frac{e^{x-a}}{e^{x-b}}\lim_{\beta\to\infty}\frac{(e^{-\beta(x-a)}+1)^{1/\beta}}{(e^{-\beta(x-b)}+1)^{1/\beta}}\right). \qquad (11)$$

We do the same transformations as in the previous case but we take e^{x-b} from the denominator, too. After these transformations the remaining quotient converges to 1, so

$$\lim_{\beta\to\infty}S_{a,b}^{(\beta)}(x)=\frac{1}{b-a}\ln\left(\frac{e^{x-a}}{e^{x-b}}\right)=\frac{1}{b-a}\ln\left(e^{x-a-(x-b)}\right)=$$

$$=\frac{1}{b-a}\ln e^{b-a}=\frac{b-a}{b-a}=1. \qquad (12)$$

■

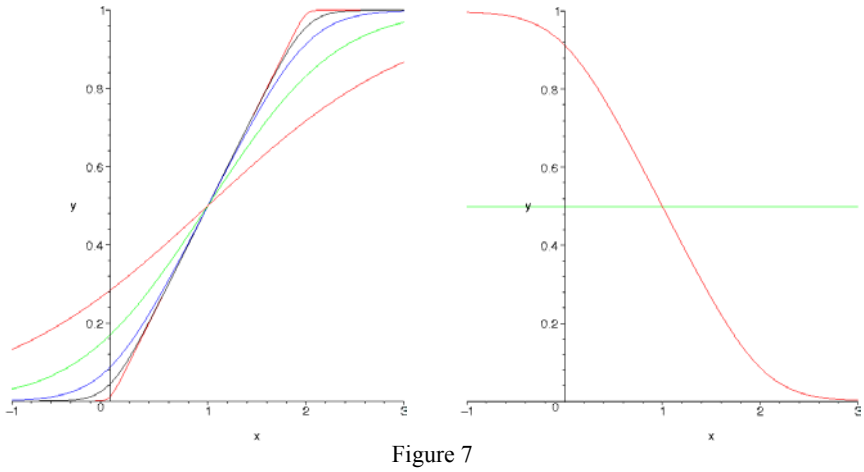

Figure 7
On the left image: the interval squashing function with an increasing β parameter (a=0 and b=2). On the right image: the interval squashing function with a zero and a negative β parameter

On figure 7 the interval squashing function can be seen with various β parameters. The following proposition states some properties of the interval squashing function.

Proposition 4

$$\lim_{\beta \to 0} S_{a,b}^{(\beta)}(x) = 1/2, \tag{13}$$

$$S_{a,b}^{(-\beta)}(x) = 1 - S_{a,b}^{(\beta)}(x). \tag{14}$$

As an another example, the Lukasiewicz conjunction is approximated with the interval squashing function on figure 8.

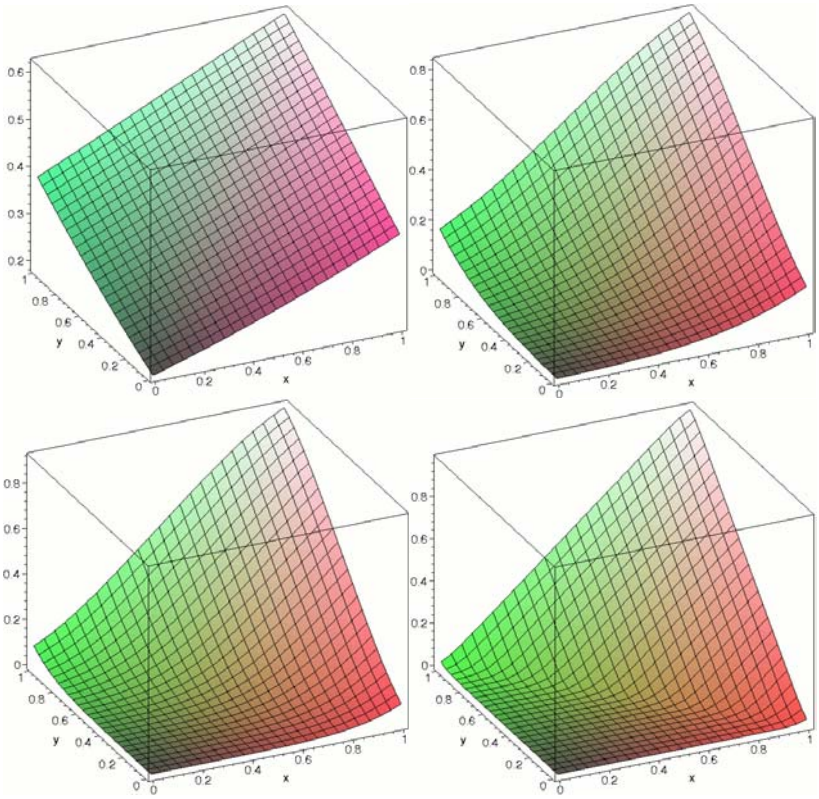

Figure 8
The approximation of the Lukasiewicz conjunction [x+y-1] with β values 1,2,8 and 32

For further use, let us introduce an another form of the interval squashing function's formula. Instead of using parameters *a* and *b* which were the "bounds" on the *x* axis, from now on we'll use *a* and δ, where *a* gives the center of the squashing function and where δ gives its steepness. Together with the new

formula we introduce its pliant notation.

Definition 5 *Let the* ***squashing function*** *be*

$$\left\langle a <_{\delta} x \right\rangle_{\beta} = S_{a,\delta}^{(\beta)}(x) = \frac{1}{2\delta} \ln \left(\frac{\sigma_{a+\delta}^{(-\beta)}(x)}{\sigma_{a-\delta}^{(-\beta)}(x)} \right)^{1/\beta}, \tag{15}$$

where $a \in R$ *and* $\delta \in R^{+}$.

If the a and δ *parameters are both 1/2 we will use the following pliant notation for simplicity:*

$$\left\langle x \right\rangle_{\beta} = S_{1/2,1/2}^{(\beta)}(x), \tag{16}$$

which is the approximation of the cut function.

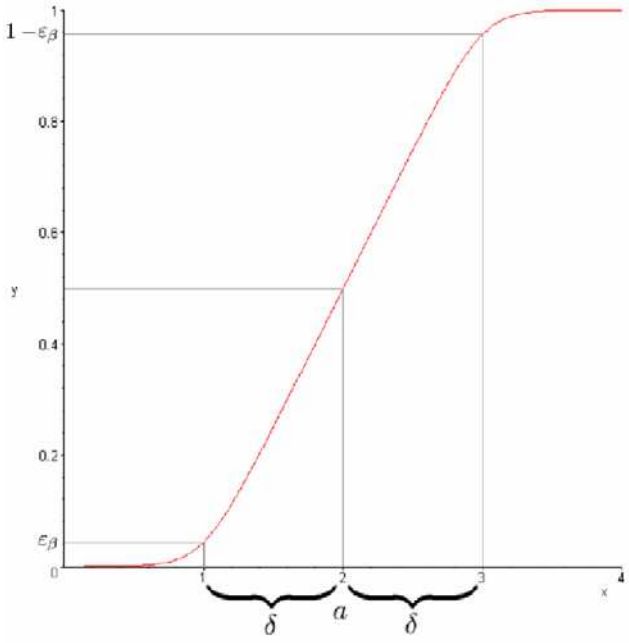

Figure 9

The meaning of $\left\langle a <_{\delta} x \right\rangle_{\beta}$

The inequality relation in the pliant notation refers to the fact that the squashing function can be interpreted as the truthness of the relation $a < x$ with decision level 1/2, according to a fuzziness parameter δ and an approximation parameter β (see figure 9).

The derivatives of the squashing function can be expressed by itself and sigmoid

functions:

$$\frac{\partial S_{a,\delta}^{(\beta)}(x)}{\partial x} = \frac{1}{2\delta}\left(\sigma_{a-\delta}^{(\beta)}(x) - \sigma_{a+\delta}^{(\beta)}(x)\right), \tag{17}$$

$$\frac{\partial S_{a,\delta}^{(\beta)}(x)}{\partial a} = \frac{1}{2\delta}\left(\sigma_{a+\delta}^{(\beta)}(x) - \sigma_{a-\delta}^{(\beta)}(x)\right), \tag{18}$$

$$\frac{\partial S_{a,\delta}^{(\beta)}(x)}{\partial \delta} = \frac{1}{2\delta}\left(\sigma_{a+\delta}^{(\beta)}(x) + \sigma_{a-\delta}^{(\beta)}(x)\right) + \frac{1}{\delta} S_{a,\delta}^{(\beta)}(x). \tag{19}$$

2.3 The Error of the Approximation

The squashing function approximates the cut function with an error. This error can be defined in many ways. We have chosen the following definition.

Definition 6 *Let the approximation error of the squashing function be*

$$\varepsilon_\beta = \left\langle 0 <_\delta (-\delta) \right\rangle = \frac{1}{2\delta} \ln\left(\frac{\sigma_{\delta}^{(-\beta)}(-\delta)}{\sigma_{-\delta}^{(-\beta)}(-\delta)} \right)^{1/\beta} \tag{20}$$

where $\beta > 0$.

Because of the symmetry of the squashing function $\varepsilon_\beta = 1 - \left\langle 0 <_\delta \delta \right\rangle$, see figure 9.

The purpose of measuring the approximation error is the following inverse problem: we want to get the corresponding β parameter for a desired ε_β error. We state the following lemma on the relationship between ε_β and β.

Lemma 7 *Let us fix the value of δ. The following holds for e_b.*

$$\varepsilon_\beta < c \cdot \frac{1}{\beta}, \tag{21}$$

where $c = \dfrac{\ln 2}{2\delta}$ *is constant.*

Proof. $\varepsilon_\beta = \dfrac{1}{2\delta\beta} \ln\left(\dfrac{1 + e^{\beta(-\delta+\delta)}}{1 + e^{\beta(-\delta-\delta)}} \right) = \dfrac{1}{2\delta\beta} \ln\left(\dfrac{2}{1 + e^{-2\delta\beta}} \right) =$

$$= \frac{\ln 2}{2\delta\beta} - \frac{\ln(1+e^{-2\delta\beta})}{2\delta\beta} < c \cdot \frac{1}{\beta} \tag{22}$$

So the error of the approximation can be upper bounded by $c \cdot \frac{1}{\beta}$, which means that by increasing parameter β, the error decreases by the same order of magnitude. ■

2.4 The Approximation of the Nilpotent Operator Class

The following theorems state that any continuous t-norm having zero divisors can be representated by the Lukasiewicz t-norm. In other words any nilpotent t-norm can be constructed using the Lukasiewicz t-norm and an appropriate automorphism of the unit interval. By these theorems the approximation of the cut function and the Lukasiewicz t-norm can be extended to the approximation of the whole class of continuous nilpotent operators.

We give the theorems using a different notation as stated in [4], especially for the cut function. By using [·] in the expressions, both the t-norm and the t-conorm case can be notated in the same way. The following lemma is needed for proving the theorems.

Lemma 8 *If c is a continuous t-norm such that c(x,n(x)) = 0 holds for all* $x \in [0,1]$ *with a strict negation n then c is Achimedean.*

Proof. Suppose that c is not Archimedean. That is, there exists $x \in (0,1)$ such that $c(x,x) = x$. If $x \le n(x)$ then $x = c(x,x) \le c(x,n(x)) = 0$, a contradiction since $x \in (0,1)$. If $x > n(x)$ then, since c is a continuous function, there exists $y \le x$ such that $n(x) = c(x,y)$. Then we have

$$n(x) = c(x,y) = c(c(x,x),y) = c(x,c(x,y)) = c(x,n(x)) = 0,$$

again a contradiction since $x \in (0,1)$. Thus our proposition is proved. ■

Theorem 9 *A continuous t-norm c is such that c(x,n(x))=0 holds for all* $x \in [0,1]$ *with a strict negation n if and only if there exists an automorphism* f *of the unit interval such that*

$$c(x,y) = f^{-1}\left[f(x) + f(y) - 1\right] \tag{23}$$

and

$$n(x) \le f^{-1}\left(1 - f(x)\right). \tag{24}$$

Proof. (Necessity) According to the previous proposition, c is Archimedean. Thus

there exists a generator f_c of c such that $c(x,y) = f_c^{(-1)}\left(f_c(x) + f_c(y)\right)$ (where $f_c^{(-1)}$ is the pseudoinverse of f_c) with $f_c(0) < \infty$. Define

$$f(x) = 1 - \frac{f_c(x)}{f_c(0)}. \tag{25}$$

Thus f is an automorphism of the unit interval. From (25) we have

$$f_c(x) = f_c(0) - f_c(0) f(x) \qquad \text{and} \qquad f_c^{(-1)}(x) = f^{-1}\left(1 - \frac{x}{f_c(0)}\right).$$

Using the above generator functional form of c(x,y) we can go on as

$$c(x,y) = f_c^{(-1)}\left(f_c(x) + f_c(y)\right) = f^{-1}\left[f_c(x) + f_c(y)\right] =$$

$$= f^{-1}\left(1 - \frac{\left[f_c(0) - f_c(0) f(x) + f_c(0) - f_c(0) f(y)\right]}{f_c(0)}\right) =$$

$$= f^{-1}\left[f(x) + f(y) - 1\right].$$

On the other hand, c(x,n(x)) = 0 is equivalent to $f(x) + f(n(x)) \le 1$, whence we obtain the inequality $n(x) \le f^{-1}\left(1 - f(x)\right)$.

Proof of sufficiency is immediate. ■

We give the theorem for t-conorms without proof since it is very similar to the above mentioned.

Theorem 10 *A continuous t-conorm d satisfies condition d(x,n(x))=1 for all* $x \in [0,1]$ *with a strict negation n if and only if there exists an automorphism* g *of the unit interval such that*

$$d(x,y) = g^{-1}\left[g(x) + g(y)\right] \tag{26}$$

and

$$n(x) \ge g^{-1}\left(1 - g(x)\right). \tag{27}$$

Using the above theorems we can state the following.

Theorem 11 *Every continuous nilpotent t-norm and t-conorm can be approximated by the squashing function in the following way:*

$$c(x,y) = f^{-1}\left\langle f(x) + f(y) - 1\right\rangle_{\beta} \tag{28}$$

$$d(x,y) = g^{-1}\left\langle g(x) + g(y)\right\rangle_{\beta} \tag{29}$$

Proof. Because $\left\langle x\right\rangle_{\beta}$ approximates [x] for all x if $\beta \to \infty$, the statement of the theorem is obvious from Theorem 9 and 10.

Conclusion

In this paper first we reviewed the cut function, which is the basis of the well known nilpotent operator class. This cut function is piecewise linear, hence it can not be continuously differentiated. We have constructed an approximation of the cut function (the squashing function) by means of sigmoid functions with good analytical properties, for example fast convergence and easy calculation. We have shown that all nilpotent operators can be approximated this way.

References

[1] R. Ackermann. *An Introduction to Many-Valued Logics*. Dover, New York, 1967

[2] P. Hájek. *Metamathematics of Fuzzy Logic*. Kluwer, 1998

[3] D. Mundici, R. Cignoli, I. M. L. D'Ottaviano. *Algebraic foundations of many-valued reasoning.* Trends in Logic, 7, 2000

[4] J. Fodor, M. Roubens. *Fuzzy Preference Modelling and Multicriteria Decision Support.* Theory and Decision Library. Kluwer, 1994

[5] J. Dombi, Zs. Gera. *The Approximation of Piecewise Linear Membership Functions and Lukasiewicz Operators.* Fuzzy Sets and Systems (manuscript, submitted for publication)

On additions of interactive fuzzy numbers

Christer Carlsson

IAMSR, Åbo Akademi University,
Lemminkäinengatan 14B, FIN-20520 Åbo, Finland
e-mail: christer.carlsson@abo.fi

Robert Fullér

Department of Operations Research, Eötvös Loránd University,
Pázmány Péter sétány 1C, H-1117 Budapest, Hungary
e-mail: rfuller@mail.abo.fi

Abstract: In this paper we will summarize some properties of the extended addition operator on fuzzy numbers, where the interactivity relation between fuzzy numbers is given by their joint possibility distribution.

1 Introduction

A fuzzy number A is a fuzzy set of the real line $\mathbb{R}$ with a normal, fuzzy convex and continuous membership function of bounded support. Any fuzzy number can be described with the following membership function,

$$A(t) = \begin{cases} L\left(\dfrac{a-t}{\alpha}\right) & \text{if } t \in [a-\alpha, a] \\ 1 & \text{if } t \in [a,b], a \leq b, \\ R\left(\dfrac{t-b}{\beta}\right) & \text{if } t \in [b, b+\beta] \\ 0 & \text{otherwise} \end{cases}$$

where $[a,b]$ is the peak of A; a and b are the lower and upper modal values; L and R are shape functions: $[0,1] \to [0,1]$, with $L(0) = R(0) = 1$ and $L(1) = R(1) = 0$ which are non-increasing, continuous mappings. We shall call these fuzzy numbers of LR-type and use the notation $A = (a,b,\alpha,\beta)_{LR}$. If $R(x) = L(x) = 1 - x$, we denote $A = (a,b,\alpha,\beta)$. The family of fuzzy numbers will be denoted by $\mathcal{F}$. A γ-level set of a fuzzy number A is defined by $[A]^\gamma = \{t \in \mathbb{R} | A(t) \geq \gamma\}$, if $\gamma > 0$ and $[A]^\gamma = \text{cl}\{t \in \mathbb{R} | A(t) > 0\}$ (the closure of the support of A) if $\gamma = 0$.

A triangular fuzzy number A denoted by (a, α, β) is defined as

$$A(t) = \begin{cases} 1 - \dfrac{a-t}{\alpha} & \text{if } a - \alpha \leq t \leq a \\ 1 & \text{if } a \leq t \leq b \\ 1 - \dfrac{t-b}{\beta} & \text{if } a \leq t \leq b + \beta \\ 0 & \text{otherwise} \end{cases}$$

where $a \in \mathbb{R}$ is the centre and $\alpha > 0$ is the left spread, $\beta > 0$ is the right spread of A.

If $\alpha = \beta$, then the triangular fuzzy number is called symmetric triangular fuzzy number and denoted by (a, α).

An n-dimensional possibility distribution C is a fuzzy set in $\mathbb{R}^n$ with a normalized membership function of bounded support. The family of n-dimensional possibility distribution will be denoted by $\mathcal{F}_n$.

Let us recall the concept and some basic properties of joint possibility distribution introduced in [30]. If $A_1, \ldots, A_n \in \mathcal{F}$ are fuzzy numbers, then $C \in \mathcal{F}_n$ is said to be their joint possibility distribution if $A_i(x_i) = \max\{C(x_1, \ldots, x_n) \mid x_j \in \mathbb{R}, j \neq i\}$, holds for all $x_i \in \mathbb{R}$, $i = 1, \ldots, n$. Furthermore, A_i is called the i-th marginal possibility distribution of C. For example, if C denotes the joint possibility distribution of A_1, $A_2 \in \mathcal{F}$, then C satisfies the relationships

$$\max_y C(x_1, y) = A_1(x_1), \quad \max_y C(y, x_2) = A_2(x_2),$$

for all $x_1, x_2 \in \mathbb{R}$. Fuzzy numbers $A_1, \ldots, A_n$ are said to be non-interactive if their joint possibility distribution C satisfies the relationship

$$C(x_1, \ldots, x_n) = \min\{A_1(x_1), \ldots, A_n(x_n)\},$$

for all $x = (x_1, \ldots, x_n) \in \mathbb{R}^n$.

A function $T : [0, 1] \times [0, 1] \to [0, 1]$ is said to be a triangular norm (t-norm for short) iff T is symmetric, associative, non-decreasing in each argument, and $T(x, 1) = x$ for all $x \in [0, 1]$. Recall that a t-norm T is Archimedean iff T is continuous and $T(x, x) < x$ for all $x \in]0, 1[$. Every Archimedean t-norm T is representable by a continuous and decreasing function $f\colon [0, 1] \to [0, \infty]$ with $f(1) = 0$ and

$$T(x, y) = f^{[-1]}(f(x) + f(y))$$

where $f^{[-1]}$ is the pseudo-inverse of f, defined by

$$f^{[-1]}(y) = \begin{cases} f^{-1}(y) & \text{if } y \in [0, f(0)] \\ 0 & \text{otherwise} \end{cases}$$

The function f is the additive generator of T. Let T_1, T_2 be t-norms. We say that T_1 is weaker than T_2 (and write $T_1 \leq T_2$) if $T_1(x, y) \leq T_2(x, y)$ for each $x, y \in [0, 1]$.

The basic t-norms are (i) the minimum: $\min(a,b) = \min\{a,b\}$; (ii) Łukasiewicz: $T_L(a,b) = \max\{a+b-1, 0\}$; (iii) the product: $T_P(a,b) = ab$; (iv) the weak:

$$T_W(a,b) = \begin{cases} \min\{a,b\} & \text{if } \max\{a,b\} = 1 \\ 0 & \text{otherwise} \end{cases}$$

(v) Hamacher [10]:

$$H_\gamma(a,b) = \frac{ab}{\gamma + (1-\gamma)(a+b-ab)},\ \gamma \geq 0$$

and (vi) Yager

$$T_p^Y(a,b) = 1 - \min\{1,\ \sqrt[p]{[(1-a)^p + (1-b)^p]}\},\ p > 0.$$

Using the concept of joint possibility distribution we introduced the following extension principle in [3].

Definition 1.1. *[3] Let C be the joint possibility distribution of (marginal possibility distributions) $A_1, \ldots, A_n \in \mathcal{F}$, and let $f\colon \mathbb{R}^n \to \mathbb{R}$ be a continuous function. Then*

$$f_C(A_1, \ldots, A_n) \in \mathcal{F},$$

will be defined by

$$f_C(A_1, \ldots, A_n)(y) = \sup_{y = f(x_1, \ldots, x_n)} C(x_1, \ldots, x_n). \tag{1}$$

We have the following lemma, which can be interpreted as a generalization of Nguyen's theorem [28].

Lemma 1. *[3] Let $A_1, A_2 \in \mathcal{F}$ be fuzzy numbers, let C be their joint possibility distribution, and let $f\colon \mathbb{R}^n \to \mathbb{R}$ be a continuous function. Then,*

$$[f_C(A_1, \ldots, A_n)]^\gamma = f([C]^\gamma),$$

for all $\gamma \in [0,1]$. Furthermore, $f_C(A_1, \ldots, A_n)$ is always a fuzzy number.

Let C be the joint possibility distribution of (marginal possibility distributions) $A_1, A_2 \in \mathcal{F}$, and let $f(x_1, x_2) = x_1 + x_2$ be the addition operator. Then $A_1 + A_2$ is defined by

$$(A_1 + A_2)(y) = \sup_{y = x_1 + x_2} C(x_1, x_2). \tag{2}$$

If A_1 and A_2 are non-interactive, that is, their joint possibility distribution is defined by

$$C(x_1, x_2) = \min\{A_1(x_1), A_2(x_2)\},$$

then (2) turns into the extended addition operator introduced by Zadeh in 1965 [29],

$$(A_1 + A_2)(y) = \sup_{y=x_1+x_2} \min\{A_1(x_1), A_2(x_2)\}.$$

Furthermore, if $C(x_1, x_2) = T(A_1(x_1), A_2(x_2))$, where T is a t-norm then we get the t-norm-based extension principle,

$$(A_1 + A_2)(y) = \sup_{y=x_1+x_2} T(A_1(x_1), A_2(x_2)). \tag{3}$$

For example, if A_1 and A_2 are fuzzy numbers, T is the product t-norm then the sup-product extended sum of A_1 and A_2 is defined by

$$(A_1 + A_2)(y) = \sup_{x_1+x_2=y} A_1(x_1)A_2(x_2), \tag{4}$$

and the $sup - H_\gamma$ extended addition of A_1 and A_2 is defined by

$$(A_1 + A_2)(y) = \sup_{x_1+x_2=y} \frac{A_1(x_1)A_2(x_2)}{\gamma + (1-\gamma)(A_1(x_1) + A_2(x_2) - A_1(x_1)A_2(x_2))}.$$

If T is an Archimedean t-norm and $\tilde{a}_1$, $\tilde{a}_2 \in \mathcal{F}$ then their T-sum

$$\tilde{A}_2 := \tilde{a}_1 + \tilde{a}_2$$

can be written in the form

$$\tilde{A}_2(z) = f^{[-1]}(f(\tilde{a}_1(x_1)) + f(\tilde{a}_2(x_2))), z \in \mathbb{R},$$

where f is the additive generator of T. By the associativity of T, the membership function of the T-sum $\tilde{A}_n := \tilde{a}_1 + \cdots + \tilde{a}_n$ can be written as

$$\tilde{A}_n(z) = \sup_{x_1+\cdots+x_n=z} f^{[-1]}\left(\sum_{i=1}^{n} f(\tilde{a}_i(x_i))\right), z \in \mathbb{R}.$$

Since f is continuous and decreasing, $f^{[-1]}$ is also continuous and non-increasing, we have

$$\tilde{A}_n(z) = f^{[-1]}\left(\inf_{x_1+\cdots+x_n=z} \sum_{i=1}^{n} f(\tilde{a}_i(x_i))\right), z \in \mathbb{R}.$$

2 Additions of interactive fuzzy numbers

Dubois and Prade published their seminal paper on additions of interactive fuzzy numbers in 1981 [5]. Since then the properties of additions of interactive fuzzy numbers, when their joint possibility distribution is defined by a t-norm have been extensively studied in the literature [1-3, 5-26]. In 1991 Fullér [6, 7] extended the results presented in [5] to product-sum and Hamacher-sum of triangular fuzzy numbers.

Theorem 2.1. *[6] Let $\tilde{a}_i = (a_i, \alpha)$, $i \in \mathbf{N}$ be symmetrical triangular fuzzy numbers and let their addition operator be defined by sup-product convolution (4). If*

$$A := \sum_{i=1}^{\infty} a_i$$

exists and it is finite, then with the notations

$$\tilde{A}_n := \tilde{a}_1 + \cdots + \tilde{a}_n,\ A_n := a_1 + \cdots + a_n,\ n \in \mathbf{N},$$

we have

$$\left(\lim_{n\to\infty} \tilde{A}_n\right)(z) = \exp(-|A - z|/\alpha),\ z \in \mathbb{R}.$$

Theorem 2.1 can be interpreted as a central limit theorem for mutually product-related identically distributed fuzzy variables of symmetric triangular form.

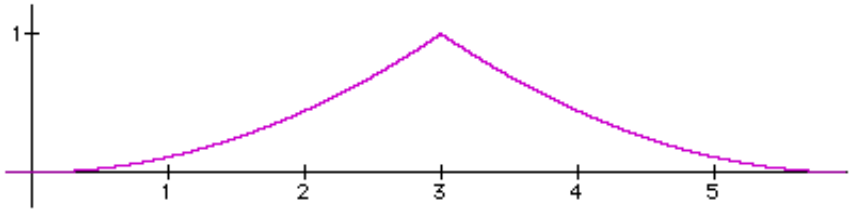

Figure 1: Product-sum of two triangular fuzzy numbers.

Theorem 2.2. *[7] Let $\tilde{a}_i = (a_i, \alpha)$, $i \in N$ and let their addition operator be defined by sup-H_0 convolution. Suppose that $A := \sum_{i=1}^{\infty} a_i$ exists and it is finite, then with the notation*

$$\tilde{A}_n = \tilde{a}_1 + \cdots + \tilde{a}_n, \quad A_n = a_1 + \cdots + a_n$$

we have

$$\left(\lim_{n\to\infty} \tilde{A}_n\right)(z) = \frac{1}{1 + |A - z|/\alpha},\ z \in \mathbb{R}.$$

Theorem 2.3. *[7] (Einstein-sum). Let $\tilde{a}_i = (a_i, \alpha)$, $i \in N$ and let their addition operator be defined by sup-H_2 convolution If $A := \sum_{i=1}^{\infty} a_i$ exists and it is finite, then with the notations of Theorem 2.2 we have*

$$\left(\lim_{n\to\infty} \tilde{A}_n\right)(z) = \frac{2}{1 + \exp(-2|A - z|/\alpha)},\ z \in \mathbb{R}.$$

In 1992 Fullér and Keresztfalvi [8] generalized and extended the results presented in [5, 6, 7]. Namely, they determined the exact membership function of the t-norm-based sum of fuzzy intervals, in the case of Archimedean t-norm having strictly convex additive generator function and fuzzy intervals with concave shape functions. They proved the following theorem,

Theorem 2.4. *[8] Let T be an Archimedean t-norm with additive generator f and let $\tilde{a}_i = (a_i, b_i, \alpha, \beta)_{LR}$, $i = 1, \ldots, n$, be fuzzy numbers of LR-type. If L and R are twice differentiable, concave functions, and f is twice differentiable, strictly convex function then the membership function of the T-sum $\tilde{A}_n = \tilde{a}_1 + \cdots + \tilde{a}_n$ is*

$$\tilde{A}_n(z) = \begin{cases} 1 & \text{if } A_n \le z \le B_n \\ f^{[-1]}\left(n \times f\left(L\left(\dfrac{A_n - z}{n\alpha}\right)\right)\right) & \text{if } A_n - n\alpha \le z \le A_n \\ f^{[-1]}\left(n \times f\left(R\left(\dfrac{z - B_n}{n\beta}\right)\right)\right) & \text{if } B_n \le z \le B_n + n\beta \\ 0 & \text{otherwise} \end{cases}$$

where $A_n = a_1 + \cdots + a_n$ and $B_n = b_1 + \cdots + b_n$.

We shall illustrate Theorem 2.4 for Yager's, Dombi's and Hamacher's parametrized t-norm. For simplicity we shall restrict our consideration to the case of symmetric fuzzy numbers $\tilde{a}_i = (a_i, a_i, \alpha, \alpha)_{LL}$, $i = 1, \ldots, n$. Denoting

$$\sigma_n := \frac{|A_n - z|}{n\alpha}$$

we get the following formulas for the membership function of t-norm-based sum $\tilde{A}_n = \tilde{a}_1 + \cdots + \tilde{a}_n$:

(i) Yager's t-norm with $p > 1$:

$$T_p^Y(x, y) = 1 - \min\left\{1, \sqrt[p]{(1-x)^p + (1-y)^p}\right\}.$$

This has additive generator

$$f(x) = (1 - x)^p$$

and then

$$\tilde{A}_n(z) = \begin{cases} 1 - n^{1/p}(1 - L(\sigma_n)) & \text{if } \sigma_n < L^{-1}(1 - n^{-1/p}) \\ 0 & \text{otherwise.} \end{cases}$$

(ii) Hamacher's t-norm with $p \le 2$:

$$H_p(x, y) = \frac{xy}{p + (1-p)(x + y - xy)}$$

having additive generator

$$f(x) = \ln \frac{p + (1-p)x}{x}$$

Then

$$\tilde{A}_n(z) = \begin{cases} \dfrac{p}{\left[(p+(1-p)L(\sigma_n))/L(\sigma_n)\right]^n - 1 + p} & \text{if } \sigma_n < 1 \\ 0 & \text{otherwise.} \end{cases}$$

(iii) Dombi's t-norm with $p > 1$:

$$D_p(x,y) = \frac{1}{1 + \sqrt[p]{(1/x-1)^p + (1/y-1)^p}}$$

with additive generator

$$f(x) = \left(\frac{1}{x} - 1\right)^p.$$

Then

$$\tilde{A}_n(z) = \begin{cases} \left[1 + n^{1/p}(1/L(\sigma_n) - 1)\right]^{-1} & \text{if } \sigma_n < 1 \\ 0 & \text{otherwise.} \end{cases}$$

(iv) Product t-norm (i.e. the Hamacher's t-norm with $p = 1$), that is $T_P(x,y) = xy$ having additive generator $f(x) = -\ln x$ Then

$$\tilde{A}_n(z) = L^n(\sigma_n),\ z \in \mathbb{R}.$$

The results of Theorem 2.4 have been extended to wider classes of fuzzy numbers and shape functions by many authors.

In 1994 Hong and Hwang [11] provided an upper bound for the membership function of T-sum of LR-fuzzy numbers with different spreads. They proved the following theorem,

Theorem 2.5. *[11] Let T be an Archimedean t-norm with additive generator f and let $\tilde{a}_i = (a_i, \alpha_i, \beta_i)_{LR}$, $i = 1, 2$, be fuzzy numbers of LR-type. If L and R are concave functions, and f is a convex function then the membership function of the T-sum $\tilde{A}_2 = \tilde{a}_1 + \tilde{a}_2$ is less than or equal to*

$$A_2^*(z) =$$

$$\begin{cases} f^{[-1]}\left(2f\left(L\left(1/2+\dfrac{(A_2-z)-\alpha^*}{(2\alpha_*}\right)\right)\right) & \text{if } A_2-\alpha_1-\alpha_2\le z\le A_2-\alpha^* \\ f^{[-1]}\left(2f\left(L\left(\dfrac{A_2-z}{2\alpha^*}\right)\right)\right) & \text{if } A_2-\alpha^*\le z\le A_2 \\ f^{[-1]}\left(2f\left(R\left(\dfrac{z-A_2}{2\beta^*}\right)\right)\right) & \text{if } A_2\le z\le A_2+\beta^* \\ f^{[-1]}\left(2f\left(R\left(1/2+\dfrac{(z-A_2)-\beta^*}{2\beta_*}\right)\right)\right) & \text{if } A_2+\beta^*\le z\le A_2+\beta_1+\beta_2 \\ 0 & \text{otherwise} \end{cases}$$

where $\beta^*=\max\{\beta_1,\beta_2\}$, $\beta_*=\min\{\beta_1,\beta_2\}$, $\alpha^*=\max\{\alpha_1,\alpha_2\}$, $\alpha_*=\min\{\alpha_1,\alpha_2\}$ *and* $A_2=a_1+a_2$.

The In 1995 Hong [12] proved that Theorem 2.4 remains valid for concave shape functions and convex additive t-norm generator. In 1996 Mesiar [25] showed that Theorem 2.4 remains valid if both $L\circ f$ and $R\circ f$ are convex functions.

In 1997 Mesiar [26] generaized Theorem 2.4 to the case of nilpotent t-norms (nilpotent t-norms are non-strict continuous Archimedean t-norms). In 1997 Hong and Hwang [14] gave upper and lower bounds of T-sums of LR-fuzzy numbers $\tilde{a}_i=(a_i,\alpha_i,\beta_i)_{LR}$, $i=1,\dots,n$, with different spreads where T is an Archimedean t-norm. They proved the following two theorems,

Theorem 2.6. *[14] Let T be an Archimedean t-norm with additive generator f and let $\tilde{a}_i=(a_i,\alpha_i,\beta_i)_{LR}$, $i=1,\dots,n$, be fuzzy numbers of LR-type. If $f\circ L$ and $f\circ R$ are concvex functions, then the membership function of their T-sum $\tilde{A}_n=\tilde{a}_1+\cdots+\tilde{a}_n$ is less than or equal to*

$$A_n^*(z)=\begin{cases} f^{[-1]}\left(nf\left(L\left(\dfrac{1}{n}I_L\left(A_n-z\right)\right)\right)\right) & \text{if } A_n-\sum_{i=1}^n\alpha_i\le z\le A_n \\ f^{[-1]}\left(nf\left(R\left(\dfrac{1}{n}I_R\left(z-A_n\right)\right)\right)\right) & \text{if } A_n\le z\le A_n+\sum_{i=1}^n\beta_i \\ 0 & \text{otherwise}, \end{cases}$$

where

$$I_L(z)=\inf\left\{\frac{x_1}{\alpha_1}+\cdots+\frac{x_n}{\alpha_n}\,\middle|\, x_1+\cdots+x_n=z,\ 0\le x_i\le\alpha_i,\ i=1,\dots,n\right\},$$

and

$$I_R(z)=\inf\left\{\frac{x_1}{\beta_1}+\cdots+\frac{x_n}{\beta_n}\,\middle|\, x_1+\cdots+x_n=z,\ 0\le x_i\le\beta_i,\ i=1,\dots,n\right\}.$$

Theorem 2.7. *[14] Let T be an Archimedean t-norm with additive generator f and let $\tilde{a}_i = (a_i, \alpha_i, \beta_i)_{LR}$, $i = 1, \ldots, n$, be fuzzy numbers of LR-type. Then*

$$\tilde{A}_n(z) \geq A_n^{**}(z) =$$

$$\begin{cases} f^{[-1]}\left(nf\left(L\left(\dfrac{A_n - z}{\alpha_1 + \cdots + \alpha_n}\right)\right)\right) & \text{if } A_n - (\alpha_1 + \cdots + \alpha_n) \leq z \leq A_n \\ f^{[-1]}\left(nf\left(R\left(\dfrac{A_n - z}{\beta_1 + \cdots + \beta_n}\right)\right)\right) & \text{if } A_n \leq z \leq A_n + (\beta_1 + \cdots + \beta_n) \\ 0 & \text{otherwise}, \end{cases}$$

In 1997, generalizing Theorem 2.4, Hwang and Hong [18] studied the membership function of the t-norm-based sum of fuzzy numbers on Banach spaces and they presented the membership function of finite (or infinite) sum (defined by the sup-t-norm convolution) of fuzzy numbers on Banach spaces, in the case of Archimedean t-norm having convex additive generator function and fuzzy numbers with concave shape function. In 1998 Hwang, Hwang and An [19] approximated the strict triangular norm-based addition of fuzzy intervals of L-R type with any left and right spreadss. In 2001 Hong [15] showed a simple method of computing T-sum of fuzzy intervals having the same results as the sum of fuzzy intervals based on the weakest t-norm T_W.

2.1 Shape preserving arithmetic operations

Shape preserving arithmetic operations of LR-fuzzy intervals allow one to control the resulting spread. In practical computation, it is natural to require the preservation of the shape of fuzzy intervals during addition and multiplication. Hong [16] showed that T_W , the weakest t-norm, is the only t-norm T that induces a shape-preserving multiplication of LR-fuzzy intervals. In 1995 Kolesarova [22, 23] proved the following theorem,

Theorem 2.8. *(a) Let T be an arbitrary t-norm weaker than or equal to the Łukasiewicz t-norm T_L; $T(x, y) \leq T_L(x, y) = \max(0, x + y - 1)$, $x, y \in [0, 1]$. Then the addition $\oplus$ based on T coincides on linear fuzzy intervals with the addition $\oplus$ based on the weakest t-norm T_W; i.e.,*

$$(a_1, b_1, \alpha_1, \beta_1) \oplus (a_2, b_2, \alpha_2, \beta_2) = (a_1 + a_2, b_1 + b_2, \max(\alpha_1, \alpha_2), \max(\beta_1, \beta_2)).$$

(b) Let T be a continuous Archimedean t-norm with convex additive generator f . Then the addition $\oplus$ based on T preserves the linearity of fuzzy intervals if and only if the t-norm T is a member of Yager's family of nilpotent t-norms with parameter $p \in [1, \infty)$, $T = T_p^Y$, and $f(x) = (1 - x)^p$. Then $T_1^Y = T_L$ and for $p \in (0, \infty)$,

$$(a_1, b_1, \alpha_1, \beta_1) \oplus (a_2, b_2, \alpha_2, \beta_2) = (a_1 + a_2, b_1 + b_2, (\alpha_1^q + \alpha_2^q)^{1/q}, (\beta_1^q + \beta_2^q)^{1/q}),$$

where $1/p + 1/q = 1$*, i.e.* $q = p/(p-1)$.

In 1997 Mesiar [27] studied the triangular norm-based additions preserving the LR-shape of LR-fuzzy intervals and conjectured that the only t-norm-based additions preserving the linearity of fuzzy intervals are those described in Theorem 2.8. He proved the following theorem,

Theorem 2.9. *[27] Let a continuous t-norm T be not weaker than or equal to* T_L *(i.e., there are some* $x, y \in [0,1]$ *so that* $T(x,y) > x + y - 1 > 0$*). Let the addition based on T preserve the linearity of fuzzy intervals. Then either T is the strongest t-norm,* $T = T_M$*, or T is a nilpotent t-norm.*

In 2002 Hong [17] proved Mesiar's conjecture.

Theorem 2.10. *[17] Let a continuous t-norm T be not weaker than or equal to* T_L*. Then the addition* $\oplus$ *based on T preserves the linearity of fuzzy intervals if and only if the t-norm T is either* T_M *or a member of Yager's family of nilpotent t-norms with parameter* $p \in (1, \infty)$*,* $T = T_p^Y$*, and* $f(x) = (1-x)^p$*.*

2.2 Additions of completely correlated fuzzy numbers

Until now we have summarized some properties of the addition operator on interactive fuzzy numbers, when their joint possibility distribution is defined by a t-norm. It is clear that in (3) the joint possibility distribution is defined *directly* and *pointwise* from the membership values of its marginal possibility distributions by an aggregation operator. However, the interactivity relation between fuzzy numbers may be given by a more general joint possibility distribution, which can not be directly defined from the membership values of its marginal possibility distributions by any aggregation operator.

Drawing heavily on [3] we will now consider some properties of the addition operator on completely correlated fuzzy numbers, where the interactivity relation is given by their joint possibility distribution.

Let C be a joint possibility distribution with marginal possibility distributions A and B, and let

$$f(x_1, x_2) = x_1 + x_2,$$

the addition operator in $\mathbb{R}^2$. In [3] we introduced the notation,

$$A +_C B = f_C(A, B).$$

Definition 2.1. *[9] Fuzzy numbers* A *and* B *are said to be completely correlated, if there exist* $q, r \in \mathbb{R}$*,* $q \neq 0$ *such that their joint possibility distribution is defined by*

$$C(x_1, x_2) = A(x_1) \cdot \chi_{\{qx_1+r=x_2\}}(x_1, x_2) = B(x_2) \cdot \chi_{\{qx_1+r=x_2\}}(x_1, x_2), \quad (5)$$

where $\chi_{\{qx_1+r=x_2\}}$*, stands for the characteristic function of the line*

$$\{(x_1, x_2) \in \mathbb{R}^2 | qx_1 + r = x_2\}.$$

In this case we have,

$$[C]^{\gamma} = \left\{(x, qx + r) \in \mathbb{R}^2 \middle| x = (1-t)a_1(\gamma) + ta_2(\gamma), t \in [0,1]\right\}$$

where $[A]^{\gamma} = [a_1(\gamma), a_2(\gamma)]$*; and* $[B]^{\gamma} = q[A]^{\gamma} + r$*, for any* $\gamma \in [0,1]$.

We should note here that the interactivity relation between two fuzzy numbers is defined by their joint possibility distribution. Fuzzy numbers A and B with $A(x) = B(x)$ for all $x \in \mathbb{R}$ can be non-interactive, positively or negatively correlated depending on the definition of their joint possibility distribution.

Definition 2.2. *[9] Fuzzy numbers A and B are said to be completely positively (negatively) correlated, if q is positive (negative) in (5).*

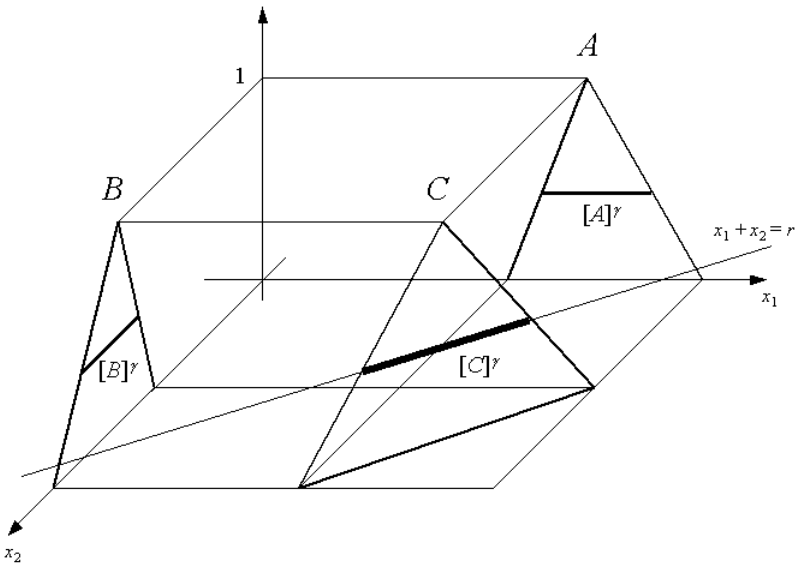

Figure 2: Completely negatively correlated fuzzy numbers with $q = -1$.

We note that if $A, B \in \mathcal{F}$ are completely positively correlated then their correlation coefficient is equal to one, furthermore, if they are completely negatively correlated then their correlation coefficient is equal to minus one [4, 9]. In the case of complete positive correlation, if $A(u) \geq \gamma$ for some $u \in \mathbb{R}$ then there exists a *unique* $v \in \mathbb{R}$ that B can take, furthermore, if u is moved to the left (right) then the corresponding value (that B can take) will also move to the left (right). In case of complete negative correlation, if $A(u) \geq \gamma$ for some $u \in \mathbb{R}$ then there exists a *unique* $v \in \mathbb{R}$ that B can take, furthermore, if u is moved to the left (right) then the corresponding value (that B can take) will move to the right (left). It is also clear that in these two cases, given q

and r, the first marginal possibility distribution completely determines the second one, and vica versa. Finally, if A and B are not completely correlated then if $A(u) \geq \gamma$ for some $u \in \mathbb{R}$ then there may exist *several* $v \in \mathbb{R}$ that B can take (see [9]).

Now let us consider the extended addition of two completely correlated fuzzy numbers A and B,

$$(A +_C B)(y) = \sup_{y=x_1+x_2} C(x_1, x_2).$$

That is,

$$(A +_C B)(y) = \sup_{y=x_1+x_2} A(x_1) \cdot \chi_{\{qx_1+r=x_2\}}(x_1, x_2).$$

Then from (2) and (5) we find,

$$[A +_C B]^\gamma = (q+1)[A]^\gamma + r, \tag{6}$$

for all $\gamma \in [0,1]$. If A and B are completely negatively correlated with $q = -1$, that is, $[B]^\gamma = -[A]^\gamma + r$, for all $\gamma \in [0,1]$, then $A +_C B$ will be a crisp number. Really, from (6) we get $[A +_C B]^\gamma = 0 \times [A]^\gamma + r = r$, for all $\gamma \in [0,1]$.

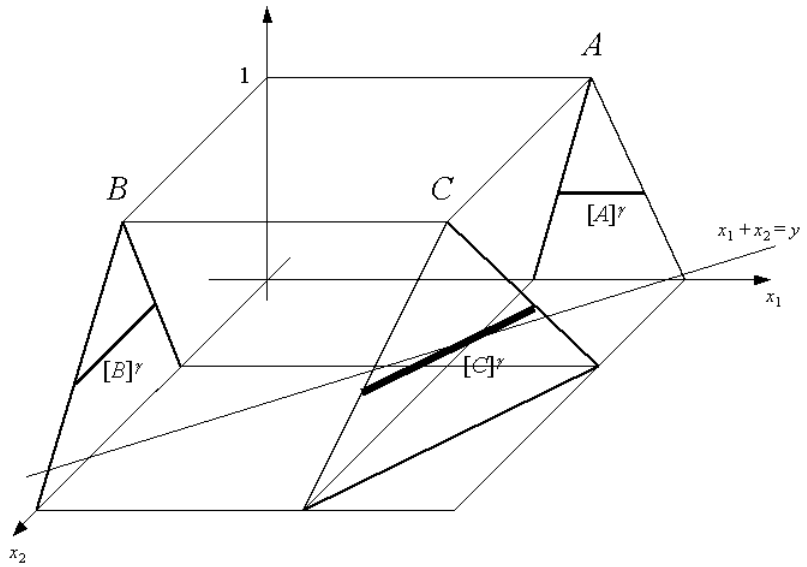

Figure 3: Completely negatively correlated fuzzy numbers with $q \neq -1$.

That is, the interactive sum, $A +_C B$, of two completely negatively correlated fuzzy numbers A and B with $q = -1$ and $r = 0$, i.e.

$$A(x) = B(-x), \forall x \in \mathbb{R},$$

will be (crisp) zero. On the other hand, a γ-level set of their non-interactive sum, $A + B$, can be computed as,

$$[A + B]^\gamma = [a_1(\gamma) - a_2(\gamma), a_2(\gamma) - a_1(\gamma)],$$

which is a fuzzy number.

In this case (i.e. when $q = -1$) any γ-level set of C are included by a certain level set of the addition operator, namely, the relationship,

$$[C]^\gamma \subset \{(x_1, x_2) \in \mathbb{R} | x_1 + x_2 = r\},$$

holds for any $\gamma \in [0, 1]$ (see Fig. 2). On the other hand, if $q \neq -1$ then the fuzziness of $A +_C B$ is preserved, since

$$[A +_C B]^\gamma = (q + 1)[A]^\gamma + r \neq \text{constant},$$

for all $\gamma \in [0, 1]$ and $y \in \mathbb{R}$. (see Fig. 3).

Really, in this case the set $\{(x_1, x_2) \in [C]^\gamma | x_1 + x_2 = y\}$ consists of a single point at most for any $\gamma \in [0, 1]$ and $y \in \mathbb{R}$.

Note 2.1. *The interactive sum of two completely negatively correlated fuzzy numbers A and B with $A(x) = B(-x)$ for all $x \in \mathbb{R}$ will be (crisp) zero.*

3 Summary

In this paper we have summarized some properties of the addition operator on interactive fuzzy numbers, when their joint possibility distribution is defined by a t-norm or by a more general type of joint possibility distribution.

References

[1] B. De Baets and A. Markova, Addition of LR-fuzzy intervals based on a continuous t-norm, in: *Proceedings of IPMU'96 Conference*, (July 1-5, 1996, Granada, Spain), 1996 353-358

[2] B. De Baets and A. Marková-Stupňanová, Analytical expressions for addition of fuzzy intervals, *Fuzzy Sets and Systems*, 91(1997) 203-213.

[3] C. Carlsson, R. Fullér and P. Majlender, Additions of Completely Correlated Fuzzy Numbers, in: FUZZY IEEE 2004 CD-ROM Conference Proceedings, Budapest, July 26-29, 2004,

[4] C. Carlsson, R. Fullér and P. Majlender, On possibilistic correlation, *Fuzzy Sets and Systems* (submitted).

[5] D. Dubois and H. Prade, Additions of interactive fuzzy numbers, *IEEE Transactions on Automatic Control*, Vol. AC-26, No.4 1981, 926-936.

[6] R. Fullér, On product-sum of triangular fuzzy numbers, *Fuzzy Sets and Systems*, 41(1991) 83-87.

[7] R. Fullér, On Hamacher-sum of triangular fuzzy numbers, *Fuzzy Sets and Systems*, 42(1991) 205-212.

[8] R. Fullér and T.Keresztfalvi, t-Norm-based addition of fuzzy numbers, *Fuzzy Sets and Systems*, 51(1992) 155-159.

[9] R. Fullér and P. Majlender, On interactive fuzzy numbers, *Fuzzy Sets and Systems* 143(2004) 355-369.

[10] H. Hamacher, Über logische Aggregationen nicht binär explizierter Entscheidung-kriterien (Rita G. Fischer Verlag, Frankfurt, 1978).

[11] D. H. Hong and S.Y.Hwang, On the compositional rule of inference under triangular norms, *Fuzzy Sets and Systems*, 66(1994) 25-38.

[12] D. H. Hong, A note on t-norm-based addition of fuzzy intervals, *Fuzzy Sets and Systems*, 75(1995) 73-76.

[13] D. H. Hong and C. Hwang, Upper bound of T-sum of LR-fuzzy numbers, in: *Proceedings of IPMU'96 Conference*, (July 1-5, 1996, Granada, Spain), 1996 343-346.

[14] D. H. Hong and C. Hwang, A T-sum bound of LR-fuzzy numbers, *Fuzzy Sets and Systems*, 91(1997) 239-252.

[15] D. H. Hong, Some results on the addition of fuzzy intervals *Fuzzy Sets and Systems*, 122(2001) 349-352.

[16] D. H. Hong, Shape preserving multiplications of fuzzy numbers, *Fuzzy Sets and Systems*, 123(2001) 81-84.

[17] D. H. Hong, On shape-preserving additions of fuzzy intervals, *Journal of Mathematical Analysis and Applications*, 267(2002) 369-376.

[18] S.Y.Hwang and D.H.Hong, The convergence of T-sum of fuzzy numbers on Banach spaces, *Applied Mathematics Letters* 10(1997) 129-134.

[19] S. Y. Hwang, J. J. Hwang, J. H. An The triangular norm-based addition of fuzzy intervals, *Applied Mathematics Letters* 11(1998) 9-13.

[20] S. Y. Hwang and Hyo Sam Lee, Nilpotent t-norm-based sum of fuzzy intervals, *Fuzzy Sets and Systems*, 123(2001) 73-80.

[21] M. F. Kawaguchi and T. Da-te, Some algebraic properties of weakly non-interactive fuzzy numbers, *Fuzzy Sets and Systems*, 68(1994) 281-291.

[22] A. Kolesarova, Triangular norm-based addition of linear fuzzy numbers, *Tatra Mt. Math. Publ.*, 6(1995), 75-82.

[23] A. Kolesarova, Triangular norm-based addition preserving linearity of t-sums of fuzzy intervals, *Mathware Soft Computing*, 5(1998), 97-98.

[24] A. Markova, T-sum of L-R fuzzy numbers, *Fuzzy Sets and Systems*, 85(1997) 379-384.

[25] R. Mesiar, A note to the T-sum of L-R fuzzy numbers, *Fuzzy Sets and Systems*, 79(1996) 259-261.

[26] R. Mesiar, Triangular-norm-based addition of fuzzy intervals, *Fuzzy Sets and Systems*, 91(1997) 231-237.

[27] R. Mesiar, Shape preserving additions of fuzzy intervals, *Fuzzy Sets and Systems* 86(1997), 73-78.

[28] H. T. Nguyen, A note on the extension principle for fuzzy sets, *Journal of Mathematical Analysis and Applications*, 64(1978) 369-380.

[29] L. A. Zadeh, Fuzzy sets, *Information and Control*, 8(1965) 338-353.

[30] L. A. Zadeh, The concept of linguistic variable and its applications to approximate reasoning, Parts I,II,III, *Information Sciences*, 8(1975) 199-251; 8(1975) 301-357; 9(1975) 43-80.

Development of Conventional and Fuzzy Controllers and Takagi-Sugeno Fuzzy Models Dedicated for Control of Low Order Benchmarks with Time Variable Parameters

Stefan Preitl[*], Radu-Emil Precup[*], Zsuzsa Preitl[*,]**

[*] "Politehnica" University of Timisoara, Dept. of Automation and Appl. Inform.
Bd. V. Parvan 2, RO-300223 Timisoara, Romania
Phone: +40-256-4032-29, -30, -24, -26, Fax: +40-256-403214
E-mail: spreitl@aut.utt.ro, rprecup@aut.utt.ro

[**] Budapest University of Technology and Economics, Dept. of Automation and Applied Informatics, MTA-BME Control Research Group
Goldmann Gy. tér 3, H-1111, Budapest, Hungary; fax : +36-1-463-2871
E-mail : preitl@aut.bme.hu

Abstract: The paper presents development and tuning tehniques and solutions for PI and PID controllers, and Takagi-Sugeno fuzzy controllers with PI and PID type dynamics meant for applications which can be characterised with low order benchmark type modeles (for example electrical and hydraulic driving and positioning systems).Two type of plants and two control structures with homogenous and with non-homogenous information processing with respect to the inputs are presented, including tuning and optimization aspects. Then Takagi-Sugeno fuzzy models dedicated to a class of plants characterized by Two Input-Single Output linear time-varying systems are presented. It is offered a stability test algorithm of the fuzzy control systems involving Takagi-Sugeno fuzzy controllers, to control the accepted class of plants. The tuning methods are briefly presented in relation with a control solution for a drive system with a variable inertia strip winding system.

Keywords: Controllers with PI and PID dynamics, Takagi-Sugeno fuzzy models, Takagi-Sugeno fuzzy controllers, stability analysis, winding system.

1 Introduction

Take the class of plants (P) having the transfer functions expressed as:

$$H_P(s) = \frac{k_P}{s(1+sT_\Sigma)} \text{ (a)}, \quad H_P(s) = \frac{k_P}{(1+sT_1)(1+sT_\Sigma)} \text{ (b)} \tag{1.1}$$

$$H_P(s)=\frac{k_P}{s(1+sT_1)(1+sT_\Sigma)} \quad \text{(a)}, \quad H_P(s)=\frac{k_P}{(1+sT_1)(1+sT_2)(1+sT_\Sigma)} \quad \text{(b)}. \qquad (1.2)$$

The parametres k_P can be constant or variable, and it is asumed that $T_\Sigma < T_2 <(<<) T_1$; this class of models characterize well enough electrical and hydraulic driving and possitioning systems (control of possition and drive applications as controlled plants) [1], [2], [6].

The paper's aim is to develop Takagi-Sugeno (TS) fuzzy controllers (FCs) based on classical development methods, meant for position control of electrical and hydraulic drives with linear constant or time-varying (LTV) parameters characterized by benchmark type models of form (1) and (2). If the parameters are continuously varying, the LTV systems may result as linearized nonlinear systems in the vicinity of a set of operating points or of an operating trajectory.

These features determine the wide application area of robust control, adaptive control and TS fuzzy models. Regarded to the use of TS fuzzy models, the application is based in spite of their drawbacks such as:

- The behavior of the global TS fuzzy model can significantly divert from the expected behavior obtained by the merge of the local models;
- The stability analysis and testing of fuzzy control systems based on TS fuzzy models is relatively difficult, because of the complex aggregation of the local models in the inference engine.

Firstly, the paper presents two classical development procedures for continuously and quasi-continuously working PI and PID controllers, based on extensions of the widely used Symmetrical Optimum Method (Section 2). Then, a class of TS models for Two Input-Single Output (TISO) LTV plants is presented (Section 3). In Section 4 there are defined the TS fuzzy controllers meant for controlling the TS fuzzy models. Based on these, a stability test algorithm is presented (based on Lyapunov's stability theory) for a class of fuzzy systems with TS fuzzy controllers controlling the TISO LTV plants (Section 5). Results concerning the development of conventional and fuzzy control solutions for a drive system with two output coupled motors, applicable to the rolls of a hot rolling mill and to a variable inertia strip winding system, are presented in Section 6. Section 7 is focused on the concluding part of the paper.

2 Development of Continuously and Quasi-Continuously Operating PI and PID Control Algorithms

Many control applications prefer structures with typical control algorithms with homogenous or non-homogenous information processing on the two input channels [1], [3], [4]. Such structures have the general form given in Fig. 2.1-a -b and -c presents some particular control laws regarding the inputs. The blocks (1) ... (5) can be described by its specific transfer functions (t.f.s); w(t) or r(t) – the reference signal (or the filtered refernce signal), y(t) - the measured output, u(t) - the control signal (or its components, with index), e(t) - the control error.

There can be established relations between such controllers and the 2-DOF controllers [3]. For example, a block diagram of a 2-DOF control structure is presented in figure 2.2. R(z) , S(z) and T(z) are the characteristic blocks of the 2-DOF controller, P is the plant; $v_1(t)$, $v_2(t)$ – plant disturbances.

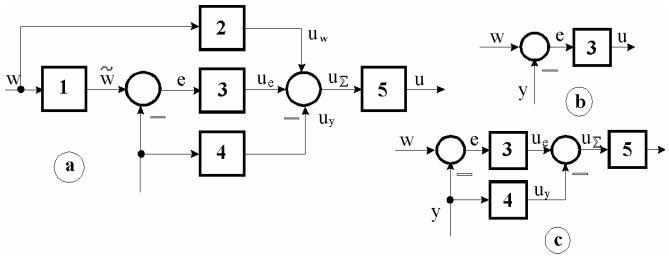

Figure 2.1
Typical I-DOF controller structures and particularization

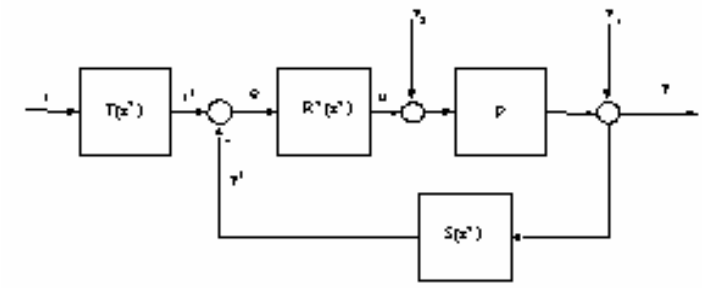

Figure 2.2
Structure of the 2-DOF controller.

The 2-DOF controller can be restructured in different ways; for the given low order plants – from a practical point of view – the presence of a conventional

controller (particularly PI or a PID and signal filters) can be highlighted. Two types of structures are detailed in figure 2.3. These rearrangements allow:

- to take over design experience from case of PI and PID controllers;
- an easy introduction of supplementary blocks specific to PI and PID controllers (Anti Windup circuit, bumpless switching and others);
- the transformation of PI and PID controllers into 2 DOF structures and vice versa.

The controllers in figure 2.3 will be characterized – for example – by continuous t.f.s $C(s)$, $C_F(s)$, $C^*(s)$, $C_P(s)$, in which the parallel realisation tuning parameters are highlighted $\{k_C,\ T_i,\ T_d,\ T_f\}$; discretizing, the digital control algorithm is obtained. Taking the basic controller C(s) of PID type, it can be written:

- for the basic PID structure in Fig. 2.1 (b) (parallel form):

$$C(s)=\frac{u(s)}{e(s)}=k_C\left(1+\frac{1}{sT_i}+\frac{sT_d}{1+sT_f}\right),\ F(s)=\frac{r^*(s)}{r(s)}=\frac{1+(1-\alpha)\,T_i s+\dfrac{(1-\beta)T_iT_ds^2}{(1+sT_f)}}{1+T_is+\dfrac{T_iT_ds^2}{(1+sT_f)}}; \tag{2.1}$$

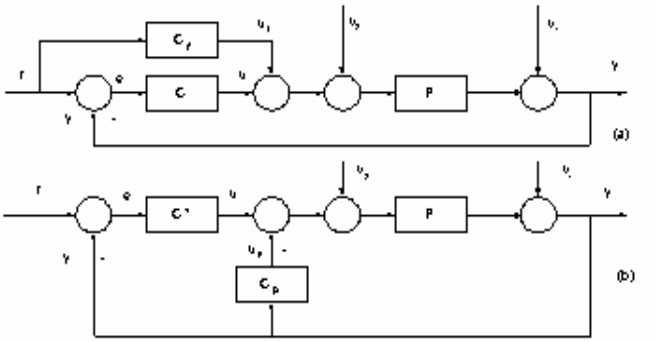

Figure 2.3
Two alternatives for rearranging a 2 DOF controller.

- for the structure (a) in figure 2.3:

$$C(s)=\frac{u(s)}{e(s)}=k_R\left(1+\frac{1}{sT_i}+\frac{sT_d}{1+sT_f}\right),\ C_F(s)=\frac{u_f(s)}{r(s)}=k_R\left(\alpha+\beta\frac{sT_d}{1+sT_f}\right); \tag{2.2}$$

- for the structure (b) in figure 2.3 (with the notation $C(s)=C^*(s)$):

$$C^*(s)=\frac{u(s)}{e(s)}=k_R[(1-\alpha)+\frac{1}{sT_i}+(1-\beta)\frac{sT_d}{1+sT_f}],\ C_P(s)=\frac{u_f(s)}{r(s)}=k_R(\alpha+\beta\frac{sT_d}{1+sT_f}). \quad (2.3)$$

Table 2.1
Connections between 2 DOF controller and extended 1 DOF controller structure.

Fig. 2.1		F(s)	-	F(s)C(s)	C(s)	Remarks
Fig. 2.3-a		-	C_F	C(s)–C_F(s)	C(s)	-
Fig. 2.3-b		-	C_P	C*(s)	C*(s)+C_P(s)	-
α	β	-	-	(ref. channel)	(feedback)	-
0	0	1	0	PID	PID	1 DOF controller
0	1	PDL2	DL1	PI	PID	1 DOF with non-homogenous behavior
1	0	PD2L2	P	PID-L1	PID	
1	1	PL2	PDL2	I	PID	
α	β	PID controller with pre-filtering (2 DOF controller)				

Remarks: P – proportional, D – derivative, L – lag, I – integrator modules.

Depending on the values of α and β parameters, for the presented blocks the behaviors from in Table 2.1 are obtained.

The choice of a certain representation of the controller depends on [3]:

- the structure of the available controller;
- the adopted algorithmic design method, and the result of this design.

In the presence of an integral (I) component and a limitation block in the controller structure, figure 2.4 (a), the use of the AWR measure (Anti-Windup-Reset) is recommended. A classical structure for introducing the AWR measure on a controller structure with integral component is presented in figure 2.4 (b). The AWR measure can be globally implemented with respect to controller output or locally, with respect to integral (I) component of the controller.

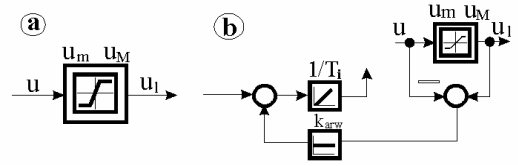

Figure 2.4
Classical structure for introducing ARW measure on the controller structure

The transfer functions of the continuous PI (PID) controllers are written related to the design procedure and the implementation (discretization) procedure. For the serial form of PI and PID controllers the t.f.s are:

PI: $\{k_c, T_c\}$ $$C(s) = \frac{k_c}{s}(1 + sT_c) \tag{2.4}$$

PID: $\{k_c, T_c, T_c'\}$ $$C(s) = \frac{k_c}{s}(1 + sT_c)(1 + sT_c') \tag{2.5}$$

The implementation of a quasi-continuously (QC) operating PID digital control algorithm can be based on the informational diagram presented in figure 2.5; the appearance of a supplementary state variables x_k, is associated to integral (I) component and the adding of the AWR measure. The *parameter values* $\{K_{pid}, K_i, K_d, K_{arw}\}$ depends on the continuous parameters $\{k_r, T_r, T_r'\}$ and on the sampling time value, T_e .

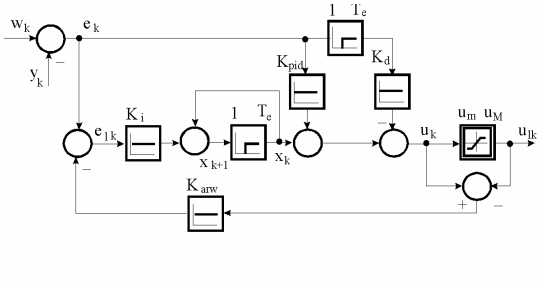

Figure 2.5
Quasi-continuously operating PID digital control algorithm implementation.

The implementation of non-homogenous information processing (Fig. 2.1-c) has two requirements [3], [4]:

- an I or PI behavior with respect to the reference channel;
- a PI or PID behavior with respect to the feedback channel. The non-homogenous information processing structure respects the following informations (Table 2.2).

Table 2.2
Transfer functions of blocks in Fig. 2.1-c (parallel form)

Case	Channel	Block 3	Block 4	Block 5	Type
(1)	*w, (r)*	I: $(1/sT_i)$	----	P: (k_C)	I: $(1/sT_i)$
	y	I: $(1/sT_i)$	P: (1)	P: (k_C)	PI: $(1+1/sT_i)$
(2)	*w, (r)*	PI: $(1+1/sT_i)$	----	P: (k_C)	PI: $(1+1/sT_i)$
	y	PI: $(1+1/sT_i)$	D: (sT_d)	P: (k_C)	PID

In order to avoid difficulties due to contradictory results obtained from design according to reference tracking and disturbance rejection, different optimal - or in special cases, optimal-like tuning techniques can be adopted. Two of these methods are considered here to be representative:

- the Modulus Optimum method, (MO-m), [1],
- the Symmetrical Optimum method (SO-m) [1] and two modified (extended versions, the Extended Symmetrical Optimum method (ESO-m) [2] and the "extended" (modified version) of the extended Symmetrical Optimum method (2E-SO-m)Criterion. The main advantage of this ESO-m and 2E-SO-m consist in the possibility to increase the control system phase reserve and – for specific cases – in a better load disturbance rejection.

The controller parameters – in its serial form – can be calculated using the relations synthetised in Table 2.3. The design parameter β belongs usually to the domain $4 \le \beta \le 16$.

In the case of implementation, the problem of bump-less transfer from one local crisp controller to another is solved in a crisp manner, exemplified here for two local controllers of digital PI-type, the "old" one with the parameters $\{q_1, q_0\}$, and the "new" one with the parameters $\{q_1^*, q_0^*\}$:

$$u_k = u_{k-1} + q_1 e_k + q_0 e_{k-1},\ u_k = u_{k-1} + q_1^* e_k + q_0^* e_{k-1}^*. \tag{2.6}$$

It is necessary to compute previously "past values" which are necessary to the new controller. As it can be observed in (16), e_{k-1}^* represent these new initial conditions (the past values).

3 A Class of Takagi-Sugeno Fuzzy Models

The following Takagi-Sugeno fuzzy model to represent a TISO LTV system will be used that models the controlled plant [7]:

Table 2.3
Tuning relations after [2], [6]

P(s)	Contr. type	Tuning relations
0	1	2
$\frac{k_p}{s(1+sT_\Sigma)}$	PI $\{k_c, T_c\}$	$k_c = \frac{1}{\beta^{3/2} k_p T_\Sigma^2}$ *(ESO-m.[2])* $T_c = \beta T_\Sigma$

$\frac{k_p}{s(1+sT_1)(1+sT_\Sigma)}$	PID $\{k_c, T_c, T_c'\}$	$k_r = \frac{1}{\beta^{3/2} k_p T_\Sigma^2}$ *(ESO-m[2])* $T_c = \beta T_\Sigma$, $T_c' = T_1$
$\frac{k_P}{(1+sT_1)(1+sT_\Sigma)}$, $m = T_\Sigma/T_1$	PI $\{k_c, T_c\}$	$k_c = \frac{1}{2 k_p T_\Sigma}$ *(MO-m)* $T_c = T_1$ $k_c = \frac{(1+m)^2}{\beta^{3/2} \cdot k_P \cdot T_\Sigma' \cdot m}$, $T_c = \frac{\beta T_\Sigma' \Delta_m(m)}{(1+m)^2}$ *(2E-SO-m) [6]* $\Delta_m(m) = 1+(2-\beta^{1/2})m+m^2$
$\frac{k_P}{(1+sT_1)(1+sT_2)(1+sT_\Sigma)}$ $m = T_\Sigma/T_1$	PID $\{k_c, T_c, T_c'\}$	$k_c = \frac{1}{2 k_p T_\Sigma}$ *(MO-m)* $T_c = T_1$, $T_c' = T_2$ $k_c = \frac{(1+m)^2}{\beta^{3/2} \cdot k_P \cdot T_\Sigma' \cdot m}$, $T_c' = T_2$ $T_c = \frac{\beta T_\Sigma' \Delta_m(m)}{(1+m)^2}$ *(2E-SO-m) [6]* $\Delta_m(m) = 1+(2-\beta^{1/2})m+m^2$

$$R^l: \text{IF } z_1(t) \text{ is } F_1^l \text{ AND } z_2(t) \text{ is } F_2^l \text{ AND } \dots \text{ AND } z_n(t) \text{ is } F_n^l \quad \text{THEN } y(s) = P_l^u(s)u(s) + P_l^v(s)v(s),\ l = 1 \dots m, \tag{3.1}$$

where:

$u(s)$, $v(s)$, $y(s)$ – the Laplace transform of the plant input (the control signal) $u(t)$, of the disturbance input $v(t)$ and of the controlled output $y(t)$;

R^l – the lth inference rule, $l = 1 \dots m$; m – the number of inference rules;

$z_i(t)$ – the measurable plant variables, $i = 1 \dots n$, and:

$$\mathbf{z}(t) = [z_1(t)\ \ z_2(t)\ \dots\ z_n(t)]^T; \tag{3.2}$$

n – the number of measurable plant (system) variables pointing out the time-variation of the plant;

F^l – the linguistic terms associated to the measurable variable $z^i(t)$ and to the rule R^l; $P_l^u(s)$ and $P_l^v(s)$ – the local t.f.s of the plant.

The TS fuzzy model (3.1) includes both the inference rules as part of the rule base and the local analytic models of the TISO LTV system. The controlled output is inferred by taking the weighted average of all local models appearing in (3.1), which characterizes the properties of the controlled plant in a local region of the input space; so it is referred to as fuzzy dynamic local model [8], [9]. The following notation is introduced:

$$\mu_l(t) = \mu_l(\mathbf{z}(t)),\ l = 1 \ldots m, \tag{3.3}$$

for the membership degrees of the normalized membership functions μ_l of the inferred fuzzy set F^l, where:

$$F^l = \bigcap_{i=1}^{n} F_i^l,\ l = 1 \ldots m,\ \text{(a)}\ \text{and}\ \sum_{l=1}^{m} \mu_l(t) = 1.\ \text{(b)} \tag{3.4}$$

By using the product inference method in (3.4) (b) and the weighted average method for defuzzification, the TS fuzzy model (3.1) can be expressed in terms of the following fuzzy dynamic global model that can be considered as TS fuzzy model of the plant:

$$\begin{aligned} &y(s) = P^u(s)u(s) + P^v(s)v(s), \\ &P^u(s) = \sum_{l=1}^{m} \mu_l(t) P_l^u(s),\ P^v = \sum_{l=1}^{m} \mu_l(t) P_l^v(s). \end{aligned} \tag{3.5}$$

The model (3.5) is LTV system because the inferred transfer functions, $P^u(s)$ and $P^v(s)$, have time-varying coefficients regarded to local linearised models.

4 Takagi-Sugeno Fuzzy Controllers. Closed-Loop System Models

The TS fuzzy models (3.1) or (3.5) could be very useful in comparison with other conventional techniques in nonlinear control. This is the case of piecewise linearization [8], where the plant model is linearized around a nominal operating point, and there are applied linear control techniques to the controller development. This approach divides the input space into crisp subspaces, and the result is in a non-smooth connection of the linear subsystems to build the closed-loop system model. These models are based on the division of the input space into fuzzy subspaces and use linear local models in each subspace. Furthermore, the fuzzy sets F_i^l and the inference method permit the smooth connection of the local models to build the fuzzy dynamic global model of the closed-loop system.

To control the TISO LTV plant (3.5) there is proposed a TS fuzzy controller with the following model:

$$R^l: \text{IF } z_1(t) \text{ is } F_1^l \text{ AND } z_2(t) \text{ is } F_2^l \text{ AND } \dots \text{ AND } z_n(t) \text{ is } F_n^l, \quad \text{THEN } u(s) = C_l(s)e(s),\ l = 1 \dots m, \tag{4.1}$$

where $e(s)$ is the Laplace transform of the control error $e(t) = r(t) - y(t)$; $r(t)$ is the reference input; $C_l(s)$ – the t.f. of the local controllers, $l = 1 \dots m$.

The local controllers in (4.1) are developed for the local analytic (linear) models in (3.1) by parallel distributed compensation [10]. By the feedback connection of the plant (3.1) and of the fuzzy controller (4.1) in terms of the conventional control structure presented in figure 4.1, the closed-loop system can be described by the following fuzzy dynamic local model:

$$R^l: \text{IF } z_1(t) \text{ is } F_1^l \text{ AND } z_2(t) \text{ is } F_2^l \text{ AND } \dots \text{ AND } z_n(t) \text{ is } F_n^l, \quad \text{THEN } y(s) = H_{r,l}(s)r(s) + H_{v,l}(s)v(s),\ l = 1 \dots m, \tag{4.2}$$

where $H_{r,l}(s)$ and $H_{v,l}(s)$ - the local t.f.s of the closed-loop system, $l = 1 \dots m$.

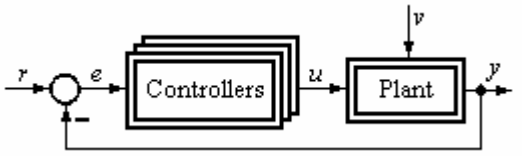

Figure 4.1
Control system structure.

In the conditions (3.3) … (3.5), by accepting the same inference method and defuzzification method as in the previous Section, the fuzzy dynamic global model of the closed-loop system can be expressed in terms of (4.3):

$$\begin{aligned} &y(s) = H_r(s)r(s) + H_v(s)v(s), \\ &H_r(s) = \sum_{l=1}^{m} \mu_l(t)H_{r,l}(s),\ H_v(s) = \sum_{l=1}^{m} \mu_l(t)H_{v,l}(s), \end{aligned} \tag{4.3}$$

where the inferred t.f.s $H_r(s)$ and $H_v(s)$ have time-varying coefficients. It is justified to consider the TS fuzzy model (4.3) as TISO LTV system; for its analysis there can be applied methods specific to LTV systems [8] … [10] which require numerical techniques for the calculation of $H_r(s)$ and $H_v(s)$.

For the development of the fuzzy controllers it is necessary to perform the stability analysis and testing; a stability analysis test algorithm for the closed-loop system (4.3) are presented in the next Section.

5 Stability Test Algorithm

To perform the stability analysis of the fuzzy control systems two approaches can be employed:

- the first one, based on the use of the fuzzy dynamic global model (4.3) and,
- the second one can be developed by starting with the definition of a piecewise smooth quadratic Lyapunov function [10], [11] based on the fuzzy dynamic local model (4.2).

In the case of the system (4.2) there can be used several approaches based on either transferring the ideas from hybrid systems [10] or by using, since this system can be considered as a variable structure one with possible discontinuous right-hand side, stability analysis methods dedicated to variable structure systems [11].

For the stability analysis and testing of the fuzzy control system modeled by the fuzzy dynamic global model (4.3) it will be presented as follows the first approach, based on the Lyapunov stability theory in terms of the definition of a piecewise smooth quadratic Lyapunov function V:

$$V = \sum_{l=1}^{m} q_l V_l, \; \mathrm{V}_l = \mathbf{x}^T \mathbf{P}_l \mathbf{x}, \tag{5.1}$$

where $\mathbf{x}$ – the state vector, dim $\mathbf{x}$ = (1, n_S), $\mathbf{P}_l$ – positive definite symmetric matrices, dim $\mathbf{P}_l$ = (n_S, n_S), q_l – weighting coefficients ensuring the smoothness of the function V, $l = 1 \ldots m$, n_S – system order.

The matrices $\mathbf{P}_l$ are obtained by ensuring the negative definiteness of the derivative of the Lyapunov function. This can be ensured by solving the algebraic Riccati equations (5.2):

$$\mathbf{A}_l^T \mathbf{P}_l + \mathbf{P}_l \mathbf{A}_l = -\mathbf{Q}_l, \; l = 1 \ldots m, \tag{5.2}$$

with $\mathbf{Q}_l$ – positive definite symmetric matrices, dim $\mathbf{Q}_l$ = (n_S, n_S), and $\mathbf{A}_l$ – the system matrices in the systemic realizations corresponding to the closed-loop transfer functions $H_{r,l}(s)$ and $H_{v,l}(s)$, dim $\mathbf{A}_l$ = (n_S, n_S).

The stability analysis test algorithm consists in four steps, detailed in [13]. Resuming:

- Step 1: based on the knowledge and experience concerning the controlled plant operation, determine the number of inference rules m for controlling the plant, the partition of the input space in fuzzy regions, assign the linguistic terms F_i^l to the measurable plant variables $z^i(t)$, $i = 1 \ldots n$, and define the membership functions corresponding to F_i^l, $l = 1 \ldots m$;

- Step 2: for each inference rule R^l, $l = 1 \dots m$, derive the linear local models of the plant, characterized by the transfer functions $P_l^u(s)$ and $P_l^v(s)$;
- Step 3: develop a conventional controller with the transfer function $H_{C,l}(s)$ for each of the local models of the plant by a linear control development technique such that the m closed-loop local systems, with the transfer functions $H_{r,l}(s)$ and $H_{v,l}(s)$, $l = 1 \dots m$, have the required control system performance;
- Step 4: set the values of the positive definite symmetric matrices $\mathbf{Q}_l$ and solve the algebraic Riccati equations (5.2); if the solutions $\mathbf{P}_l$ of (5.2) prove to be not positive definite, then jump to the step 3; otherwise, the system is stable.

The solving of the algebraic Riccati equations (5.2) and the required analysis requires the largest computational effort.

6 Application: Winding System Control Solution

A typical application for electrical drives with variable inertia (Variable Inertia Drive System, VIDS) is in the field of rolling mills and of winding mechanisms. The control of such systems represents a difficult task due to:

- the existence of output coupling between several subsystems requires the development of control systems with reference input compensation;
- the presence of possible oscillations due to the elasticity of the shaft;
- the nonlinearities of the controlled plant including backlash and stick-slip;
- the modification of the inertia during the plant operation determine time-varying parameters of the controlled plant.

The simplified functional diagram and the informational diagram of an electrical drive with DC motor variable inertia appearing in applications where a strip is winded on a drum are shown in Fig. 6.1-a and -b [12]. In the winding process, the reference input must be correlated with the modification of work roll radius. In this context, two basic aspects occur at the development of the control structure: the modification of the reference input ($\omega_0(t)$), and tuning the controller parameters.

For the first one, the condition (6.1) must be fulfilled by the control solution:

$$v(t) = \text{const} \rightarrow \omega_o(t) = k/r(t), \tag{6.1}$$

where by the measurement of $r(t)$ there can be ensured the continuous modification of the reference input $\omega_o(t)$.

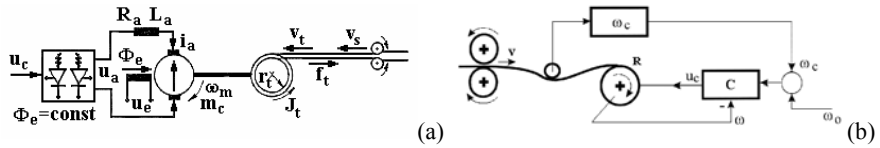

Figure 6.1
Functional diagram of VIDS and reference input correction system.

The problem of controlling the speed of the winding system can be solved in various ways: by the use of a cascade control structure with two, current and speed, controllers, or by the use of a state feedback control structure. For both versions, the variance of the moment of inertia, according to (6.2):

$$J(t) = (1/2)\,\rho\ \pi\ l\,R^4(t), \tag{6.2}$$

requires much attention in the controller design. In this paper will be presented a solutions based on control loops with linear PI and PI-fuzzy controllers with parameter adaptation.

The state-space mathematical model of VIDS has the state variables $\{x_1=i_a,\ x_2=\omega_m,\ x_3=f_t\}$, and a corresponding informational block diagram given in figure 6.2 [12].

$$\begin{aligned}
&x_1'(t)=-(R_a/L_a)x_1(t)-(k_e/L_a)x_2(t)+(k_{ch}/L_a)u_c(t)\ ,\\
&x_2'(t)=(k_m/J_e(t))x_1(t)-(1/J_e(t))m_f(x_2(t))-(r_t(t)/J_e(t))x_3(t))-(1/J_e(t))(J_e'(t))r_t(t),\\
&x_3'(t)=c_b r_t(t)x_2(t)-c_b v_s(t)\ .
\end{aligned} \tag{6.3}$$

Linearizing the models in some representive functional points, mathematical models (benchmark t.f.s) in form of (1.1) and (1.2) can be obtained.

Concerning the local linearized plant models (1.1), (1.2), the speed controller design is based on the tuning methods described in chapter 2, applied in its various, dedicated versions [2], [4], [6]. An atractive tuning version, regarding TS fuzzy models, TS fuzzy controllers and TS fuzzy closed-loop system models (Sections 3 and 4), by accepting that the controller parameters ensure a maximum phase reserve for each local linearised plant model and the corresponding TISO LTV systems are handled as in Sections 3-5. It can be considered equivalent with a re-tuning of the controller parameters as function of radius modification. This version permits the obtaining of better control system performance.

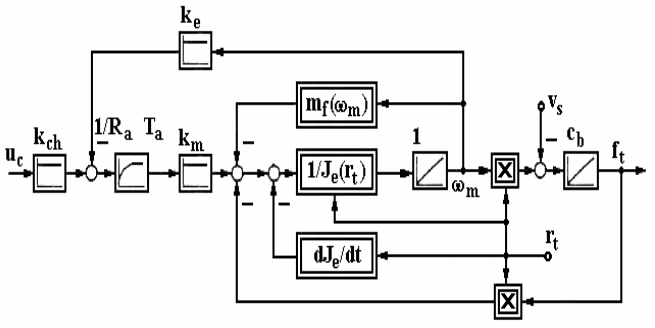

Figure 6.2
Informational block diagram of VIDS.

The envisaged control structure contains two loops, the inner regarded to the curent and the external regarded to the speed. The inner loop controller is calculated based on the Modulus Optimum method with fixed parameter values.

For the development of the speed control loop, in the development step 1 it can be used only one plant variable, r_t. For obtaining a bump-less transfer from one local controller to another at the same time with ensuring a relatively simple implementation, the authors recommend that the membership functions of the linguistic terms F_i^l should have triangular type and m should not exceed 3 or 5.

Some details regarding the development step 3 dedicated to the development of the local controllers are presented as follows.

For the considered controlled plant, after linearization in the vicinity of some significant operating points the model can be brought to a simplified form characterized by the following local transfer functions:

$$P_l^u(s) = \frac{k_P}{s(1+sT_\Sigma)},\ l = 1 \ldots m, \tag{6.4}$$

where the parameters:

- T_Σ (the small time constant coresponding to the sum of parasitic time constants) is a constant value, and
- k_P (the controlled plant gain) is time-varying due to the time-varying J_e; note that for the sake of simplicity the index l was omitted.

There can be used several versions of local transfer functions $P_l^v(s)$ depending on the types of disturbance inputs $v(t)$ applied to the controlled plant.

For the local plants (6.4) the use of PI controllers having the transfer functions:

$$C_l(s) = \frac{k_c}{s}(1 + sT_c),\ l = 1 \ldots m, \tag{6.5}$$

can ensure very good control system performance when the controllers are tuned in terms of the ESO-m [2]; the controller parameters are k_c (the controller gain) and T_c (the integral time constant) (see table 2.3). By the choice of the parameter $\beta = 9 \ldots 14$ the control structure ensures a good maximum phase reserve ($55^0 < \varphi_{r,m} < 60^0$); this phse reserve is changing during the plant operating. The choice of such a value ensures good robustnes, so that the stability analysis was not performed.

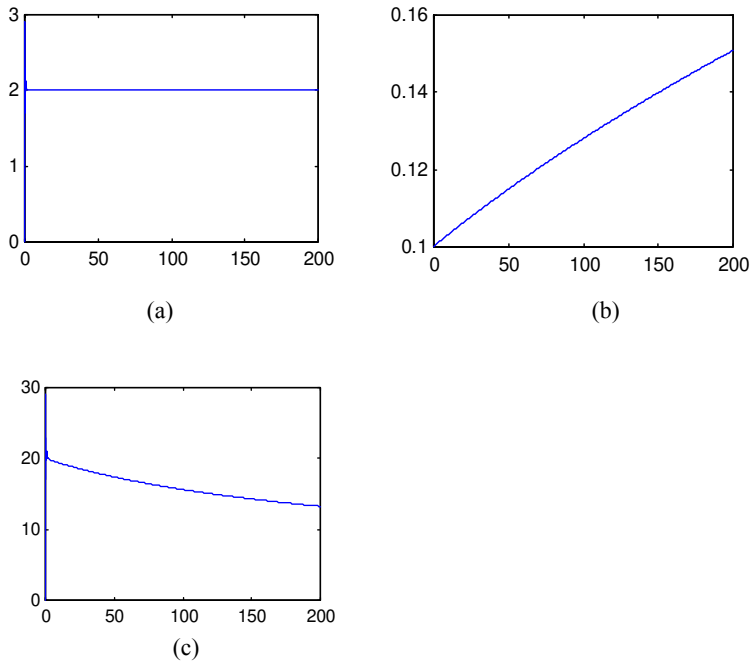

Figure 6.3
Simulation results

The local control system performance can be improved by adding a first- or second-order reference filter [2], [6]. This is the way the control structure obtains the features specific to control structures with 2 DOF controllers.

For to test the method, a theoretical application closely connected to practice was considered. The non-linear Simulink model of the plant is presented in Appendix 1. Three PI controllers were calculated and the change of the controllers during the plant operating was based on a very simple fuzzy selection rule. The problem of bump-less transfer from one local crisp controller to another is solved in a crisp manner.

Some simulation results are presented in figure 6.3: (a) the change of the linear speed, v(t); (b) the change of the radius changing r(t); (c) the change of the angular speed, ω(t).

The results can be accepted as good and confirm the possibilitie of use Takagi-Sugeno fuzzy models to represent a TISO LTV as models of the controlled plant.

Conclusions

The paper presents continuous-time development solutions for electrical drives with variable inertia. The tuning relations are deduced for classical but generally accepted benchmark type plant models.

The presented TS fuzzy models dedicated to TISO LTV systems are suitable for control structures where the plant mathematical model linearization offers local linear models.

A stability test algorithm for the fuzzy control systems modeled by TS fuzzy models based on Lyapunov stability theory is presented. The main limitation of the stability analysis algorithm concerns its computational complexity.

The models and the stability analysis algorithm can be used in the development of conventional but also of TS fuzzy controllers based on the parallel distributed compensation with several applications. One real-world application can be in the area of electrical drives with variable inertia, where the development of the local controllers can be performed in terms of the ESO-m or 2E-SO-m.

The simulated application is regarded to a VIDS where the reference input must be correlated with the modification of working roll radius.

References

[1] Åström, K. J. and T. Hägglund: PID Controllers Theory: Design and Tuning, Instrument Society of America, Research Triangle Park, 1995

[2] Preitl, St. and R.-E. Precup, An extension of tuning Relations after symmetrical optimum method for PI and PID controllers, Automatica, Elsevier Science, vol. 35, pp. 1731 – 1736, 1999

[3] Preitl, Zsuzsa, Controller development by algebraic methods. Analysis and Matlab-Simulink programs (in romanian). Master thesis, "Politehnica" University of Timişoara, Romania, 2003

[4] Precup, R.-E. and St. Preitl, Development of Some Fuzzy Controllers with Non-homogenous Dynamics with Respect to the Input Channels Meant for a Class of Systems, *Proceedings of ECCC-1999,* (e-format) Karlsruhe, Germany

[5] Preitl, St., R.-E. Precup, Zsuzsa Preitl, Two Degree of Freedom Fuzzy Controllers: Structure and Development, Proceedings of the "In

Memoriam John von Neumann" Symposium, December, 2003, ISBN 963-7154-21-3, pp. 49 – 60, Budapest, Hungary

[6] Preitl, Zsuzsa, PI and PID Controller Tuning Method for a Class of Systems, SACCS 20017th International Symposium on Automatic Control and Computer Science, October 2001, Iasi, Romania (e-format)

[7] Preitl St. and R.-E. Precup, On the Fuzzy Control of a Class of Linear Time-Varying Systems, A&QT-R 2004, IEEE-TTC- Conference on Automation, Quality and Testing, Robotics, May 13–15, 2004, Cluj-Napoca, Romania

[8] Kóczy, L. T., Fuzzy If-Then Rule Models and Their Transformation into One Another. IEEE Trans. on SMC – part A, 26, (1996) 621-637

[9] H. O. Wang, K. Tanaka and M. F. Griffin, An Approach to Fuzzy Control of Nonlinear Systems: Stability and Design Issues, IEEE Transactions on Fuzzy Systems, (1996), vol. 4, pp. 14 – 23

[10] M. Johansson and A. Rantzer, Computation of Piecewise Quadratic Lyapunov Functions for Hybrid Systems, IEEE Transactions on Automatic Control, (1998), vol. 43, pp. 555 – 559

[11] M. Johansson, A. Rantzer and K. -E. Arzen, Piecewise Quadratic Stability of Fuzzy Systems, IEEE Transactions on Fuzzy Systems, (1999), vol. 7, pp. 713 – 722

[12] St. Preitl and R.-E. Precup. "PI controller design for speed control of DC drives with variable moment of inertia". Bul.St. U.P.T., Trans. AC&CS. Timisoara, Vol. 42(56), pp. 97 – 105. 1997

[13] St. Preitl, R.-E. Precup, On the Fuzzy Control of a Class of Linear Time-Varying Systems, AQTR 2004 (THETA 14), IEEE-TTTC- Conference on Automation, Quality and Testing, Robotics May, 2004, Cluj-Napoca, Romania

Appendix 1. The non-linear Simulink model of the plant

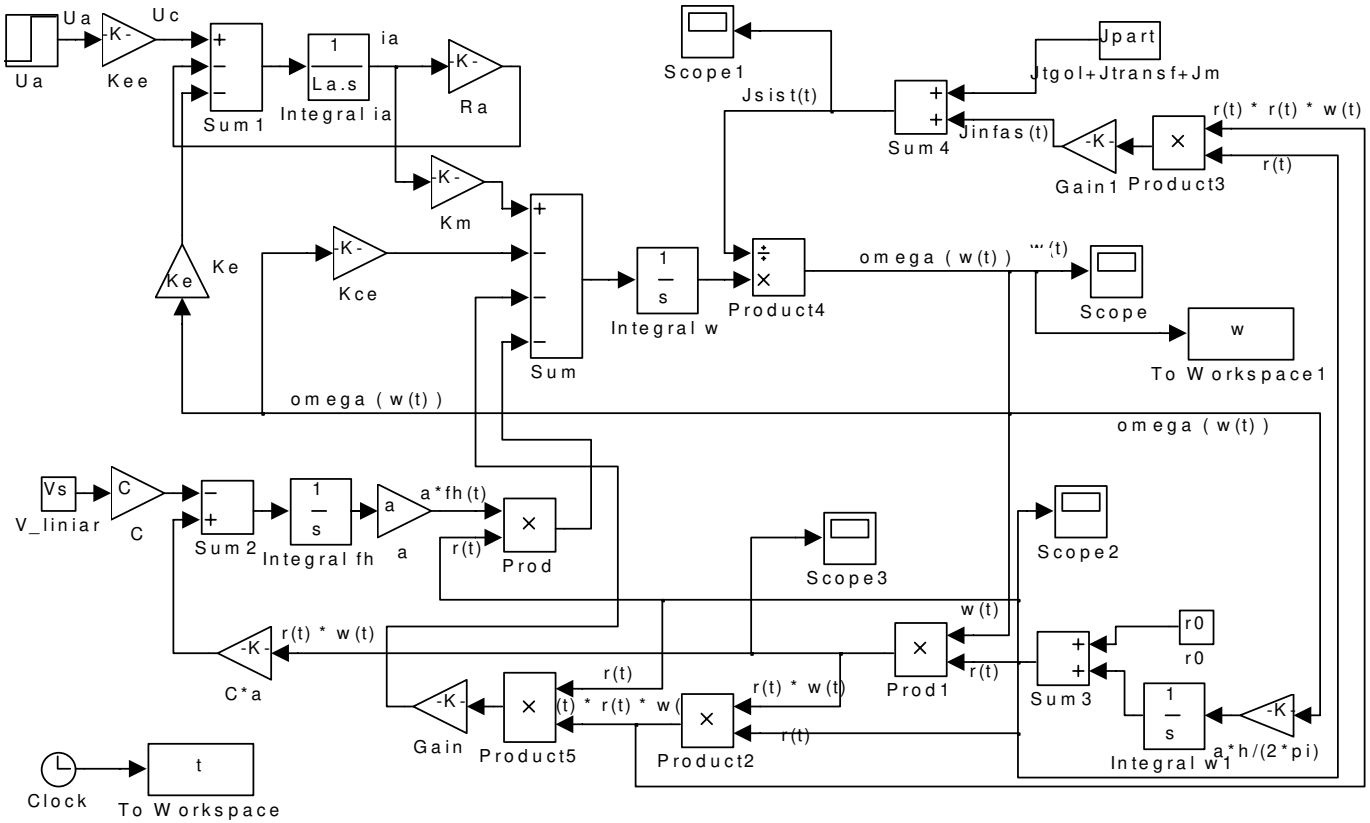

Interpolation-based Fuzzy Reasoning as an Application Oriented Approach

Szilveszter Kovács

Department of Information Technology, University of Miskolc,
Miskolc-Egyetemváros, Miskolc, H-3515, Hungary
szkovacs@iit.uni-miskolc.hu

Intelligent Integrated Systems Japanese Hungarian Laboratory,
Budapest University of Technology and Economics, Hungary

Abstract: Some difficulties emerging during the construction of fuzzy rule bases are inherited from the type of the applied fuzzy reasoning. The fuzzy rule base requested for many classical reasoning methods needed to be complete. In case of fetching fuzzy rules directly from expert knowledge, the way of building a complete rule base is not always straightforward. One simple solution for overcoming the necessity of the complete rule base is the application of interpolation-based fuzzy reasoning methods, since interpolation-based fuzzy reasoning methods can serve usable (interpolated) conclusion even if none of the existing rules is hit by the observation. These methods can save the expert from dealing with derivable rules and help to concentrate on cardinal actions only. For demonstrating the benefits of the interpolation-based fuzzy reasoning methods in construction of fuzzy rule bases a simple example will be introduced briefly in this paper too.

Keywords: Interpolation-based Fuzzy reasoning, rule base construction

1 Introduction

Since the classical fuzzy reasoning methods (e.g. compositional rule of inference) are demanding complete rule bases, the classical rule base construction claims a special care of filling all the possible rules. In case if there are some rules missing, there are observations may exist which hit no rule in the rule base and therefore no conclusion is obtained. Having no conclusion in a fuzzy control structure is hard to explain. E.g. one solution could be to keep the last real conclusion instead of the missing one, but applying historical data automatically to fill undeliberately missing rules could cause unpredictable side effects. Another solution for the same problem is the application of the interpolation-based fuzzy reasoning methods, where the derivable rules are deliberately missing. Since the rule base of a fuzzy interpolation-based controller, is not necessarily complete, it could contain the

most significant fuzzy rules only without risking the chance of having no conclusion for some of the observations. In other words, during the construction of the fuzzy rule base, it is enough to concentrate on the cardinal actions; the "filling" rules (rules could be deduced from the others) can be deliberately omitted.

In the followings, first an approximate fuzzy reasoning method based on interpolation in the vague environment of the fuzzy rule base [4], [5], [6] will be introduced. The main benefit of the proposed method is its simplicity, as it could be implemented to be simple and quick enough to be applied in practical direct fuzzy logic control too. Then its adaptation to fuzzy control structures through a simple rule base construction example will be discussed briefly.

2 Interpolation-based Fuzzy Reasoning

One way of interpolative fuzzy reasoning is based on the concept of vague environment [2]. Applying the idea of the vague environment the linguistic terms of the fuzzy partitions can be described by scaling functions [2] and the fuzzy reasoning itself can be replaced by classical interpolation. The concept of vague environment is based on the similarity or indistinguishability of the elements. Two values in the vague environment are ε-distinguishable if their distance is grater than ε. The distances in vague environment are weighted distances. The weighting factor or function is called *scaling function (factor)* [2]. Two values in the vague environment X are ε-distinguishable if

$$\varepsilon > \delta_s(x_1, x_2) = \left| \int_{x_2}^{x_1} s(x)dx \right| , \tag{1}$$

where $\delta_s(x_1, x_2)$ is the vague distance of the values x_1, x_2 and $s(x)$ is the scaling function on X. For finding connections between fuzzy sets and a vague environment the membership function $\mu_A(x)$ can be introduced as a level of similarity **a** to x, as the degree to which x is indistinguishable to **a** [2]. The □-cuts of the fuzzy set $\mu_A(x)$ are the sets which contain the elements those are ($\tilde{1}$□)-indistinguishable from **a** (see fig. 1):

$$\delta_s(\mathrm{a},\mathrm{b}) \le 1-\alpha \ , \quad \mu_A(x) = 1 - \min\{\delta_s(\mathrm{a},\mathrm{b}),1\} = 1 - \min\left\{\left|\int_{\mathrm{a}}^{\mathrm{b}} s(x)dx\right|,1\right\} . \tag{2}$$

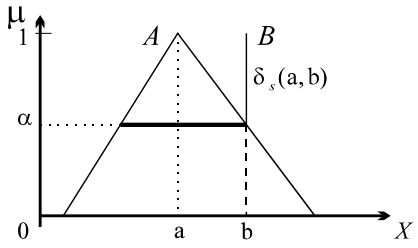

Figure 1
The □-cuts of $\mu_A(x)$ contains the elements that are (1-□)-indistinguishable from a

This case (see fig. 1) the vague distance of points a and b ($\delta_s(\mathrm{a},\mathrm{b})$) is the *Disconsistency Measure* (S_D) of the fuzzy sets *A* and *B* (where *B* is a singleton):

$$S_D = 1 - \sup_{x \in X} \mu_{A \cap B}(x) = \delta_s(\mathrm{a},\mathrm{b}) \text{ if } \delta_s(\mathrm{a},\mathrm{b}) \in [0,1], \quad \textbf{(3)}$$

where $A \cap B$ is the min t-norm, $\mu_{A \cap B}(x) = \min[\mu_A(x), \mu_B(x)]$ $\forall\, x \in X$.

From the viewpoint of fuzzy reasoning and fuzzy rule bases, where an observation fuzzy set is needed to be compared to rule antecedents built up member fuzzy sets (linguistic terms) of the antecedent fuzzy partitions (2) and (3) means that the disconsistency measures between member fuzzy sets of a fuzzy partition and a singleton, can be calculated as vague distances of points in the vague environment of the fuzzy partition. The main difference between the disconsistency measure and the vague distance is, that the vague distance is a value in the range of [0,∞], while the disconsistency measure is limited to [0,1].

Therefore if it is possible to describe all the fuzzy partitions of the primary fuzzy sets (the antecedent and consequent universes) of the fuzzy rule base by vague environments, and the observation is a singleton, the "extended" disconsistency measures of the antecedent primary fuzzy sets of the rule base, and the "extended" disconsistency measures of the consequent primary fuzzy sets and the consequence can be calculated as vague distances of points in the antecedent and consequent vague environments.

The vague environment is described by its scaling function. For generating a vague environment of a fuzzy partition an appropriate scaling function is needed to be find, which describes the shapes of all the terms in the fuzzy partition. A fuzzy partition can be characterised by a single vague environment if and only if the membership functions of the terms fulfil the following requirement [2]:

$$s(x) = |\mu'(x)| = \left|\frac{d\mu}{dx}\right| \text{ exists iff } \min\{\mu_i(x), \mu_j(x)\} > 0 \Rightarrow |\mu'_i(x)| = |\mu'_j(x)|, \quad \textbf{(4)}$$

$\forall i, j \in I$, where $s(x)$ is the vague environment (see e.g. on fig. 2 and fig. 3).

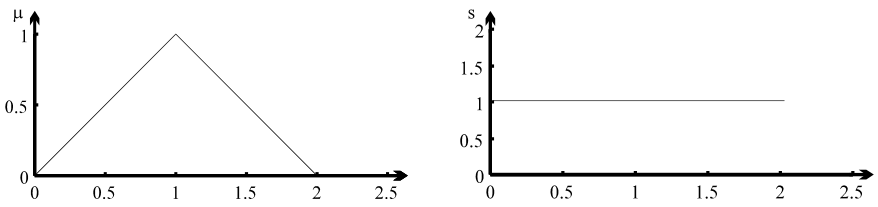

Figure 2
A fuzzy set and its scaling function

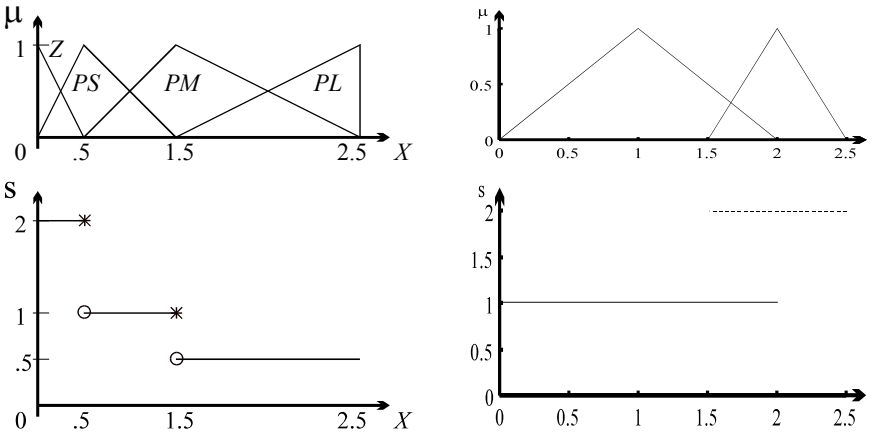

There is a scaling function $s(x)$ exists, which describes all the fuzzy sets

There is no scaling function, which describes both the fuzzy sets

Figure 3
A fuzzy partition and its scaling function

Generally condition (4) is not fulfilling, so the question is how to describe all fuzzy sets of the fuzzy partition with one "universal" scaling function. For this task the concept of *approximate scaling function*, as an approximation of the scaling functions describes the terms of the fuzzy partition separately is proposed. See e.g. a partition built-up triangular fuzzy sets on fig. 4 and the corresponding approximate scaling functions on fig. 5 (linear interpolation) and fig. 6 (non-linear interpolation). See more detailed the questions of approximate scaling functions in [4], [5], [6].

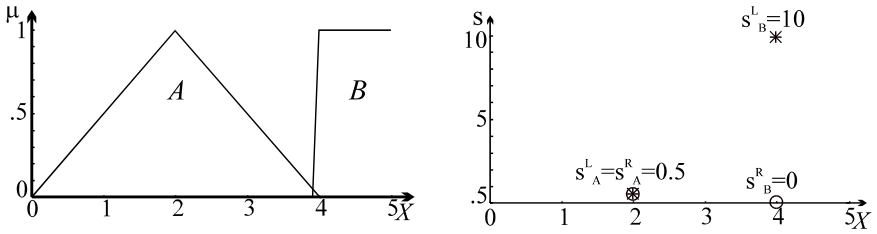

Figure 4

Fuzzy partitions built-up triangular fuzzy sets can be characterised by triples, by the values of the left s^L and the right s^R scaling factors and the cores.

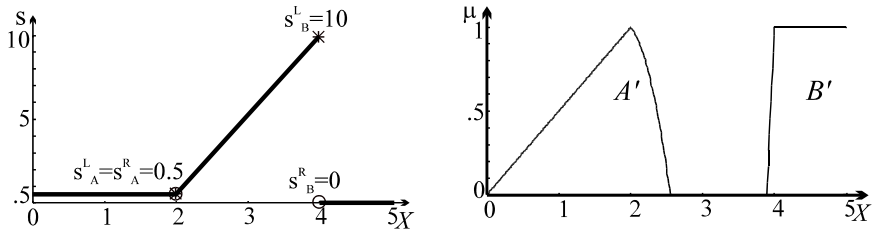

Figure 5

Linearly interpolated scaling function of the fuzzy partition shown on fig. 4, and the partition as the approximate scaling function describes it (*A'*,*B'*).

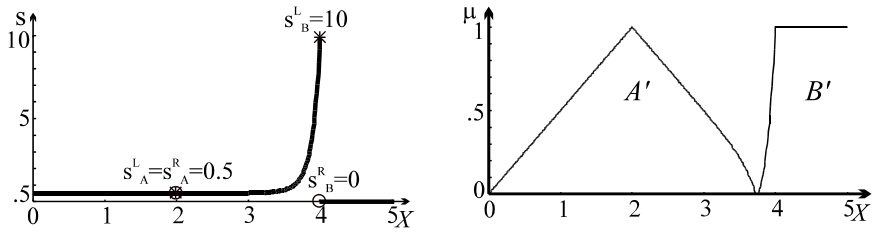

Figure 6

Approximate scaling function generated by non-linear interpolation [4], [5], [6] of the fuzzy partition shown on fig.4., and the partition as the approximate scaling function describes it (*A'*,*B'*).

If the vague environment of a fuzzy partition (the scaling function or the approximate scaling function) exists, the member sets of the fuzzy partition can be characterised by points in the vague environment. (These points are characterising the cores of the fuzzy terms, while the membership functions are described by the scaling function itself.) If all the vague environments of the antecedent and consequent universes of the fuzzy rule base are exist, all the primary fuzzy sets (linguistic terms) built-up the fuzzy rule base can be characterised by points in their vague environment. Therefore the fuzzy rules (built-up from the primary

fuzzy sets) can be characterised by points in the vague environment of the fuzzy rule base too. This case the approximate fuzzy reasoning can be handled as a classical interpolation task. Applying the concept of vague environment (the distances of points are weighted distances), any interpolation, extrapolation, or regression methods can be adapted very simply for approximate fuzzy reasoning [4], [5], [6].

Because of its simple multidimensional applicability, for interpolation-based fuzzy reasoning in this paper the adaptation of the *Shepard operator* based interpolation (first introduced in [1]) is suggested. Beside the existing deep application oriented investigation of the Shepard operator e.g. [3], it is also successfully applied in the *Kóczy-Hirota fuzzy interpolation* [12]. (The stability and the approximation rate of the Shepard operator based Kóczy-Hirota fuzzy interpolation is deeply studied in [7] and [8].) The Shepard interpolation method for arbitrarily placed bivariate data was introduced as follows [1]:

$$S_0(f,x,y)=\begin{cases} f_k & \text{if } (x,y)=(x_k,y_k) \text{ for some } k, \\ \left(\sum_{k=0}^{n} f(x_k,y_k)/d_k^{\lambda}\right)\Big/\left(\sum_{k=0}^{n} 1/d_k^{\lambda}\right) & \text{otherwise,} \end{cases} \qquad (5)$$

where measurement points x_k, y_k ($k \in [0,n]$) are irregularly spaced on the domain of $f \in \Re^2 \to \Re$, $\lambda > 0$, and $d_k = \left[(x-x_k)^2+(y-y_k)^2\right]^{1/2}$. This function can be typically used when a surface model is required to interpolate scattered spatial measurements.

The adaptation of the Shepard interpolation method for interpolation-based fuzzy reasoning in the vague environment of the fuzzy rule base is straightforward by substituting the Euclidian distances d_k with vague distances $\delta_{s,k}$:

$$\delta_{s,k} = \delta_s(\mathbf{a}_k,\mathbf{x}) = \left[\sum_{i=1}^{m}\left(\int_{a_{k,i}}^{x_i} s_{X_i}(x_i)\,dx_i\right)^2\right]^{1/2}, \qquad (6)$$

where s_{X_i} is the i^{th} scaling function of the m dimensional antecedent universe, $\mathbf{x}$ is the m dimensional crisp observation and $\mathbf{a}_k$ are the cores of the m dimensional fuzzy rule antecedents $\boldsymbol{A}_k$.

Thus in case of singleton rule consequents fuzzy rules R_k

If $x_1 = A_{k,1}$ **And** $x_2 = A_{k,2}$ **And** … **And** $x_m = A_{k,m}$ **Then** $y = c_k$ (**7**)

by substituting (6) to (5) the conclusion of the interpolative fuzzy reasoning can be obtained as:

$$y(\mathbf{x}) = \begin{cases} c_k & \text{if } \mathbf{x} = \mathbf{a}_k \text{ for some } k, \\ \left(\sum_{k=1}^{r} c_k / \delta_{s,k}^{\lambda}\right) \Big/ \left(\sum_{k=1}^{r} 1/\delta_{s,k}^{\lambda}\right) & \text{otherwise.} \end{cases} \quad (\mathbf{8})$$

The interpolative fuzzy reasoning (8) can simply extend to be able to handle fuzzy conclusions by introducing the vague environment (scaling function) of the consequence universe. This case the fuzzy rules R_k has the following form:

If $x_1 = A_{k,1}$ **And** $x_2 = A_{k,2}$ **And** … **And** $x_m = A_{k,m}$ **Then** $y = B_k$ (**9**)

By introducing vague distances on the consequence universe:

$$\delta_s(b_k, y) = \left[\left(\int_{b_k}^{y} s_Y(y)dy\right)^2\right]^{1/2}, \quad (\mathbf{10})$$

where s_Y is the i^{th} scaling function of the one dimensional consequent universe, b_k are the cores of the one dimensional fuzzy rule consequents B_k.

Introducing the first element of the one dimensional consequence universe b_0 the (Y: $b_0 \le y \quad \forall \; y \in Y$), based on (8) and (10) the requested one dimensional conclusion $y(\mathbf{x})$ can be obtained from the following formula:

$$\delta_s(y(\mathbf{x}), b_0) = \begin{cases} \delta_s(b_k, b_0) & \text{if } \mathbf{x} = \mathbf{a}_k \text{ for some } k, \\ \left(\sum_{k=1}^{r} \delta_s(b_k, b_0)/\delta_{s,k}^{\lambda}\right) \Big/ \left(\sum_{k=1}^{r} 1/\delta_{s,k}^{\lambda}\right) & \text{otherwise.} \end{cases} \quad (\mathbf{11})$$

A simple one-dimensional example for the approximate scaling function and the Shepard operator based interpolation (11) is introduced on fig. 7-10.

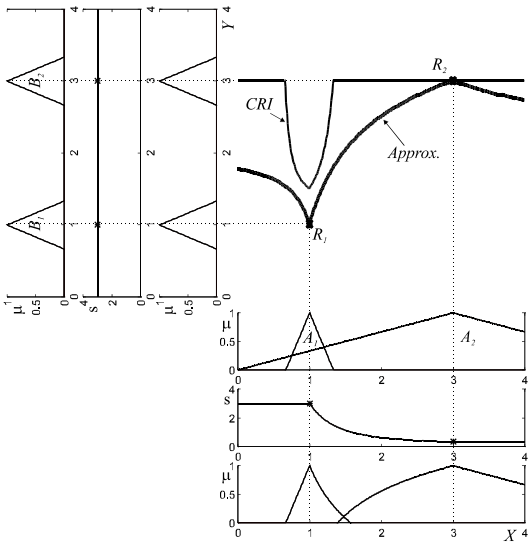

Figure 7
Interpolation of two fuzzy rules (R_i: $A_i \rightarrow B_i$) (see fig. 10 for notation)

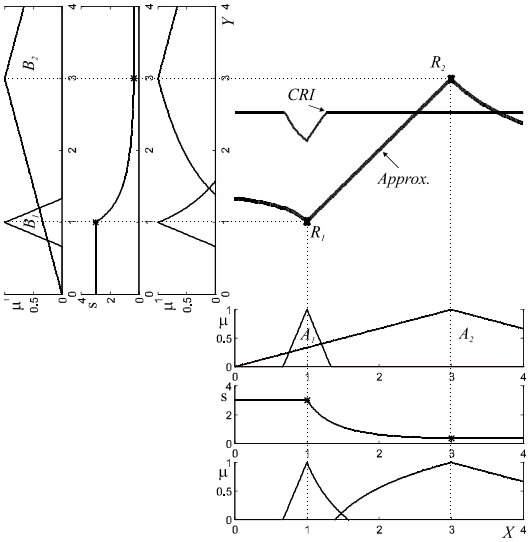

Figure 8
Interpolation of two fuzzy rules (R_i: $A_i \rightarrow B_i$) (see fig. 10 for notation)

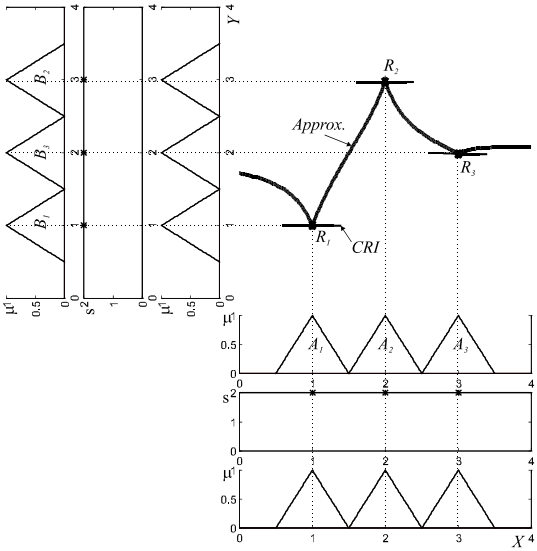

Figure 9
Interpolation of three fuzzy rules (R_i: $A_i \rightarrow B_i$) (see fig. 10 for notation)

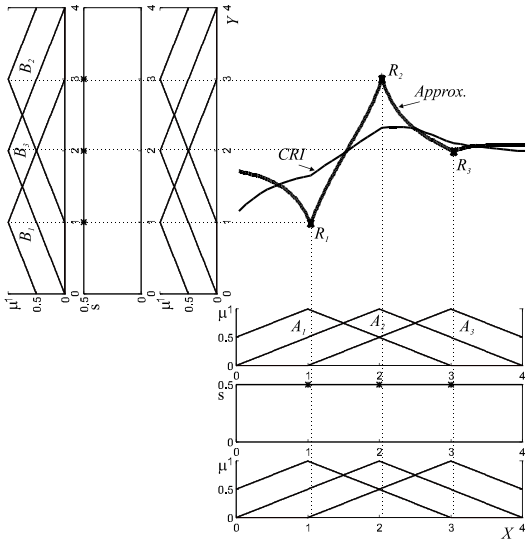

Figure 10
Interpolation of three fuzzy rules (R_i: $A_i \rightarrow B_i$) in the approximated vague environment of the fuzzy rule base, using the Shepard operator based interpolation (11) ($\lambda = 1$) (*Approx.*), and the min-max. CRI with the centre of gravity defuzzification (CRI), where μ is the membership grade, and s is the scaling function.

For comparing the crisp conclusions of the interpolation-based fuzzy reasoning and the classical methods, the conclusions generated by the max-min compositional rule of inference (CRI) and the centre of gravity defuzzification for the same rule base is also demonstrated on the example figures (fig. 7-10). More detailed description of the proposed approximate fuzzy reasoning method can be found in [4], [5], [6].

3 Application Example

The main benefit of the interpolation-based fuzzy reasoning method, introduced in the previous chapter, is its simplicity. Applying look-up tables for pre-calculating the vague distances, it could be implemented to be simple and quick enough to fit the speed requirements of practical real-time direct fuzzy logic control systems too. The calculation efforts of many other interpolation-based fuzzy reasoning methods "wasted" for determining the exact membership shape of the interpolated fuzzy conclusion prohibits their practical application in real-time direct fuzzy logic control. The lack of the fuzziness in the conclusion is a disadvantage of the proposed method, but it has no influence in common applications where the next step after the fuzzy reasoning is the defuzzification.

For demonstrating the simplicity of defining rule base for interpolation-based fuzzy reasoning, as an example, the construction of the state-transition rule base of a user adaptive information retrieval system will be introduced briefly in the followings.

In this user adaptive information retrieval system example (introduced in [10] and [11] in more details) the user adaptivity is handled by combination of existing (off-line collected) human opinions (user models) in the function of their approximated similarity to the actual user opinions. The goal of the state-transition control is to estimate the "current state", the actual suitability of the existing user models. Based on the observations (inputs) – the conclusion of the user feedback (the similarity of the user feedback to the existing user models SS_i for all the possible models $\forall i \in [1, N]$) and the previous state S_i (estimation) the state-transition rule base has to estimate the new state values, the next approximation of the vector of the suitability of the existing user models.

The heuristic we would like to implement in our example is very simple. If we already found a suitable model (S_i) and the user feedback is still supporting it (SS_i), we have to keep it even if the user feedback began to support some other models too. If there were no suitable model, but the user feedback began to support one, we have to pick it at once. In case of interpolation-based fuzzy reasoning, the above heuristic can be simply implemented by the following state-

transition rule base [10], [11]. For the i^{th} state variable S_i, $i \in [1, N]$ of the state vector **S**:

If S_i=One **And** SS_i=One **Then** S_i=One (**12.1**)

If S_i=Zero **And** SS_i=Zero **Then** S_i=Zero (**12.2**)

If S_i=One **And** SS_i=Zero
And SS_k=Zero **Then** S_i=One $\forall k \in [1, N], k \neq i$ (**12.3**)

If S_i=Zero **And** SS_i=One
And S_k=Zero **And** SS_k=Zero **Then** S_i=One $\forall k \in [1, N], k \neq i$ (**12.4**)

If S_i=Zero **And** SS_i=One
And S_k=One **And** SS_k=One **Then** S_i=Zero $\exists k \in [1, N], k \neq i$ (**12.5**)

where SS_i is the similarity of the user feedback to the i^{th} existing user model $\forall i \in [1, N]$; N is the number of known user models (state variables). The structure of the state-transition rules is similar for all the state variables. Zero and One are linguistic labels of fuzzy sets (linguistic terms) representing high and low similarity. The interpretations of the Zero and One fuzzy sets can be different in each S_i, SS_i universes.

Please note that rule base (12) is sparse. It contains the main rules for the following straightforward goals only: Rule (12.1) simply keeps the previously chosen state values in the case if the symptom evaluation also agrees. The rule (12.2) has the opposite meaning, if the state values were not chosen, and moreover the symptom evaluation is also disagrees the state value should be suppressed. The rule (12.3) keeps the already selected state values (previous approximation), even if the symptom evaluation disagrees, if it has no better "idea". Rules (12.4) and (12.5) have the task of ensuring the relatively quick convergence of the system to the sometimes unstable (changeable) situations, as new state variables which seem to be fit, can be chosen in one step, if there is no previously chosen state, which is still accepted by the symptom evaluation (12.4). (Rule (12.5) has the task to suppress this selection in the case if exists a still acceptable state which has already chosen.) The goal of this heuristic is to gain a relatively quick convergence for the system to fit the opinions of the actual user, if there is no state value high enough to be previously accepted. This quick convergence could be very important in many application areas e.g. in case of an on-line user adaptive selection system introduced in [10], where the user feed-back information needed for the state changes are very limited.

Some state changes of the state-transition control (fuzzy automaton) in the function of the user feedback (SS_1, SS_2) for the two states case (applying the state-transition rule base (12)) are visualised on fig. 11 and fig. 12.

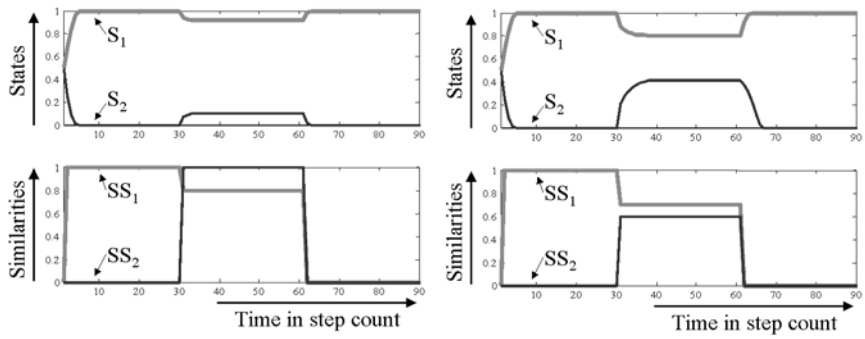

Figure 11
Do not "pick up" a new state if the previous approximation is still adequate.

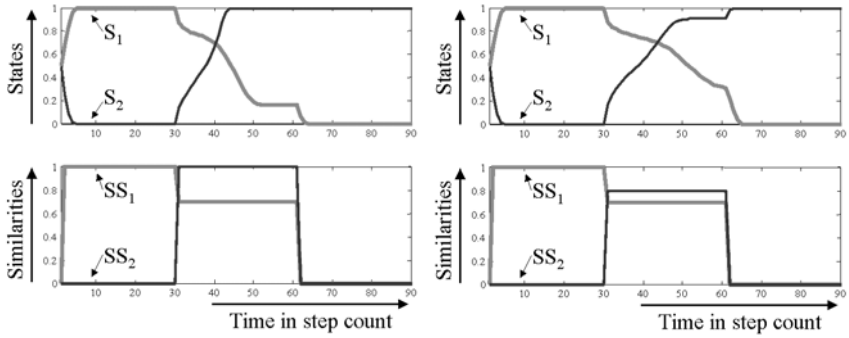

Figure 12
But "pick it up" if it seems better.

Counting the rules of the classical (e.g. compositional) fuzzy reasoning for the same strategy we find, that in the two state case the complete rule base needs 16 rules (as we have four observation universes (S_1, SS_1, S_2, SS_2) each with two terms fuzzy partitions (Zero, One) - 2^4 rules), while the sparse rule base (12) contains 5 rules only (see table 1 for the state-transition rule base of state S_1). Taking into account that in the proposed behaviour-based control structure a separate rule base is needed for each state variables, the behaviour coordination needs 32 rules, while 10 is enough in case of applying the proposed interpolation-based fuzzy reasoning method. Increasing the number of the state variables the situation became even worse. In case of three state variables (S_1, S_2, S_3) the rate become $3 \cdot 2^6$ ($n \cdot 2^{2 \cdot n}$, where n is the number of the states) and $3 \cdot 6$ ($n \cdot (n+3)$) up to the interpolation-based method (see table 2).

Table 1
State-transition rule base of state S_1 in case of two state variables (S_1,S_2) according to rule base (12)

R_{S1}:	S_1	SS_1	S_2	SS_2	S_1	
1.,	One	One			One	(according to (12.1))
2.,	Zero	Zero			Zero	(according to (12.2))
3.,	One	Zero		Zero	One	(according to (12.3))
4.,	Zero	One	Zero	Zero	One	(according to (12.4))
5.,	Zero	One	One	One	Zero	(according to (12.5))

Table 2
State-transition rule base of state S_1 in case of three state variables (S_1,S_2,S_3) according to rule base (12)

R_{S1}:	S_1	SS_1	S_2	SS_2	S_3	SS_3	S_1	
1.,	One	One					One	(12.1)
2.,	Zero	Zero					Zero	(12.2)
3.,	One	Zero		Zero		Zero	One	(12.3)
4.,	Zero	One	Zero	Zero	Zero	Zero	One	(12.4)
5.,	Zero	One	One	One			Zero	(12.5)
6.,	Zero	One			One	One	Zero	(12.5)

The exponential rule number "explosion" in case of increasing the number of the input variables makes many heuristic ideas unimplementable and therefore useless. E.g. in the case of the original source of the example application of this paper (introduced in [10]), the behaviour coordination module applied for user adaptive information retrieval system had 4 state variables (one for each emotional models), which makes our simple rule base (12) practically unimplementable as a complete rule base ($4 \cdot 2^8 = 1024$ rules). While our working demonstrational example had only 28 rules thanks to the applied interpolation-based fuzzy reasoning method. A downloadable and runable code of the above mentioned application example together with the code of other examples and the code of the interpolation-based Fuzzy reasoning method introduced in this paper can be found at [13].

Conclusions

The goal of this paper was to introduce an interpolation-based fuzzy reasoning method, which could be implemented to be simple and quick enough to fit the

requirements of real-time direct fuzzy logic control systems. The suggested approximate fuzzy reasoning method based on interpolation in the vague environment of the fuzzy rule base gives an efficient way for designing direct fuzzy logic control applications. The lack of the fuzziness in the conclusion is a disadvantage of the proposed method, but it has no influence in common applications where the next step after the fuzzy reasoning is the defuzzification.

To give some guidelines for interpolation-based fuzzy reasoning rule base design, some highlights of the state-transition rule base of a user adaptive information retrieval system application ([10], [11]) is also introduced in this paper.

The implementation of interpolation-based fuzzy reasoning methods in fuzzy control structures simplifies the task of fuzzy rule base creation. Since the rule base of a fuzzy interpolation-based controller is not necessarily complete, it could contain the most significant fuzzy rules only without risking the chance of having no conclusion for some of the observations. In other words, during the construction of the fuzzy rule base, it is enough to concentrate on the cardinal actions; the "filling" rules (rules could be deduced from the others) could be deliberately omitted. Thus, compared to the classical fuzzy compositional rule of inference, the number of the fuzzy rules needed to be handled during the design process could be dramatically reduced.

The necessity of the complete rule base in many classical fuzzy reasoning methods (e.g. max-min CRI) and hence the exponential rule number "explosion" in case of increasing the number of the input variables makes numerous rule base ideas unimplementable and therefore useless. The application of interpolation-based fuzzy reasoning methods could provide some implementation chances for many of them (see e.g. our simple example in section 3).

Acknowledgements

This research was supported by the Japan Gifu Prefecture Research Institute of Manufacturing Information Technology and the Intelligent Integrated Systems Japanese Hungarian Laboratory.

References

[1] Shepard, D.: A two dimensional interpolation function for irregularly spaced data, Proc. 23rd ACM Internat. Conf., (1968) 517-524

[2] Klawonn, F.: Fuzzy Sets and Vague Environments, Fuzzy Sets and Systems, 66 (1994) 207-221

[3] Barnhill, R., Dube, R., Little, F.: Properties of Shepard's surfaces, Rocky Mountain J. Math. 13 (1991) 365–382

[4] Kovács, Sz.: New Aspects of Interpolative Reasoning, Proceedings of the 6th International Conference on Information Processing and Management of Uncertainty in Knowledge-Based Systems, Granada, Spain (1996) 477-482

[5] Kovács, Sz., Kóczy, L. T.: Approximate Fuzzy Reasoning Based on Interpolation in the Vague Environment of the Fuzzy Rule base as a Practical Alternative of the Classical CRI, Proceedings of the 7th International Fuzzy Systems Association World Congress, Prague, Czech Republic, (1997) 144-149

[6] Kovács, Sz., Kóczy, L. T.: The use of the concept of vague environment in approximate fuzzy reasoning, Fuzzy Set Theory and Applications, Tatra Mountains Mathematical Publications, Mathematical Institute Slovak Academy of Sciences, Bratislava, Slovak Republic, vol. 12 (1997) 169-181

[7] Tikk, D., Joó, I., Kóczy, L. T., Várlaki, P., Moser, B., Gedeon, T. D.: Stability of interpolative fuzzy KH-controllers, Fuzzy Sets and Systems, 125, (2002), 105-119

[8] Tikk, D.: Notes on the approximation rate of fuzzy KH interpolator, Fuzzy Sets and Systems, 138(2), September, (2003), 441-453

[9] Kovács, Sz.: Interpolative Fuzzy Reasoning and Fuzzy Automaton in Adaptive System Applications, Proceedings of the IIZUKA2000, 6th International Conference on Soft Computing, October 1-4, Iizuka, Fukuoka, Japan (2000) 777-784

[10] Kovács, Sz., Kubota, N., Fujii, K., Kóczy, L. T.: Behaviour based techniques in user adaptive Kansei technology, Proceedings of the VSMM2000, 6th International Conference on Virtual Systems and Multimedia, October 3-6, Ogaki, Gifu, Japan (2000) 362-369

[11] Kovács, Sz.: Fuzzy Reasoning and Fuzzy Automata in User Adaptive Emotional and Information Retrieval Systems, Proceedings of the 2002 IEEE International Conference on Systems, Man and Cybernetics, October 6-9, Hammamet, Tunisia, 02CH37349C, ISBN: 0-7803-7438-X, WP1N5 (2002) 6

[12] Kóczy, L. T., Hirota, K.: Interpolative reasoning with insufficient evidence in sparse fuzzy rule bases, Information Sciences 71, (1992) 169-201

[13] www.iit.uni-miskolc.hu/~szkovacs

Sign Language in the Intelligent Sensory Environment

Ákos Lisztes*, Ákos Antal, Andor Gaudia*, Péter Korondi***

Budapest University of Technology and Economics
*Department of Automation and Applied Informatics, Budapest, Hungary
** Department of Mechatronics, Optics and Instrumentation Technology

Abstract: It is difficult for most of us to imagine, but many who are deaf rely on sign language as their primary means of communication. They, in essence, hear and talk through their hands. This paper proposes a system which is able to recognize the signs using a video camera system. The recognized signs are reconstructed by the 3D visualization system as well. To accomplish this task a standard personal computer, a video camera and a special software system was used. At the moment the software is able to recognize several letters from the sign language alphabet with the help of color marks. The sign language recognition is a function of an Intelligent Space, which has ubiquitous sensory intelligence including various sensors, such as cameras, microphones, haptic devices (for physical contact) and actuators with ubiquitous computing background.

Keywords: sign language, deaf, image processing, marker, CCD, camera, OpenGL, WISDOM, recognition, reconstruction, intelligent space

1 Introduction

Sign languages are visual languages. They are natural languages which are used by many deaf people all over the world, e.g. HSL (Hungarian Sign Language) or ASL (American Sign Language). In 1988, the European Parliament passed a resolution stating that the sign languages of the European Community should be officially recognized by the Member States. To date only Sweden, Greece, Portugal and Finland have ratified this resolution into legislation. Nevertheless, the sign languages of Europe are living and developing languages. They can be characterized by manual (hand shape, hand-orientation, location, motion) and non-manual (trunk, head, gaze, facial expression, mouth) parameters. Mostly one-handed and two handed signs are used. Sign languages occupy a 3D signing space usually considered to be within the arms reach horizontally and from the top of the head to the waist [1].

In sign language the hands convey most of the information. Hence, vision-based automatic sign language recognition systems have to extract relevant hand features from real life image sequences to allow correct and stable gesture classification. Using only the position information of the hands [2] or additionally their 2D orientation and some simple 2D shape properties [3] [4], recognition results of up to 97.6% for 152 different single gestures have been achieved so far. Nevertheless, more detailed information about the hand shape becomes necessary if a general recognition system is supposed to be constructed with a significantly larger gesture vocabulary and with the aim of distinguishing between so-called minimal pairs of signs, which merely differ in hand shape.

Most recent gesture recognition applications use either low level geometrical information [5], 2D models of the contour [6] or appearance models [7] [8] to describe the 2D hand image. The resulting parameters are appropriate to distinguish between a few clearly separable hand shapes from a fixed viewing angle. Although there are only a small number of different hand shapes employed during the performance of sign language, these can appear at any posture, creating a large amount of different hand images. The problem is that the degree of similarity between these 2D appearances does not correspond well to the degree of similarity between the corresponding constellations of the real hand. Because of this, an improvement of recognition results through direct usage of any extracted 2D features cannot be expected.

The most suitable information for gesture classification are the real hand parameters which include the finger constellation and the 3D hand posture. Several approaches have been published to extract these from images without the usage of any aids like marked gloves. In [9] the given image is compared with a large database of rendered hand images using a set of similarity criteria. The natural hand parameters of each image are included in the database. Another approach is to detect relevant points like the finger tips in the image and to adapt a simple 3D model to the positions found [10]. Furthermore, different methods have been developed to construct a deformable 3D model of the hand and to adapt it to the image content.

The main goals of the proposed system are the following:

- To recognize some very basic elements of manual sign language, based on 2D visual information.
- To visualize the positions of the fingers with a 3D graphical Hand Simulation.
- To make connection with other users in order to exchange sign language data over the Internet.

This paper is structured as follows: Section 2 gives a general description about our system. Section 3 introduces the details of the system. Finaly in Section 4 the results are summarized and further plans are explained.

2 General Description

2.1 Intelligent Space

The main problem is the bandwith of the existing LAN applications. We can acquire bigger amout of information than we can transfer through the fastes computer network line. To reduce the data transfer the intelligence of the system must be distributed. A conceptual figure of the Intelligent Space with ubiquitous sensory intelligence is shown in Figure 1.

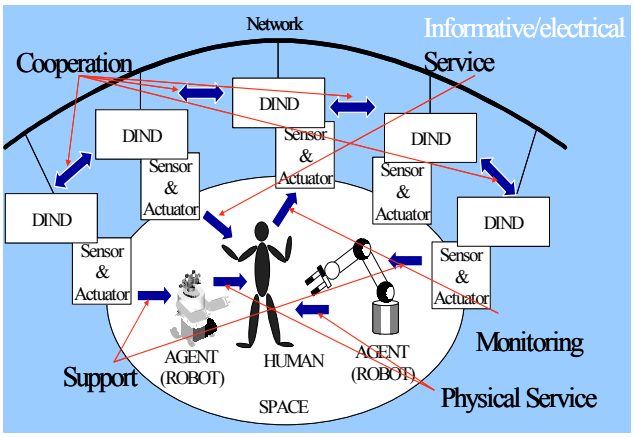

Figure 1
Intelligent Space Concept

The Ubiquitous Sensory Intelligence is realised by Distributed Intelligent Networked Devices [11], robots, which are physical agents of the Intelligent Space, and Human. In the Intelligent Space, DINDs monitor the space, and achieved data are shared through the network. Since robots in the Intelligent Space are equipped with wireless network devices, DINDs and robots organize a network. The Intelligent Space based on Ubiquitous Sensory Intelligence supply information to the Human beings and it can help them physically by using robot agents. Conventionally, there is a trend to increase the intelligence of a robot (agent) operating in a limited area. The Ubiquitous Sensory Intelligence concept is the opposite of this trend. The surrounding space has sensors and intelligence instead of the robot (agent). A robot without any sensor or own intelligence can operate in an Intelligent Space. The difference of the conventional and Intelligent Space concept is shown in Figure 2. There is an intelligent space, which can sense and track the path of moving objects (human beings) in a limited area. There are some mobile robots controlled by the intelligent space, which can guide blind persons in this limited area. The Intelligent Space tries to identify the behaviour of moving objects (human beings) and tries to predict their movement in the near future.

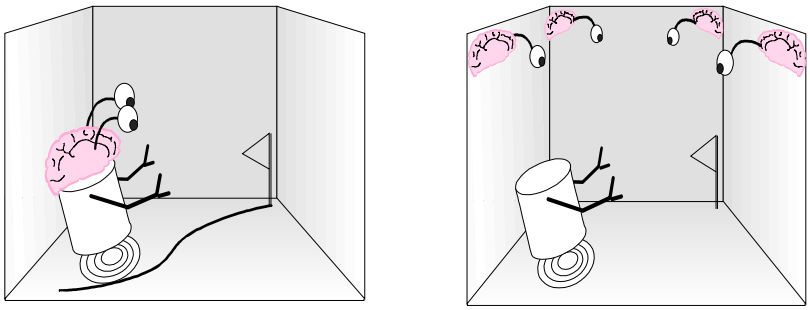

Conventional concept

Ubiquitous Sensory Intelligence concept

Figure 2
Comparison of conventional and Ubiquitous Sensory Intelligence concept

Using this knowledge, the intelligent space can help avoiding the fixed objects and moving ones (human beings) in the Intelligent Space. A mobile robot with extended functions is introduced as a mobile haptic interface, which is assisted by the Intelligent Space. The mobile haptic interface can guide and protect a blind person in a crowded environment with the help of the Intelligent Space. The Intelligent Space learns the obstacle avoidance method (walking habit) of dynamic objects (human beings) by tracing their movements and helps to the blind person to avoid the collision. The blind person communicates (sends and receives commands) by a tactile sensor. The prototype of the mobile haptic interface and simulations of some basic types of obstacle avoidance method (walking habit) are presented. Some other Intelligent Space projects can be found in the Internet [12, 13, 14, 15].

2.2 Sign Language Recognition as a Type of DINDs

We can use as a definition: A space becomes intelligent, when Distributed Intelligent Network Devices (DINDs) are installed in it [11]. DIND is very fundamental element of the Intelligent Space. It consists of three basic elements. The elements are sensor (camera with microphone), processor (computer) and communication device (LAN). DIND uses these elements to achieve three functions. First, the sensor monitors the dynamic environment, which contains people and robots. Second, the processor deals with sensed data and makes decisions Third, the DIND communicates with other DINDs or robots through the network. Figure 3 hows the basic structure of human decision and DIND.

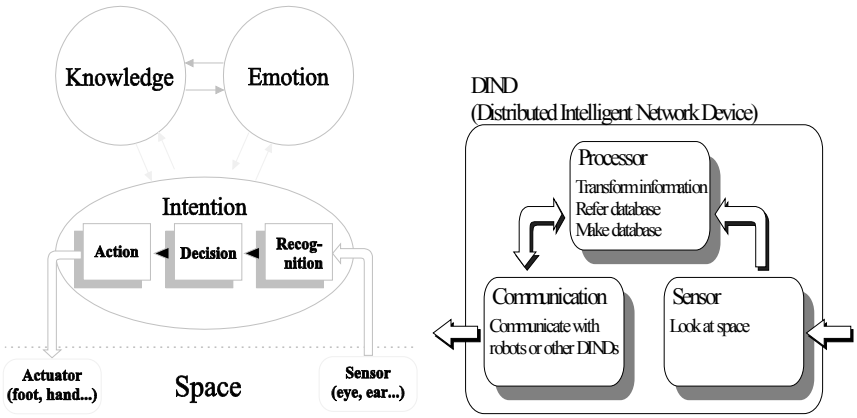

Figure 3
Fundamental structures of human decision and DIND

2.3 The Alphabet of the Sign Language

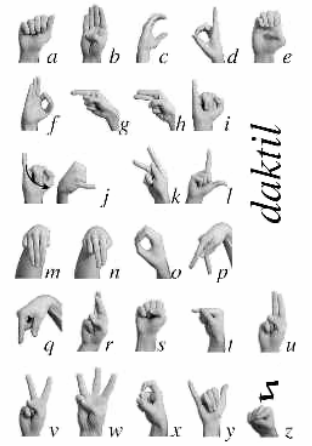

Figure 4
Alphabet of the Sign Language

A, B, E, I, U, V and W letters can be recognized without examining the position of the thumb (see in Fig. 5-11).

Figure 5
Camera picture of letter A

Figure 6
Camera picture of letter B

Figure 7
Camera picture of letter C

Figure 8.
Camera picture of letter I

Figure 9
Camera picture of letter U

Figure 10
Camera picture of letter V

Figure 11
Camera picture of letter W

To recognize all of the letters two or more cameras and a rather complicated marking system is needed so we limited our system's facilities to recognize those letters which neglect the use of thumb.

2.4 Marker Points

For finding the joints of the fingers on the picture of the camera we had to sign them. First we mark the joints with red points but in this case two problems appeared: which point belongs to which finger and this point an inner point or an outer point. To solve this problem, different colors would have to be used as it shown in Figure 12. and 13., but in that case the finding of the joints would be more difficult, because there are more colors.

Figure 12
The inner color points of the prepared glove

Figure 13
The outer color points of the prepared glove

2.5 System Elements

We designed a system which uses a CCD video camera to recognize the finger positions(see in Fig. 14) To help our system we used specially marked gloves as described in section 2.4. The image of the observed hand is transferred to a standard desktop computer - using a video digitalisator card - where an image is analyzed by our image recognition program. If the analyzed hand is recognized as a sign for deaf people the corresponding letter is displayed on the screen. While displaying a recognized letter the program is able to display the signs using a 3D hand visualization software (see in Fig. 15). Multiple hand visualization programs can be connected to the recognition software through the Internet.

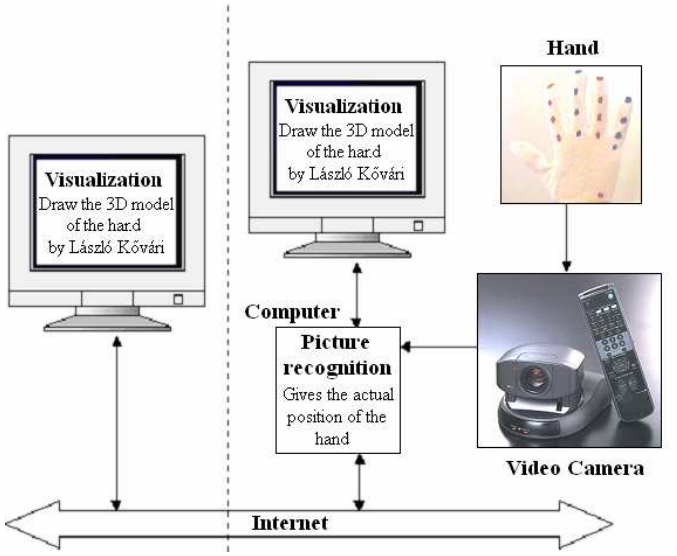

Figure 14
Block diagram of the sign recognition and sign reconstruction system

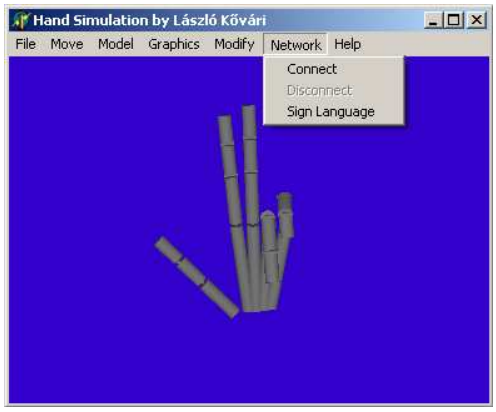

Figure 15
The Hand Simulation software

3 Detailed Description

The video camera system produces a standard composite video signal which is recognized by a video digitalisator card. The captured image is transferred to the image recognition software 10 times per second.

The image recognition software scans the image pixel by pixel using the algorithm described as follows:

3.1 Algorithm for Finding the Marker Points

The problem at finding the marker point is that they are bigger than one pixel. That is why after finding for example a red pixel it must be decided whether this pixel belongs to an earlier found joint or it belongs to a new one. This problem is well known, there exist many so-called edge detection algorithms. But these algorithms are quite sophisticated, usually not too fast, and they know much more than what we need. This is why we decided to use a self-created algorithm, which is worse than any of these edge detection algorithms, but enough for our purposes. We are interested only about the en frame rectangle of the joints. So the algorithm works in the following way:

The computer starts to scan the picture, and after it finds a red point the following two things can happen:

- If this point is not further to the middle of a previously found rectangle than a given limit, then we suppose, the point belongs to that rectangle. In this case we increase the size of that rectangle, so that it encloses this new point too.
- If it is not enough close to any other rectangles, then we suppose that it is a new joint, and we make a new rectangle for it.

To find the color marks the program gets RGB component of each pixel. Instead of looking for a concrete color we are examining a range of colors. We can set this range with the help of the scroll bars or edit boxes which can be seen in the left bottom quarter of the program screen. (see in Fig. 16) It is important to the lighting conditions are to be nearly constant so the RGB components of the color points change in narrow range.

3.2 Evaluation of the Positions of the Points

First of all a red dot at the lower right corner of the palm of the hand is found; this will be the base point of the further analysis. Four different groups of the points are created, one for each finger. The points are separated into those groups by reading their color code and position according to the base point. Each group should contain 4 points. If some points are missing, they are automatically added by the program.

Each group is examined by the algorithm and the angles of the joints' are calculated. These calculated angles are compared to the stored values – angle values for letters A, B, E, I, U, V and W – and the result of the comparison will be the recognized letter.

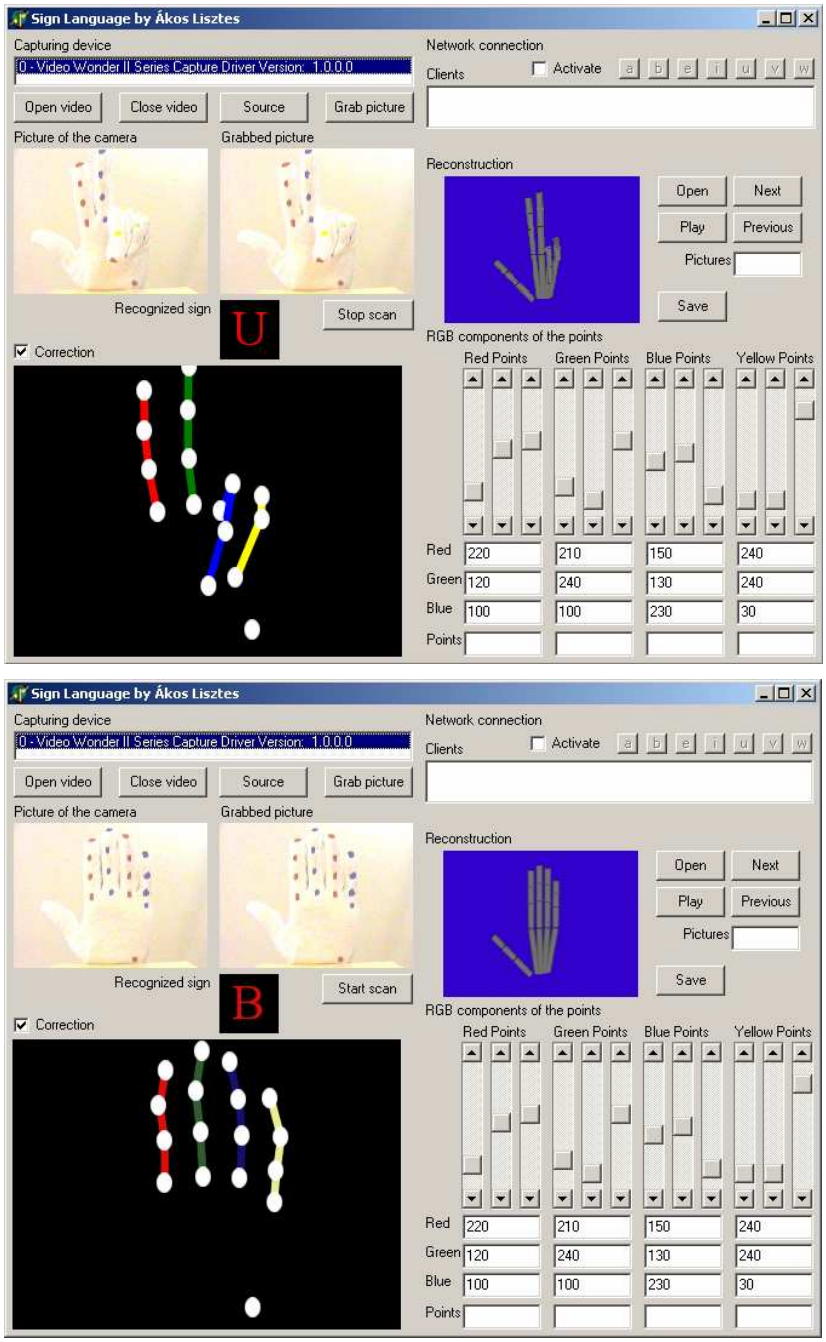

Figure 16
Sign Recognition of letter U and B

3.3 The Sign Reconstruction Software

A 3D hand animation software was developed to give a visual feedback of signs [16] (see in Fig. 15). Visual feedback has the aim of giving a quite real representation of the environment, and although at the moment this environment is far from complete, the program enables the user to wonder in full three-dimensional space.

4 Results and Further Plans

4.1 Performed Tasks

A Sign Recognition program was written in Delphi 6 which can detect the positions of the fingers' expect the thumb and can recognize the A, B, E, I, U, V and W letters. A Hand Simulation Program correctly reconstructs the recognized signs.

A network connection between the sign recognition software and the hand simulation software has been established and tested; It was able to transfer the recognized signs through the Internet.

Using this technique the network load was significantly lower than sending the whole video stream through the network.

4.1.1 Performance Test Results

We used the following system components for testing:

- Sony EVI D30/D31 Pan/Tilt/Zoom CCD camera
- Genius Video Wonder Pro III video digitalisator card
- GeForce4 MX440 video card
- Intel Pentium II 366 MHz processor
- 128 Mb RAM
- Windows 95 OSR2

The signal produced by the CCD camera is a standard composite video signal; This can be digitalised using a video digitalisator card. The video signal contains 25 frames per second but the digitalisator card was able to digitalise 16-25 frames per second. Our algorithm was able to process 10 frames per second (average) at 100% CPU utilization.

4.1.2 Functionality Test Results

The efficiency of the algorithm was around 90%. We tested the algorithm in ideal light conditions and the signs were shown for at least 5 seconds. No mistakes were made during the test only few times the program wasn't able to recognize the sign.

4.2 Further Plans

A video recognition system should be extended to handle the thumb and to recognize every used sign. Rendundancy of the recognition system should be improved to tolerate different light conditions as well.

The marker system should be simplified or neglected and the recognition system should work without any additional help. Later this system can be integrated to Intelligent Space systems as a DIND (Distributed Intelligent Network Device).

Conclusion

As we know there is a growing need for space monitoring systems all over the World but these systems' need larger and larger operating staff as well; The tendency in the World is that salaries are growing and to employ a security staff to operate these monitoring systems becomes uneconomical. Contrarily computer systems are getting cheaper and cheaper so they might substitute humans in this field.

We think that there is a growing need for cheap intelligent space systems which can be easily taught to make difference between usual and unusual situations. Intelligent space systems are able to communicate with humans in the monitored area, but we have to make them as flexible as possible. The proposed system fits into the Intelliget Space because it can be used as the interface between deaf people and computers.

Acknowledgement

The authors wish to thank the JSPS Fellowship program, National Science Research Fund (OTKA T034654, T046240), Hungarian-Japanese Intergovernmental S & T Cooperation Programme and Control Research Group of Hungarian Academy of Science for their financial support.

References

[1] Liddel, S. K. and R. E. Johnson. American Sign Language The phonological base. In: Sign Language Studies, 64: 195-277, 1989

[2] Yang, M.-H., N. Ahuja, and M. Tabb, "Extraction of 2D Motion Trajectories and its application to Hand Gesture Recognition", IEEE Transactions on Pattern Analysis and Machine Intelligence, 24(8), 2002, pp. 1061-1074

[3] Starner, T., J. Weaver, and A. Pentland, "Real-time American sign language recognition using desk and wearable computer based video", IEEE Transactions on Pattern Analysis and Machine Intelligence, 20(12), 1998, pp. 1371-1375

[4] Akyol, S., "Non-intrusive recognition of isolated gestures and signs", Ph.D. thesis, Achen University (RWTH), Germany, 2003

[5] Hardenberg, C. v. and F. Bérard, "Bare-Hand Human-Computer Interaction", ACM Workshop on Perceptive User Interfaces, Orlando, Florida, Nov. 2001

[6] Bowden, R. and M. Sarhadi, "Building temporal models for gesture recognition", BMVC, 2000, pp. 32-41

[7] Martin, J. and J. Crowley, "An Appearance-Based Approach to Gesture recognition", ICIAP (2), 1997, pp. 340-347

[8] Triesch, J. and C. v. d. Malsburg, "Robust Classification of Hand Postures against Complex Backgrounds", IEEE International Conference on Automatic Face and Gesture Recognition, 1996, pp. 170-175

[9] Athitsos, V. and S. Sclaroff, "An Appearance-Based Framework for 3D Hand Shape Classification and Camera Viewpoint Estimation", Technical Report 2001-22, Boston University, 2001

[10] Nölker, C. and H. Ritter, "GREFIT: Visual Recognition of Hand Postures", Gesture-Based Communication in Human-Computer Interaction, Springer, 1999, pp. 61-72

[11] J.-H. Lee and H. Hashimoto, "Intelligent Space - Its concept and contents – ", Advanced Robotics Journal, Vol. 16, No. 4, 2002

[12] Hashimoto Laboratory at The University of Tokyo http://dfs.iis.u-tokyo.ac.jp/~leejooho/ispace/

[13] MIT Project Oxygen MIT Laboratory for Computer Science MIT Artificial Intelligence Laboratory http://oxygen.lcs.mit.edu/E21.html

[14] Field Robotics Center, Carnegie Mellon University Pittsburgh, PA 15213 USA http://www.frc.ri.cmu.edu/projects/spacerobotics/publications/intellSpaceRobot.pdf

[15] [Institut of Neuroinformatics Universität/ETH Zürich Winterthurerstrasse 190 CH-8057 Zürich http://www.ini.unizh.ch/~expo/2_0_0_0.html

[16] Kővári, L.: Visual Interface for Telemanipulation, Final Project, Budapest University of Technology and Economics, 2000

[17] T. Akiyama, J.-H. Lee, and H. Hashimoto, "Evaluation of CCD Camera Arrangement for Positioning System in Intelligent Space", International Symposium on Artificial Life and Robotics, 2001